Gene-immunotherapy

with TRAIL and bispecific antibody EpCAMxCD3

for the selective induction of apoptosis

in advanced pancreatic and prostate cancer

Dissertation

submitted to the

Combined Faculties for the Natural Sciences and for Mathematics

of the Ruperto-Carola University of Heidelberg, Germany

for the degree of

Doctor of Natural Sciences

presented by Ariane Groth
Master of Science

born in: Wolfen, Germany

Oral-examination:...

Referees: First referee: PD Dr. Philipp Beckhove

                   Second referee: Prof Dr. Ingrid Herr

Declaration by candidate

I hereby confirm that this work submitted for assessment is my own and is expressed in my own words. Any uses made within it of the works of other authors in any form (i.e. ideas, equations, figures, text, tables, programs) are properly acknowledged at the point of their use. A full list of the references employed has been included. Where other sources of information have been used, they have been indicated or acknowledged.

Signature:

Acknowledgement

This dissertation was carried out under the supervision of Prof Dr. rer. nat. Ingrid Herr and PD Dr. med. Philipp Beckhove, from September 2006 till March 2010 as a cooperative project of the German Cancer Research Center and the Department of Molecular OncoSurgery at the University Hospital of Heidelberg.

My first acknowledgement goes to my doctoral supervisor Ingrid Herr for her guidance, constant support and encouragement during my doctoral research. I am very grateful for the opportunity to work in her group, for her constant support, advice and guidance in my dissertation and the freedom she granted me in my research.

Further, I am very grateful to PD Dr. Philipp Beckhove for taking on the task of the first referee of my dissertation and for the reviews of this work.

I owe a huge debt of gratitude to Dr. Alexei Salnikov and PD Dr. Gerhard Moldenhauer for their constant guidance, assistance and advice. They greatly contributed to my dissertation by sharing ideas and suggestions at every stage of my work. A special thank you goes to Alexei Salnikov for his support, the time and the patience in reading, evaluating and commenting my writings. I learned a great deal from him and thank him for many fruitful discussions and the time in the lab with him.

I extend my thanks to all current and former members of my lab group, especially Vanessa Rausch, Benjamin Beckermann, Georgious Kallifatidis, Sabine Schlesinger and Jury Gladkich. They all contributed in various forms of support to my work and the time in this lab. I especially want to acknowledge the work of Jury Gladkirch and Sabine Schlesinger for their help in the animal experiments and with immunohistochemistry.

Next, I wish to thank Isabel Vogler and Prof. Dr. Manuel Grez, for their time in Frankfurt and their cooperation. I am also very grateful for the scientific advice of Prof Dr. Wolfgang Uckert, his contribution was essential for the vector construction.

I also want to express my gratitude to all the people who have willingly donated blood for the numerous experiments with lymphocytes.

Particular thanks go to Martin Mollenhauer for advice in vector cloning and in reading and commenting the dissertation.

Most importantly, I want to thank my parents to for their love, encouragement and constant support. They have always believed in me and helped me reach my goals.

My final acknowledgement goes to Sandro Giannattasio, who has been my emotional anchor during the preparation and writing of this dissertation. His unselfish support kept me focused and well in balance during the major phase of my doctoral thesis. Thank you.

Abstract

Patients with pancreatic and prostate cancer have a poor survival rate and new therapeutic strategies are needed. Epithelial cell adhesion molecule (EpCAM), suggested as a marker for cancer stem cells, is over-expressed on most pancreatic and prostate tumor cells but not on normal cells and may be an ideal therapeutic target. The anti-tumor efficiency of bispecific EpCAMxCD3 antibody linking tumor cells and T lymphocytes was evaluated. Furthermore, it was tested whether the combination of bsAb EpCAMxCD3 with lymphocytes over-expressing the death ligand TRAIL, inducing apoptosis in cancer cell but not on normal cells, would be effective. In NOD/SCID mice, EpCAMxCD3 had a long serum half-life ($t_{1/2} \sim 7$ days). Co-transplanted pre-activated lymphocytes and EpCAMxCD3 effectively retarded the tumor growth of BxPc-3 pancreatic and PC-3 prostate xenografts. TRAIL-over-expressing lymphocytes strongly enhanced the efficacy of very low doses of EpCAMxCD3 and retarded the tumor growth. Furthermore, TRAIL-over-expressing lymphocytes enhanced EpCAMxCD3 treatment in a BxPc-3 xenograft model with developed tumors. Tumor growth retardation was associated with a reduced tumor cell proliferation and with a reduced blood vessel density. In 3D *in vitro* tumor reconstructs, TRAIL-over-expressing lymphocytes dramatically increased the expression of apoptosis-related proteins, compared to pre-activate lymphocytes and EpCAMxCD3. For mimicking a pancreatic cancer microenvironment *in vitro*, we used a three-dimensional tumor reconstruct system, in which lymphocytes were co-cultured with tumor cells and fibroblasts in a collagen matrix. In this *in vivo*–like system, EpCAMxCD3 potently stimulated production of the effector cytokines IFN-γ and TNF-α by extracorporally pre-activated lymphocytes. Moreover, compared with a bivalent anti-CD3 antibody, EpCAMxCD3 more efficiently activated the production of TNF-α and IFN-γ by non-stimulated peripheral blood mononuclear cells. Most excitingly, we demonstrate for the first time that EpCAMxCD3 induces prolonged contacts between lymphocytes and tumor cells, which may be the main reason for the observed anti-tumor effects. In addition, EpCAMxCD3 stimulated the expression of multiple chemokines in 3D tumor reconstructs. Those chemokines could potentially contribute to the increased infiltration of the tumor tissues with CD68^{+} and F4/80^{+} macrophages. Conclusively the combination of TRAIL-transduced lymphocytes and the bispecific antibody EpCAMxCD3 was very efficient in pancreatic and prostate xenograft models *in vivo* and *in vitro*. This combination of gene therapy with immunotherapy may open a way to improve the immune response and treatment outcome in patients with pancreatic, prostate cancer and most likely other tumor entities.

Summary

The aim of this project was to test the efficacy of a novel therapeutic approach for cancer therapy. This approach combines immunotherapy with bispecific antibody (bsAb) EpCAMxCD3 and gene therapy with TRAIL. The potential efficacy of this approach was tested in experimental models of pancreatic and prostate carcinoma. Specific aims were i) to construct a lentiviral vector suitable for the transduction of human lymphocytes and the over-expression of TRAIL. The next aim was ii) to establish and to evaluate suitable xenograft models for the study of the chosen approach, iii) to test the efficacy and the anti-tumor potential of TRAIL-over-expressing lymphocytes and bsAb EpCAMxCD3 *in vivo* and iv) to elucidate the functional mechanisms underlying observed anti-tumor effects of TRAIL-over-expressing lymphocytes and bsAb EpCAMxCD3 *in vivo* and *in vitro*.

In conclusion, this is the first study, which shows the effective lentiviral transduction of human lymphocytes with the death ligand TRAIL. The vector pV3TP2A effectively transduced human lymphocytes to over-express TRAIL. The majority of these TRAIL-over-expressing lymphocytes were CD8+ T cells and retained their cytotoxic functions, their migratory and proliferative properties after the transduction. Furthermore, this study showed that EpCAMxCD3 possesses a potent anti-tumor activity *in vivo*. In NOD/SCID mice, EpCAMxCD3 had a long serum half-life (t1/2 ~ 7 days). In two mouse models the combination of EpCAMxCD3 with lymphocytes significantly retarded the growth of BxPc-3 pancreatic and PC-3 prostate cancer xenografts. For mimicking a pancreatic cancer microenvironment *in vitro* a 3D tumor reconstruct system was used, in which lymphocytes were co-cultured with EpCAM-expressing tumor cells and fibroblasts in a collagen matrix. In this *in vivo*-like system EpCAMxCD3 potently stimulated the production of the effector cytokines IFN-γ and TNF-α by extracorporally pre-activated lymphocytes. Moreover, compared with a bivalent anti-CD3 antibody, EpCAMxCD3 more efficiently activated production of TNF-α and IFN-γ by non-stimulated PBMCs. We demonstrate for the first time that EpCAMxCD3 induces prolonged contacts between lymphocytes and tumor cells, which may be one of the main reason for the observed anti-tumor effects. The combination with lymphocytes over-expressing the death ligand TRAIL could effectively enhance the anti-tumor effects of bsAb EpCAMxCD3. The combination with TRAIL-over-expressing lymphocytes enabled us to strongly reduce the dose of EpCAMxCD3 necessary for an anti-tumor effect. This is a great advantage, which could minimize potential side effects of bsAb

treatment. EpCAMxCD3 did not alter lymphocyte migration as measured by time-lapse video microscopy, which is an important prerequisite for future use in patients. Apoptosis induction in tumor cells by TRAIL-over-expressing lymphocytes was confirmed *in vitro* in 3D tumor reconstructs. In cytotoxic killing assays, the anti-tumor effect of TRAIL-over-expressing lymphocytes was significantly enhanced by EpCAMxCD3. In 3D gels, lymphocytes were effective producers of IFN-γ, TNF-α and chemokines, which could also be detected *in vivo* from tumor lysates. An increased infiltration of the tumor islets with macrophages and granulocytes was observed upon treatment with TRAIL-over-expressing lymphocytes and EpCAMxCD3. A potential explanation for the demonstrated anti-tumor effect of EpCAMxCD3 and TRAIL-over-expressing lymphocytes combination therapy, is an enhancement of the observed effects of single treatment, namely the reduced proliferation in tumor cells, decreased blood vessels formation, local production of cytokines and chemokines, apoptosis and an increased infiltration of tumor tissue with macrophages. Conclusively, the combination of TRAIL-over-expressing lymphocytes and the bispecific antibody EpCAMxCD3 was very efficient in pancreatic and prostate xenograft models *in vivo*. This combination of gene therapy with immunotherapy could potentially be a possible therapeutic option for the clinical application in the future.

Zusammenfassung

Ziel dieser Studie war einen neuartigen Therapieansatz für die Krebstherapie zu testen. Dieser Ansatz kombiniert die Immuntherapie mit dem bispezifischem Antikörper (bsAk) EpCAMxCD3 mit einer Gentherapie mit TRAIL. Die potentielle Wirksamkeit dieser Therapie wurde in experimentellen Modellen des Prostata und des Pankreaskarzinoms getestet. Konkrete Ziele dabei waren i) die Generierung eines lentiviralen Vektors, der geeignet für die Transduktion von humanen Lymphozyten ist und die Überexpression des Todesliganden TRAIL ermöglicht, ii) die Etablierung und die Evaluierung eines geeigneten Xenograft Models, iii) die Untersuchung der Effektivität und der Anti-Tumor Wirkung TRAIL-überexprimierender Lymphozyten mit bsAk EpCAMxCD3 *in vivo* und *in vitro* und iv) die Analyse des Funktionsmechanismus der beobachteten Anti-Tumor Wirkung von TRAIL-überexprimierender Lymphozyten und EpCAMxCD3 *in vivo* und *in vitro*.

Zusammenfassend zeigte diese Studie dass EpCAMxCD3 eine potente Anti-Tumor-Wirkung *in vivo* besitzt. In NOD/SCID Mäusen besaß EpCAMxCD3 eine lange Serum Halbwertszeit von ungefähr 7 Tagen. In zwei unabhängigen Mausmodellen reduzierte EpCAMxCD3 zusammen mit Lymphozyten effizient das Tumorwachstum von pankreatischen BxPc-3 und prostata PC-3 Xenografts. Um die Mikroumgebung eines Karzinoms *in vitro* nachzuahmen, wurde ein 3D Tumor Rekonstrukt benutzt in dem Lymphozyten zusammen mit EpCAM-exprimierenden Tumorzellen in Fibroblasten in einer Kollagenmatrix co-kultiviert wurden. In diesem *in vivo* artigem System stimulierte EpCAMxCD3 die Produktion der Effektorzytokine IFN-γ und TNF-α in voraktivierten Lymphozyten. Verglichen mit bivalenten anti-CD3 Antikörpern, stimulierte EpCAMxCD3 sogar die Produktion von IFN-γ und TNF-α von unstimulierten Lymphozyten. Wir demonstrieren hier erstmalig dass EpCAMxCD3 die Kontaktzeit zwischen Lymphozyten und Tumorzellen verlängert, was die Grundlage für die Anti-Tumor Wirkung sein könnte. Als eine wichtige Vorraussetzung für eine mögliche klinische Anwendung hatte EpCAMxCD3 keinen Einfluß auf die Migration von Lymphozyten, was mit Time-lapse Video Mikroskopie demonstriert wurde. Die Kombination mit Lymphozyten die den Todesliganden TRAIL überexprimierten verstärkte die Anti-Tumor-Wirkung von EpCAMxCD3 sehr effizient. Schon geringe Dosen von EpCAMxCD3 genügten um eine Anti-Tumor Wirkung zu erzielen in dieser Kombination mit TRAIL-überexprimierenden Lymphozyten. Diese Tatsache könnte vorteilhaft sein um mögliche Nebeneffekte der Behandlung zu minimieren. Die Induktion von Apoptose in Tumorzellen

konnte in 3D Tumor Rekonstrukten *in vitro* gezeigt werden. In Versuchen zur Zytotoxizität von Lymphozyten auf Tumorzellen wurde die Wirkung von TRAIL-überexprimierendev Lymphozyten noch durch EpCAMxCD3 signifikant gesteigert. In 3D Tumor Rekonstrukten wurden neben den Zytokinen IFN-γ und TNF-α auch Chemokine produziert, die sowohl *in vitro* als auch in Tumor Lysaten detektiert werden konnten. Diese Chemokine stehen höchstwahrscheinlich im Zusammenhang mit der vermehrten Infiltrierung des Tumorgewebes mit Makrophagen und Granulozyten nach der Behandlung mit TRAIL-überexprimierenden Lymphozyten und mit EpCAMxCD3. Eine mögliche Erklärung für die gezeigte Anti-Tumor Wirkung von TRAIL-überexprimierenden Lymphozyten und EpCAMxCD3 ist eine Reduktion der Blutgefäße, die lokale Produktion von Zytokinen und Chemokinen mit einer vermehrten Einwanderung von Makrophagen in das Tumor Gewebe.

Zusammenfassend konnte die Kombination aus TRAIL-überexprimierenden Lymphozyten und dem bispezifischen Antikörper EpCAMxCD3 erfolgreich für die Therapie experimenteller Pankreas und Prostata Tumor Xenografts *in vivo* getestet werden.

Table of contents

"Gene-immunotherapy with TRAIL and bispecific antibody EpCAMxCD3 for the selective induction of apoptosis in advanced pancreatic and prostate cancer"

Abbreviations

WHO	World Health Organization
%	Percent
°C	Degree celsius
3D	three dimensional
aa	Amino acids
AAV	Adeno associated virus
Ad	Adeno virus
ADCC	Antibody-dependent cell-mediated cytotoxicity
Apo2/TRAIL	Tumor nekrosis factor related apoptosis inducing ligand
Bad	Pro-apoptotic protein Bad
Bak	Pro-apoptotic protein Bak
Bax	Pro-apoptotic protein Bax
Bcl-2	Anti-apoptotic protein B cell lymphoma 2
BCR/Abl	Fusion protein of the BCR gene and the V-abl Abelson murine leukemia viral oncogene homolog 1
BiTE	Bi-specific T cell engagers
bsAb	Bispecific antibody
CD19xCD3	Bispecific antibody dual specific for CD19 and CD3
CDC	Complement dependent cytotoxicity
CEA	Carcinoembryonic antigen
cm^3	Cubic centimeter
CML	Chronic myelogenous leukemia
CTL	Cytotoxic T lymphocytes
Db	Diabody
DC	Dendritic cell

DISC	Death-Inducing Signalling Complex
Dox	Doxycycline
EGF	Epithelial Growth Factor
EGFP	Enhanced green fluorescent protein
EGFR	Epithelial Growth Factor Receptor
ELISA	Enzyme-linked immunosorbent assay
EpCAM	Epithelial cell adhesion molecule
EpCAMxCD3	Bispecific antibody dual specific for EpCAM and CD3
FACS	fluorescence activated cell sorting
FADD	Fas-Associated protein with Death Domain
FasL	Death ligand Fas Ligand
Fig	Figure
FITC	Fluorescin isothyocyanate
FLIP	FLICE-like inhibitory Protein
g	gram
h	hour
H+E	Hematoxylin and eosin
HBV	Hepatitis B virus
HCV	Hepatitis C virus
HEA125	Anti human EpCAM monoclonal antibody
HER-2	Human Epidermal growth factor Receptor 2
HIV	Human immunodeficiency virus
HPV	Human papilloma virus
hTERT	Human telomerase reverse transcriptase
i.e.	for example
i.p.	Intra peritoneal
i.v.	Intra venous
IAP	Inhibitors of apoptosis
IFN-γ	Interferon gamma

IgG	Immunoglobulin G
IL-x	Interleukin
IRES	Internal ribosomal entry site
Iso	Iso-type control
K-ras	Small GTPase
Kg	Kilogram
Ki-67	Proliferation marker Ki-67
L	Liter
LPS	Lipopolysaccharid
Lt-α	Lymphotoxin alpha
Lt-β	Lymphotoxin beta
LTR	Long terminal repeats
LV	Lentivirus
M&M	Materials and methods
mAb	Monclonal antibody
MAGE	Melanoma associated antigen
mg/kg	Milligram per kilogram
Min	Minutes
Ml	milliliter
MMAC1/PTEN	Tumor suppressor gene MMAC1/PTEN
MOCK-L	Mock transduced lymphocytes
MOI	Multiplicity of infection
MSC	Mesenchymal stem cells
n	Number of animals
Nf-κB	nuclear factor kappa-light-chain-enhancer of activated B cells
ng	Nanogram
ng/ml	Nanogram per milliliter
NHL	Non-Hodgekin Lymphoma
NK cell	Natural killer cell

NKT	Natural killer T cell
nm	nanometer
NOD/ SCID	Non-obese diabetic/ severe combined immunodeficient mice
NY-ESO-1	cancer/testis family of human tumour-associated antigens
OKT3	Anti CD3 monoclonal antibody
OPG	Osteoprotegerin
P16/INK4A/retinoblastoma protein	Pathway for tumor suppressor gene p16/ INK4A and retinoblastoma protein
p21	Tumor suppressor gene p21
p2A	2A element of porcine teschovirus
p53	Tumor suppressor gene p53
p73	Tumor suppressor gene p73
pAb	Polyclonal antibody
PBMC	Peripheral blood mononuclear cell
PBS	Phosphate buffered saline
PE	phycoerythrin
pg/ml	Picogram per milliliter
PI3/Akt	Pathway for phosphoinositide 3-kinase and protein kinase B Akt
recTRAIL	Recombinant TRAIL
rpm	Rotations per minute
RV	Retrovirus
s.a.	such as
s.c.	Subcutaneous
ScFv	Single chain variable fragment
SIN	Self-inactivating vector
SIV	Simian immunodeficiency virus
ssDNA	single strand DANN
ssRNA	Single strand RNA

t½	Half life
TCR	T cell receptor
TGF-α	Transforming Growth Factor alpha
TNF-α	Tumor necrosis factor alpha
TNM	Classification system of malignant carcinoma
TRAIL	Tumor nekrosis factor related apoptosis inducing ligand
TRAIL-L	TRAIL-transduced lymphocytes
TRAIL-R1/ DR4	Tumor nekrosis factor related apoptosis inducing ligand receptor 1/ death receptor 4
TRAIL-R2/ DR5	Tumor nekrosis factor related apoptosis inducing ligand receptor 1/ death receptor 5
TRE	Tet responsive element
TU	Transducing units
TUNEL	TdT-mediated dUTP-biotin nick end labeling
v/v	Volume per volume
VEGF	Vacular endothelial growth factor
WPRE	Woodchuck hepatitis virus B post-transcriptional regulatory element
µg/ml	Microgram per milliliter
µl	microliter
µm	Mycrometer

1   Introduction

1.1   Epidemiology of pancreatic and prostate cancer

1.1.1   Prostate cancer

In 2008, approximately 110.000 men died of prostate cancer in the EU and 350.000 died worldwide, thus causing 0.6% of all causes of death (WHO 2008). According to the Robert-Koch-Institut statistics, 28.53% of all estimated cancer deaths in Germany will be prostate cancer, making it the most prevalent tumors in males. With 58.000 newly diagnosed patients in 2008, and increasing incidents, prostate cancer remains one of the major public health problems in the western world. The rising numbers are caused mainly by demographic factors, especially the increasingly elderly population, and the improvement of the diagnostic tools (i.e. prostate-specific antigen test). The improvements in the diagnosis and the treatment of prostate cancer increased the 5-year survival rate for all prostate cancer patients to almost 99%. The relative 10-year survival rate is 91% and 76% for 15 years. However, 10-20% of all patients are already diagnosed with advanced prostate carcinoma with metastasis and many other develop metastasis in spite of clinical intervention.

The natural history of the prostate carcinoma is not completely understood and the disease ranges from aggressive to slow growing tumors [1]. There are several risk factors. The strongest factor is age, prostate cancer is rare under the age of 40 and its incidence increases exponentially with age. More than 70% of all patients are older than 65 years at the time of diagnosis [2]. There is a varying geographical incidence and ethnicity also plays a role in the development of the disease, with the highest incidents in African Americans (about twice that in white men) and lowest in Asian, American Indians and Hispanic-Latinos [3]. An estimated 9% of prostate cancer are related to inherited predisposition [4]. Among environmental factors, dietary factors like a high intake of saturated fat, mainly animal fat, and low levels of dietary selenium, vitamin E and vitamin D, may increase the risk [5, 6]. Prostate cancer is thought to arise after a sequence of at least eight genetic mutational events. Early events include the loss of tumor suppressor genes such as p53, which is mutated in up to 64% of tumors and p21 in up to 55%. The p73 tumor suppressor gene, with significant homology to p53, is also mutated in prostate cancer [7]. However, MMAC1/PTEN is the most widely mutated suppressor gene in prostate cancer and may contribute to the acquisition of the metastatic phenotype [8]. The development of the hormone refractory phenotype appears to

be related to the over-expression of mutant p53 and bcl-2 family of proteins as well as amplification of the androgen receptor [9].

Pathologically, 95% of all prostate cancers are adenocarcinomas. Primary carcinoid tumors of the prostate, sarcomas, and primary small cell carcinomas are rare. The prostate cancer cell cytoplasm may contain large amounts of acid phosphatase and prostate specific antigen (PSA), which is used diagnostically. The clinical features of prostate cancer include localized prostate cancer, confined within the prostate capsule, locally advanced prostate cancer, where the cancer extends outside the prostate capsule, and metastatic prostate cancer most commonly graded by the Gleason method and staged by the TNM system [10]. The treatment options for the prostate carcinoma vary depending on age, stage of the cancer and medical condition of the patient. Management of primary prostate cancer includes the treatment modalities of radical prostatectomy, external beam radiotherapy, interstitial radiotherapy and watchful waiting. However, the prostate carcinoma is relatively radiation insensitive. The tumor has a low growth rate and hence a slow response to radiotherapy. To improve the disease control in patients, radiotherapy is combined with adjuvant therapy with gonadotropin releasing hormone (GnRH) analogues. The hormonal therapy supports the disease management at least in initial stages of the treatment [10].

1.1.2 Pancreatic cancer

In 2008, approximately 97.000 people died of pancreatic cancer in the EU and 285.000 worldwide, this makes statistically 0.5% of all causes of death (WHO 2008). According to the Robert-Koch-Institut statistic, 30.73% of all estimated cancer deaths in Germany will be pancreatic cancer. This number makes pancreatic cancer the fourth leading cause of cancer death. Approximately 13.000 patients were newly diagnosed in the year 2008. The early detection is still a clinical challenge and more sensitive detection methods are under development. Hence, in more than 50% of the patients advanced pancreatic carcinoma with metastasis is diagnosed. The 5-year survival rate of only 5% reflects this diagnosis problem and the 5-year survival rate of patients diagnosed with an early metastasis free stage is only 20%.

The major risk factors for pancreatic cancer are increasing age, smoking [11], new onset diabetes mellitus [12], increased body mass index [11], chronic pancreatitis [13, 14], hereditary pancreatitis [15] and an inherited predisposition for pancreatic cancer [16]. Dietary factors are also associated with an increased risk like the comsumption of red and processed meat and a reduced intake of methionine and folate from food sources [17-19]. The molecular

lesions in pancreatic cancers are classified into late and early lesions. Activating mutations in K-ras and the PI3/Akt signaling pathway, regulating growth factor mediated signaling pathways and cell survival, proliferation and resistance to apoptosis, respectively, are commonly found. Several growth factors and their receptors i.e. the epidermal growth factor receptor (EGFR), HER-2, EGF and TGF-α are over-expressed by pancreatic cancer cells. Genetic lesions in the molecular pathways occur with a varying degree in pancreatic carcinomas. The most commonly affected pathways are the pathways of the tumor suppressor genes such as p16/INK4A/retinoblastoma protein pathway, p53 transcription factor pathway or Smad4/TGFb pathway and a reactivation of the developmental signaling by Notch and Hedgehog [19].

Ductal adenocarcinoma is the most common malignant tumor of the pancreas. The late presentation and the aggressive tumor biology of this disease makes an early diagnosis difficult and only a minority of 10-15% of patients can undergo potentially curative surgery. Another problem is the high resistance of ductal adenocarcinoma to conventional methods of cytotoxic treatment and radiotherapy. The most widely used chemotherapeutic for advanced pancreatic cancer has been 5-Fluoracil, an inhibitor of thymidylate synthetase or combinations with gemcitabine. External beam radiotherapy is routinely used with 5-Fluoracil, but the main drawback is the limit of the dosage owing to the close proximity of adjacent radiosensitive organs. Patients with advanced pancreatic carcinoma, which are inoperable, are subjected to palliative or to adjuvant therapy to improve survival and quality of life, but the median survival dates do not offer a good prognosis [19].

1.2 Novel experimental approaches for the cancer therapy

The evolution of these two cancer diseases and their insensitivity to conventional therapies or the late diagnosis urgently increases the need for alternative therapeutic approaches. As radiation and chemotherapy often have a limited effect and a substantial toxicity, there is a strong need to test new therapeutic approaches or to find supportive treatments for the combination with conventional treatments.

The understanding of the biological abnormalities of cancer has generated a large number of studies targeting cancer cells on the cellular and on the molecular level. The tumorigenesis in humans has been widely recognized as a multistep process, underlying a stepwise evolution from normality via a series of pre-malignant states into an invasive cancer. Cancers are as distinct and complex as the cells and tissues of which they are derived, and only distinct hallmarks discriminate them from a normal cell. Hanahan *et al.* and Schreiber *et al.* suggested

seven essential alterations in cell physiology that collectively dictate malignant growth [20, 21]. Those hallmarks are the self-sufficiency in growth signals, the insensitivity to growth-inhibitory signals, the evasion of programmed cell death (apoptosis), a limitless replicative potential, a sustained angiogenesis, the avoidance of immuno surveillance and tissue invasion and metastasis. Each of these physiological changes – novel capabilities acquired during tumor development – represents the successful breaching of an anti-cancer defense mechanism.

Based on these "hallmarks" the research on novel therapeutic strategies has several directions to target a cancer cell. Central considerations include the inhibition of angiogenesis, cell proliferation and migration, the re-sensitization to apoptosis, immunotherapeutic boosting of the tumor-specific immunity by vaccines, cytokines and immune modulators or by the transfer of tumor-reactive cells In addition, there are gene therapy approaches by the restoration of lost genes, the inhibition of over-expressed or dys-regulated genes or the direct cancer eradication by introducing suicide-genes, lytic viruses only to mention a few.

1.3 Gene therapy

Gene therapy is one of the most promising therapeutic strategies for cancer. Gene therapy - the introduction of one or more foreign genes into an organism - has the potential to correct the genetic changes that were acquired by the tumor cells. Gene therapy approaches differ as much as the targeted malignancies. The concept of gene therapy was envisioned in the late 1970s and early 1980s shortly after the emergence of restriction enzymes and subcloning of mammalian genes in plasmids and phages. Today, major gene therapy research areas for cancer include tumor suppressor gene therapy, suicide gene therapy, anti-angiogenic and pro-apoptotic gene therapy, the genetic enhancement of antitumor immune response by strategies using dendritic and T cells and by cytokine-based gene transfer strategies and drug resistant gene therapy (reviewed in [22]).

1.3.1 Vectors for gene therapy

Different vectors have been developed for the transfer of genetic information. These vectors are nonviral, integrating virus vectors (gammaretrovirus and lentivirus), and non-integrating virus vectors (adenovirus, adeno-associated virus, and herpes simplex virus vectors).

1.3.1.1 Nonviral vector systems

Non-viral vectors deliver genes i.e. in liposomes, by a chemical linking of DNA to carrier

molecules, which will bind to a specific receptor, by nanoparticles and cationic liposomes/lipoplexes, by transfection or by electroporation [23]. However, the non-viral delivery systems have a significantly reduced transfection efficiency as they are hindered by numerous extra- and intracellular obstacles.

1.3.1.2   Viral vector systems

For many applications, the vehicles of choice are the viral vectors. An ideal vector is efficient, non-pathogenic, capable of transferring genetic material into a broad range of cells and tissues and can maintain expression for an appropriate period of time. Viruses have an innate invasive ability to infect cells and to deliver their genes, which makes them highly efficient tools for gene therapy. In general, viral vectors are derived from wild-type strains and the parts of the viral genome required for replication and pathogenesis are deleted. Thereby, the virus is converted into a recombinant vector with insertional space for therapeutical genes and regulatory sequences. For the production of viral vectors, these essential genes are expressed in trans by the producer cells. Out of the clinical studies for gene therapy until 2009 more than 64,5% were directed against cancer (Databank in the Journal of Gene Medicine and NIH). Out of these 1019 studies, 23% were conducted with adenoviral, 18% with retroviral and only 0.5% with lentiviral vectors.

In most virus-based approaches recombinant adenoviruses and adeno-associated viruses have been the main vectors. The adenoviral vectors (Adv) are derived from the *Adenoviridae* family, a icosahedral, non-enveloped virus with a broad tropism, which can infect both dividing and quiescent cells. This large double stranded DNA virus does not integrate into the genome, making it limited to transient, episomal expression. Most adenoviral vectors are derived from adenovirus type 5 with deletions of the E1 and E3 region, essential for replication. Adv is currently the most widely used gene delivery vector, with a high delivery efficiency, a great packaging capacity for therapeutical genes (<30kb), a fast and efficient production to high titers, it is non-oncogenic and allows a high expression of the transgene. Adenoviral vectors have been successfully applied in the clinical setting, but express transgenes only for less than a week. The transgene will not persist because adenovirus-based vectors do not integrate into the host genome. Furthermore, adenovirus is immunogenic and most people have been exposed to adenovirus at some point in their life [24, 25]. A specially engineered adenovirus is the oncolytic adenovirus. These viruses exhibit lytic properties of virus replication for the selective infection and lysis of tumor cells [26].

The adeno-associated virus (AAV), a ssDNA virus of the *Parvoviridae* family, is naturally replication-deficient and requires the presence of adenovirus to complete its life cycle. AAV can infect non-dividing cells and in can integrate into the host genome (<10% of the viruses). AAV has a broad host range, low level of immune response and the longevity of gene. There are 8 well defined serotypes (serotypes 1 – 5 and 7 – 9) and more than 100 variants with a different selective tissue tropism [27]. Disadvantages of the AAV vectors are the small packaging limit (<5kb) and adaptive immune responses to their capsids. Although AAV can mediate site-selective integrations into the target cell genome, it has not successfully been applied to T cells.

Chromosome-integrating vectors derived from retroviruses or lentiviruses have been most useful for long-term gene expression and in lymphocyte –based therapies. These viruses integrate into the host-genome, resulting in the permanent expression of the transgene and in a low intrinsic immunogenicity.

The retroviruses (RV), sRNA viruses, are gamma retroviruses from the *Orthoretrovirinae* family, stably integrates into the host genome. Most vectors are derived from murine leukaemia virus. The advantages of RV are an easy production with high titers and a stable and efficient integration into the host genome. However, the inability to transduce non-dividing cells and observed insertional mutagenesis with secondary malignancies limits their potential use for gene therapy.

Lentivirus-derived vectors can also integrate into the genome of non-dividing cells and they are less susceptible to gene silencing by host restriction factors. The lentiviruses, a ssRNA virus, also belongs to the *Orthoretrovirinae* family. They mediate long-term integration of the therapeutic gene, but unlike RV, do not require cellular mitosis to access the host genome for integration [28].

1.3.1.3 The lentiviral vector system

Lentiviral vectors are derived from human immunodeficiency virus (HIV) [29], but also other lentiviruses like the simian immunodeficiency virus (SIV) have been studied. From the viral genome, the polyproteins gag, pol and env are required in trans for viral replication and packaging. Required in cis are the 5' and 3' long terminal repeats (LTR), the integration sequences as well as the packaging site ψ, the transport RAN-binding site and finally additional sequences involved in reverse transcription. The accessory genes *vif, vpr, vpu, nef, tat* and *ref* play crucial roles in virus replication. Unlike retrovirus, lentiviruses are capable of

transducing quiescent cells [28], although for some cell types (T cells) a progression through the cell cycle from G_0 to G_{1b} is necessary to complete reverse transcription [30]. To generate replication-deficient vectors, deletions in the viral genome were generated. The design of lentiviral vectors is based on the separation of *cis*- and *trans*-acting sequences. Generally, lentiviral particles are generated through transient transfection of three plasmids in the human embryonal kidney (HEK) 293T producer cell line. The three plasmids are: (1) a packaging plasmid, (2) a transfer/vector plasmid and (3) an envelope-encoding plasmid.
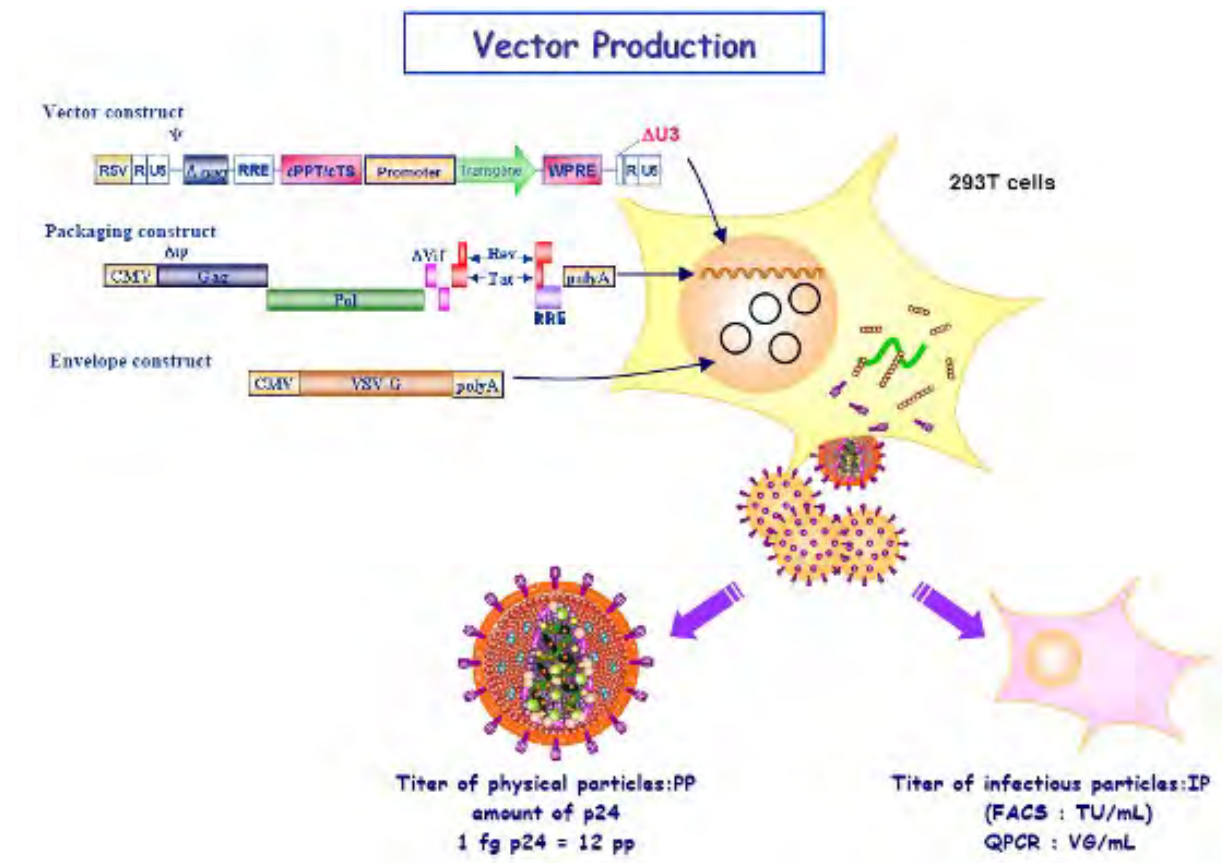
Fig 1 Schematic representation of lentiviral vector production in 293T cells (adapted from www.tronolab.epfl.ch)

The lentiviral particles are divided into 'generations' according to the packaging plasmid which was used for virus production (Fig 2). The first-generation packaging construct provided the entire *gag* and *pol* sequences in *trans* to enable packaging of the transfer construct and contains the viral regulatory genes *tat* and *rev* along with the accessory genes *vif, vpr, vpu* and *nef*. Identification of the HIV genes that are necessary for virulence, but disposable for transfer of the genetic cargo, allowed the engineering of multiple-attenuated packaging systems [31]. In these second-generation packaging systems, up to four accessory genes (*vif, vpr, vpu* and *nef*) were removed without negative effects on yield or infection

efficiency in most cell types. These minimal packaging systems gained in safety, because any replication-competent lentivirus (RCL) that was still generated would be devoid of all virulence factors. In the third generation, safety was further improved by engineering split-genome packaging systems, where the *rev* gene is expressed from a separate plasmid. Also, *tat* could be removed by placing a strong constitutional promoter in the 5' LTR of the transfer vector [32].

The transfer plasmid consists of an expression cassette and the HIV *cis*-acting factors necessary for packaging, reverse transcription and integration. Engineering of self-inactivating (SIN) transfer vectors by deleting the U3 region of the 3' LTR not only further minimized the risk of emergence of RCL, but also decreased problems related to promoter interference [31, 33]. Nuclear import of the transfer construct was improved by including the cPPT and its central termination sequence, together forming a triple helix (TRIP). This structure mediates the transport of the preintegration complex through the nuclear pores. TRIP/cPPT-containing transfer vectors yield higher virus titers and provide enhanced transgene expression in the target cells [34, 35]. Addition of post-transcriptionally active elements, such as the woodchuck hepatitis B post-transcriptional regulatory element (WPRE), represents another strategy to improve the lentiviral vector design. WPRE may improve gene expression by modification of polyadenylation, RNA export or translation [36].

The third plasmid required for lentivirus production provides a heterologous envelope. In most cases it is the glycoprotein of vesicular stomatitis virus (VSV.G), which allows the formation of mixed particles or pseudotypes, displaying the tropism of the virus from which the envelope is derived.
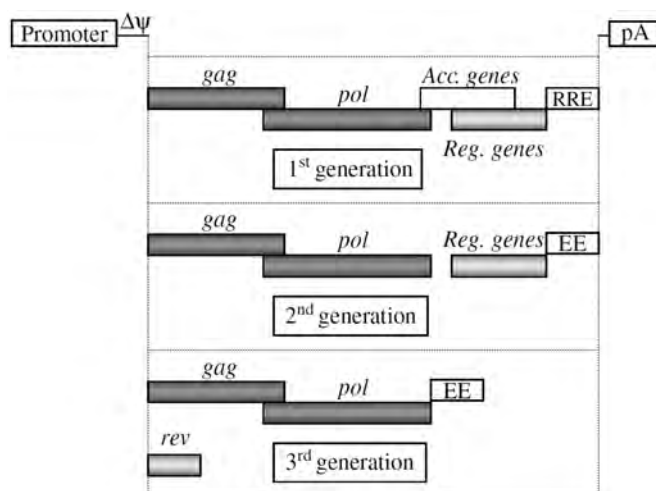
modified from Delenda et al. J Gene Med. 2004 Feb;6 Suppl 1:S125-38.

Fig 2 Schematic representation of the different LV packaging generations.

The commonly maintained structures in all LV packaging elements are shown by the cis-acting sequences (the promoter and polyadenylation regions that replace the original 5' and 3'-LTR elements, respectively, as well as the deletion of the encapsidation site ($\Delta\psi$) and the trans-viral helper genes (gag-pol). Depending on the vector generation, the accessory (Acc.) and regulatory (Reg. or rev alone) genes are conserved in the packaging constructs.

1.3.2   Gene therapy targeting apoptosis

Cancer is partly caused by the uncontrolled proliferation of malignant cells that harbour multiple oncogenic mutations. The increasing understanding of the apoptosis-signaling pathway offers many options for the therapeutic intervention in cancer. There are two apoptotic pathways characterized - the extrinsic pathway and the intrinsic pathway. The extrinsic pathway operates through cell surface death receptors. The intrinsic pathway is tightly controlled by the Bcl-2 family of proteins and involves the disruption of mitochondrial membrane integrity in response to cellular insults or other danger signals. Both pathways converge at the level of effector caspases – proteolytic enzymes that carry out the cell death response (Fig 3). These two pathways are localized within a broader superstructure of other signaling pathways and molecular targets with links to apoptosis. The main focus of research are strategies targeting the extrinsic and/or the intrinsic pathways. These include the targeted activation of the extrinsic pathway through pro-apoptotic receptors agonists, inhibition of the Bcl-2 family of proteins and the interfaces of extrinsic and intrinsic pathways by caspase modulation and IAP inhibition.

1.3.2.1   The extrinsic and the intrinsic apoptotic pathway

The intrinsic apoptotic pathway is activated by cellular stress (Fig 3). Stress like chemotherapy or radiotherapy induces DNA damage and activates the p53 tumour-suppressor protein. p53 initiates the intrinsic pathway by upregulating Puma and Noxa, which in turn activate Bax and Bak [37, 38]. By contrast, the kinase Akt, which acts downstream of many growth factors, inhibits the intrinsic pathway by phosphorylating Bad [39]. Bax and Bak permeabilize the outer mitochondrial membrane, resulting in efflux of cytochrome c, which binds to the adaptor Apaf-1 to recruit the initiator procaspase 9 into a signalling complex termed the apoptosome. Activated caspase 9 then cleaves and activates the effector caspases 3, 6 and 7 to trigger apoptosis [40]. The mitochondrial protein Smac/DIABLO augments apoptosis by binding inhibitor of apoptosis proteins (IAP) and reversing their grip on several caspases [41].

The extrinsic apoptotic pathway: cytotoxic immune cells produce pro-apoptotic ligands such as Apo2L/TRAIL (Fig 3). The homotrimeric ligand binds to the pro-apoptotic receptors DR4 and/or DR5 on the surface of a target cell. Ligand binding induces receptor clustering and recruitment of the adaptor protein Fas-associated death domain (FADD) and the initiator caspases 8 and 10 as pro-caspases, forming a death-inducing signalling complex (DISC). This triggers activation of the apical caspases, driving their autocatalytic processing and release into the cytoplasm, where they activate the effector caspases 3, 6 and 7. DISC formation is modulated by several inhibitory mechanisms, including c-FLIP, which associates with the DISC by interacting with FADD to block initiator caspase activation and decoy receptors, which can block ligand binding or directly interfere with receptor activation.

Although the extrinsic and intrinsic pathways can function separately, they often interact. p53 mainly stimulates the intrinsic pathway, but it also upregulates some of the pro-apoptotic receptors such as DR5 and augments extrinsic signalling [42]. Extrinsic-pathway activation leads to caspase 8-mediated processing of Bid; truncated Bid subsequently stimulates Bax and Bak to engage the intrinsic pathway [43, 44]. The effector caspases can then feed back to promote further caspase 8 processing.
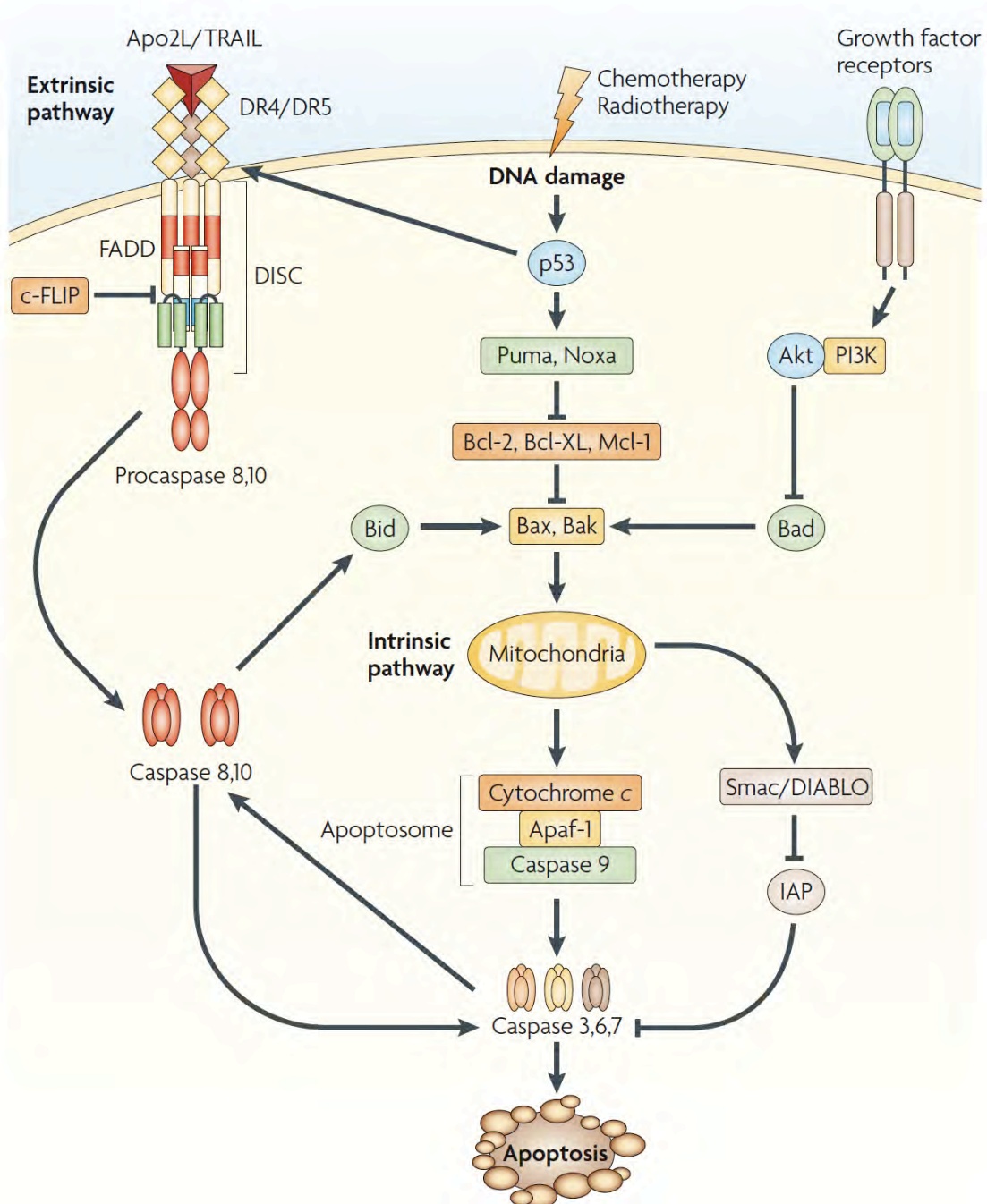
Fig 3 Key steps in the intrinsic and extrinsic apoptotic signaling pathways (adapted from Ashkenazi *et al.*, 2008 Nature Reviews [45])

1.3.2.2   TRAIL as an effector molecule in cancer therapy

Promoting apoptosis involves the signaling through members of the tumor necrosis factor (TNF) superfamily. The family members TNF and Fas ligand (FasL) can efficiently induce apoptosis in a variety of tumor cells. However, the administration of TNF and FasL is associated with extreme toxicity, precluding their development for cancer therapy. Native

TNF-related apoptosis-inducing ligand (TRAIL) shares certain similarity to the most related members FasL, TNF-α, Lt-α und Lt-β [46]. The TRAIL gene is located on chromosome 3 and spans approximately 20kb. It is composed of five exons and four introns. The TRAIL transcripts are detected in various human tissues, most predominantly in spleen, lung and prostate. TRAIL is a type II transmembrane protein and consists of 281 amino acids in the human and 291 amino acids in the murine forms, sharing 65% identity [46]. TRAIL has an N-terminal domain, which is not conserved across the family members, while the C-terminal domains show a most significant conservation. TRAIL is the only protein of the TNF family that contains cysteine residues, with the capacity to bind and interact with a zinc-ion, which allows the interaction of three molecules of TRAIL. After cleavage of the extracellular C-terminal portion of TRAIL from the cell surface, TRAIL can be released by the cells as a soluble molecule [47]. Both forms rapidly induce apoptosis in susceptible cells by the extrinsic apoptotic pathway via clustering with their cognate cell surface death receptors DR4/TRAIL-R1 and DR5/TRAIL-R2 [48, 49]. Three additional TRAIL receptors exist: DcR1/TRAILs-R3 and DcR2/TRAIL-R4 and osteoprotegerin (OPG), incapable of transmitting an apoptotic signal [49, 50]. The trimerization of the death receptor is reqired for the recruitment of an adaptor protein Fas-associated death domain (FADD) and the formation of the death-inducing signal complex (DISC) through recruiting the initiator caspases caspase 8 and 10 in the extrinsic apoptosis pathway [51]. TRAIL is expressed by a wide variety of human tissues, and is expressed on multiple cell types within the immune system such as B and T cells [47], mononuclear phagocytes [52], dendritic cells (DCs) [53], and natural killer cells (NK cells) [54] and plays a role in shaping and regulating the immune system. TRAIL is not expressed by freshly isolated human T cells, B cells, DCs and NK cells [47]. The regulation of TRAIL expression in the immune system is cytokine driven. Interferon alpha (IFN-α) and interferon gamma (IFN-γ) stimulate TRAIL expression in monocytes and dendritic cells [52, 53], IFN-α and IFN-β stimulate TRAIL expression in T lymphocytes and NK cells. Interleukins 2, 7 and 15 can also induce NK cell expression of TRAIL [55, 56].

TRAIL has several functions *in vivo*. TRAIL contributes to the host immunosurveillance against primary tumor development and metastasis (reviewed in [57, 58]). TRAIL has been shown to influence viral infections and to contribute to autoimmune diseases. TRAIL can boost the host responses to the tumor and change the tumor microenvironment for enhanced antigen presentation and tissue infiltration [59, 60]. Although the TRAIL receptors are expressed constitutively in a variety of normal tissues [61], TRAIL has the unique characteristic to induce apoptosis selectively in tumorigenic or transformed cells [48] without

toxicity to normal cells [51, 62]. All above mentioned makes TRAIL an ideal tool in anti-cancer therapy.

1.3.2.3 TRAIL delivery in cancer therapy

Based on the characteristic of TRAIL to induce apoptosis selectively in tumorigenic cells, many strategies have been developed for the delivery of TRAIL. Many recombinant preparations of TRAIL (recTRAIL) have been developed and tested *in vivo* [48, 63]. Another strategy to deliver TRAIL to tumor cells has been the transfer in normal cells as carriers or the direct transduction of the tumor cells with viral vector encoding for the TRAIL gene. In animal experiments, the treatment with recTRAIL substantially inhibited the growth of a variety of human tumors including breast and colon carcinomas [63], gliomas and multiple myeloma [64-66] and many other. RecTRAIL was also effective in patient samples [63]. However, frequently observed hepatocyte toxicity [67, 68], the required high dose of bioactive TRAIL and its short half life *in vivo* [63] have delayed the entrance into the clinics. Although improved recTRAILs are now in phase II clinical trials (reviewed in [69]), the pharmacokinetic and pharmacodynamic problems of a systemic delivery and the safety for the patient are still a major concern.

TRAIL is also used by gene therapy. TRAIL can be delivered by normal cells like mesenchymal stem cells (MSCs), which have tumor targeting properties, for the targeted delivery and local production of TRAIL in tumors [70-73]. Another way to use TRAIL in gene therapy is the transduction of the TRAIL coding sequence into the tumor cell directly. The vectors encoding TRAIL can be administered directly, locally or systemically. The most studied vector have been the adenoviral vectors [74-83] while also other vectors are tested for their suitability [84-87]. The delivery of TRAIL by lentiviral vectors for this application has rarely been described [88-90]. The intention of this strategy is to kill the tumor cells present at the injection site and to generate sufficient apoptotic tumor debris to stimulate a systemic, tumor-specific immune response. In this study transduced lymphocytes are used as carrier cells for the delivery of TRAIL to pancreatic and prostate cancer cells.

1.4 Immunotherapy

Immunotherapy is a promising approach for cancer therapy. Immunotherapy in general is the treatment of disease by inducing, enhancing or suppressing an immune response. Immunotherapies, designed to elicit or amplify an immune response, are classified as activating immunotherapies. Immunotherapies, designed to reduce, suppress or direct an

existing immune response, as in cases of autoimmunity or allergy, are classified as suppressing immunotherapies. A central problem in tumor immunology is that an established tumor creates an environment of immune tolerance that promotes tumor growth, protects the tumor from immune attack and attenuates the efficacy of immunotherapy. Several mechanisms have been described by which tumors can suppress the immune system. It includes secretion of cytokines, alterations in antigen-presenting cells, alterations in costimulatory and coinhibitory molecules and altered ratios of regulatory T cells to effector T cells. These barriers of tolerance have to be overcome in a successful cancer therapy. Addiotionally, tumors are a heterogenious mass of cells with numerous subpopulations undergoing changes during their proliferation. Also tumor cells can vary in the expression of their specific antigens. Since cancers differ in their immunological protection and their antigen expression, a immunotherapy against cancer is not universally applicable, but has to be adapted to the individual tumor. The observation by William Coley in the 1890s, that soft tissue sarcoma in patients having acute bacterial infections would regress, was one of the starting points for immunotherapies against cancer. One of the first indications that metastatic human cancers could be eliminated using immunological manipulations came from studies of the administration of autologous lymphokine-activated killer cells and IL-2 to patient with metastatic melanoma, colon cancer or renal-cell cancer [91]. At this time the question whether the immune system can recognize and eliminate tumor cells was highly controversial. This view has changed and the fact that the immune system is capable of targeting tumors is accepted. Cancer immunotherapy approaches concentrate on killing the tumor cells through effector cells of the immune system, which include B-cells, producing antibodies, $CD8^+$ CTL, $CD4^+$ helper T cells, NK cells and NK T cells. Cancer immunotherapies are either active i.e. immunization or passive i.e. adoptive transfer. These approaches target the innate immunesytem by inducing humoral immunity or/and the adaptive immune system by stimulating cellular immunity [92].

The cells of the innate immune system such as NK, γδ T cells or NKT cells have lytic effector functions. They can produce activating cytokines like IL-12 which mediate an innate immune response and can also initiate an adaptive immune response. Immunotherapy trageting the innate immune system also selectively activate these cells of the innate immunity by *in vitro* expansion and activation, by directly providing effector cytokines like TNF-α or IFN-γ, by stimulating a local tumor inflammation by the administration of adjuvants like bacterial products like LPS or by activating and increasing the number of circulating antigen presenting cells like DCs.

Immunotherapy stimulating cellular immunity attempts to circumvent the problem of poor immunogenicity of tumors by presenting tumor antigens through activated DCs. Therefore the stimulus and the antigens are provided to DCs, Tregs which also intervene with T cell responses in tumors are depleted, or effector cells such as T cells are transferred. This adoptive therapy transfers ex vivo selected and expanded tumor reactive T cells or T cells with engineered T cell receptors.

The activation of B cells is central in humoral immunotherapy. B cells produce antibodies that can bind to immunogenic cell surface protein and initiate complement-mediated lysis, bridge NK cells or macrophages to the tumor for antibody-dependent cell-mediated cytotoxicity (ADCC). Tumor-reactive B cell responses can also be enhanced by cancer vaccines or by antigen pulsed DCs. The passive transfer of antibodies has been successfully used in cancer therapy. Thus, engineered monoclonal antibodies (mAb) against cancer specific antigens are successfully used in the clinics. Examples of an application of antibody therapies in oncology are the introduction and approval of mAbs such as trastuzumab (Herceptin, anti-HER2/neu receptor), bevacizumab (Avastin, anti-vascular endothelial growth factor (VEGF) antibody), of cetuximab (Erbitux, an anti-epidermal growth factor (EGF) antibody), epratuzumab (Lymphocide, anti-CD22) and Rutixan (rituximab, anti-CD20). In combination with standard chemotherapy, these agents received a significant anti-tumor response in patients with breast cancer, metastatic cancers of the colorectum, breast and lungs and in chemotherapy-refractory cancers of the colon and rectum, or leukemia.

Additionally, several new classes of recombinant antibodies such as the bispecific antibodies are developed. The application of antibodies in cancer-therapy, include the direct and indirect interference with cancerous signaling pathways, angiogenesis, proliferation and the facilitated detection of malignant cells.

1.4.1   Bispecific antibodies in cancer therapy

Bispecific antibodies are artificial molecules (bsAb) carrying a different antigen-binding site on each arm (reviewed in [93, 94]). This dual specificity makes them trifunctional molecules. The hybridoma technique introduced by Kohler and Milstein in 1975 [95] allowed the formation of hybrid cell lines (called hybridomas) by fusing a specific antibody-producing B cell with a myeloma (B cell cancer) generating antibodies all of a single specificity (monoclonal antibodies). The fusion of two hybridomas yields hybrid-hybridomas or quadromas. These quadromas expressing two different heavy and two different light chains produce a variety of different antibody species resulting from the random pairing of the heavy

and the light chains. From this process, bispecific antibodies are generated, carrying a different specificity on each arm [96, 97]. Besides the quadroma technique, other methods have been developed to generate different formats of bsAbs (Fig 4). Recombinant bsAb formats include the development of chemically linked bsAb [98], BiTE [99], bispecific single chain ScFv antibodies [100] and diabodies [101]. The antibodies additionally can be chimerized or fully humanized [93]. The dual specificity enable bsAbs completely different target strategies such as a) the simultaneous inhibition of two signaling pathways either by blocking two receptors or two ligands or a combination of both, b) increased specificity by the ability to bind two different antigens simultaneously and c) a retargeting of cells (one binding specificity is directed against a target cell, whereas the other binding site is used to recruit a toxic activity or moiety).
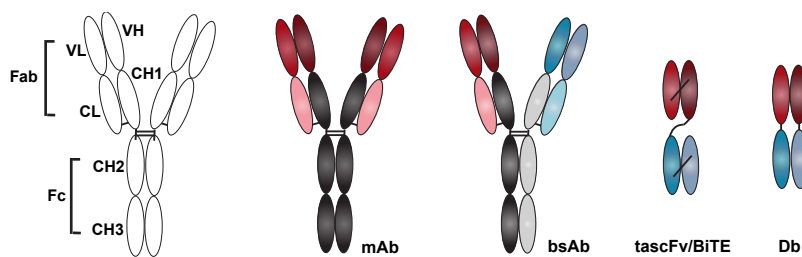
Fig 4 Schematic representation of therapeutic antibodies

The application of bsAbs in cancer therapy takes advantage of the feature that one arm of the antibody can bind to a tumor-associated antigen on cancer cells and the other to abundant molecules i.e. on immune cells. This feature brings tumor and immune cells in a close contact, triggers immune cell activation and can redirect immune cells to kill tumor cells [102-104].

1.4.2 Tumor antigen targets in immunotherapy

The discrimination of a tumor cell from a healthy cell is essential for a therapeutic targeting of cancer. The targeting of cancers by antibodies requires the expression of tumor antigens that are exclusively expressed or over-expressed on the tumor. A tumor can be discriminated by tumor-specific antigens or tumor-associated antigens. These tumor antigens comprise several categories. There are the oncogenic viral antigens for example from EBV in Burkitt's lymphoma, HBV and HCV in hepatoma, HPV in cervical and perineal carcinoma. Additionally, there are certain fusion genes like BCR/ABL in CML, antigens with a limited normal expression in the testes and placenta in healthy tissue like MAGE and antigens that

are expressed in development but not in adult tissue for example CEA and αFP. In addition, there is a number of molecules, which are expressed on many normal cell types but whose phenotype is altered in malignant cells. This includes the molecules ras, p53, hTERT, NY-ESO-1, altered self-epitopes like gangliosides, mucins or EpCAM.

1.4.2.1 EpCAM as target molecule in immunotherapy

The epithelial cell adhesion molecule (EpCAM) is one of the promising tumor associated antigens. EpCAM was initially described as a tumor associated antigen by Koprowski and colleagues in 1979 [105]. EpCAM expression is highly upregulated by several carcinoma cells [106], making it a favorable target for tumor therapy. Furthermore, EpCAM is considered a potential prognostic tumor marker [106-108] and the over-expression correlates with decreased in survival as in breast or in ovarian cancers. An exception is renal cell carcinoma, where the opposite is the case. Cancers with upregulated EpCAm expression are i.e. lung, colorectal, prostate and pancreatic carcinoma.

EpCAM is a type I membrane protein of 314aa. EpCAM is a non-typical member of the CAM family, with an extracellular signaling sequence, followed by an epidermal growth factor-like repeat, a human thyroglobulin repeat and a cystein-poor domain. EpCAM has one single-spanning transmembrane domain and an intracellular domain containing an NPXY internalization motif and several actin-binding sites. In contrast to the broad expression pattern of most other CAMs in normal tissues, the expression of EpCAM is restricted to normal epithelial cells. EpCAM is mainly expressed in adult tissues and restricted to cells of epithelial origin but it is also found during certain stages of early embryonic development and during differentiation and morphogenesis. In adult tissues, EpCAM is virtually expressed in all simple epithelia without any major change. EpCAM is known to mediate cell-cell adhesion but has several more roles. It is involved in cellular processes such as signaling in cell migration, proliferation and differentiation. Binding partners include actin and the cytoskeleton, mediating adhesion to the epithelial microenvironment, but also CD44v4-V7, tetraspanins and Claudin-7, which influence not only cell-cell adhesion, cell-matrix adhesion, but also apoptosis resistance, carcinogenesis promotion and metastasis (reviewed in [109]). On the other hand, EpCAM is typically over-expressed in a variety of epithelial cancers and derived metastasis, including prostate cancer and pancreatic adenocarcinoma. Nevertheless, EpCAM distribution and their location varies in these carcinomas. Upon tissue inflammation EpCAM is upregulated. Although little is known about the molecular mechanism of EpCAM

regulation, it has been observed that TNF-α can down-regulate EpCAM and that this coincides with NF-κB activation.

Several different antibody constructs have been generated against EpCAM expressed by tumor cells [110-117] with promising results in phase I/II clinical trials [118, 119]. Adecatumumab (MT201 Micromet), a fully human anti-EpCAM antibody [120], is currently in three ongoing clinical trials: two phase II studies with metastatic breast cancer and early stage prostate cancer and a phase I study testing the safety of the combination of Abs with taxotere. Pre-clinical studies have shown that MT201 mainly acts through antibody-dependent cellular (ADCC) and complement-dependent cytotoxicity (CDC) [121]. EpCAM-directed bsAb immunotherapies are already very advanced into the clinics. MT110, a single-chain EpCAMxCD3 bispecific antibody construct of the BiTE class [122], led to the successful eradication of established tumors from human cancer cell lines mixed with human T cells and in ovarian cancer tissue of patients. Catumaxomab (Removab, Trion Pharma/Fresenius), a hybrid mouse/rat antibody trispecific for EpCAM, CD3 and - via its Fc portion – for antigen-presenting as well as for a variety of other cytotoxic immune cells, has been shown to efficiently reduce ovarian cancer patients suffering from ascites and in gastric cancer patients in phase II clinical studies. However, a relatively short half-time, overt productions of cytokines, Fc-mediated side effects and bsAb immunogenicity limit the clinical application [94].

1.4.3 Engaging effector cells by bispecific antibodies

There is a choice of immunological effector cells for the engagement by bsAbs. BsAb have been designed for many immunological effector cells i.e. macrophages, NK cells, neutrophils, B and T cells. One of the most potent effector cells of the immune systems are T cells. Engaging T cells by bispecific antibodies is advantageous due to their high cytotoxic potential. They are present in the body in abundance, have intrinsic search and destroy functions, and there is evidence for their potential to initially control malignant diseases. There are numerous reports on tumor rejection by T cells in animal models, and the presence of T cells inside tumors can significantly correlate with overall survival, as recently reported for patients with colon cancer and NHL [123, 124]. The invariant CD3 signaling complex on lymphocytes is the most common T cell antigen for bsAbs. Targeting T cell by bispecific antibodies to tumor cells has several advantages. This therapeutic strategy does not rely on the laborious generation of tumor specific T cell clones and does not require a regular antigen presentation by dendritic cells. Furthermore, it has been shown, that T cells can be engaged by

a bispecific antibody to recognize a frequent surface antigen on the tumor cell, and that the expression of MHC class I, usually required for antigen recognition, is not required ([125]). Moreover, not only cytotoxic CD8$^+$ T cells can be targeted and redirected for lysis, but also CD4$^+$ T cells.

1.4.4   Bispecific antibody EpCAMxCD3

The bispecific antibody EpCAMxCD3 is used in this work. It has a dual specificity for the binding of EpCAM and CD3. Both EpCAM and CD3 molecules are attractive targets for the generation of bsAb and bispecific single-chain antibody constructs for anti-cancer treatment [115, 122, 126, 127]. EpCAMxCD3 has been generated by the hybrid-hybridoma techique from the parental hybridoma anti human EpCAM (HEA125, IgG$_1$) and anti human CD3 (OKT3, IgG$_{2A}$). Hence, EpCAMxCD3 is composed of mouse IgG$_1$ and IgG$_{2A}$ constant heavy chain regions. This antibody has been shown to reduce the ascites formation in ovarian cancer patients [117, 128].

1.5   Combination therapy for pancreatic and prostate cancer

Both gene therapy and immunotherapy strategies have been tested for cancer therapy. However, in most studies only on approach is applied. The aim of this project was to test whether a combination of immunotherapy with EpCAMxCD3 and gene therapy with TRAIL-over-expressing lymphocytes would be effective in pancreatic and prostate carcinoma. This is the first time, such an combined approach is tested (Fig 5).
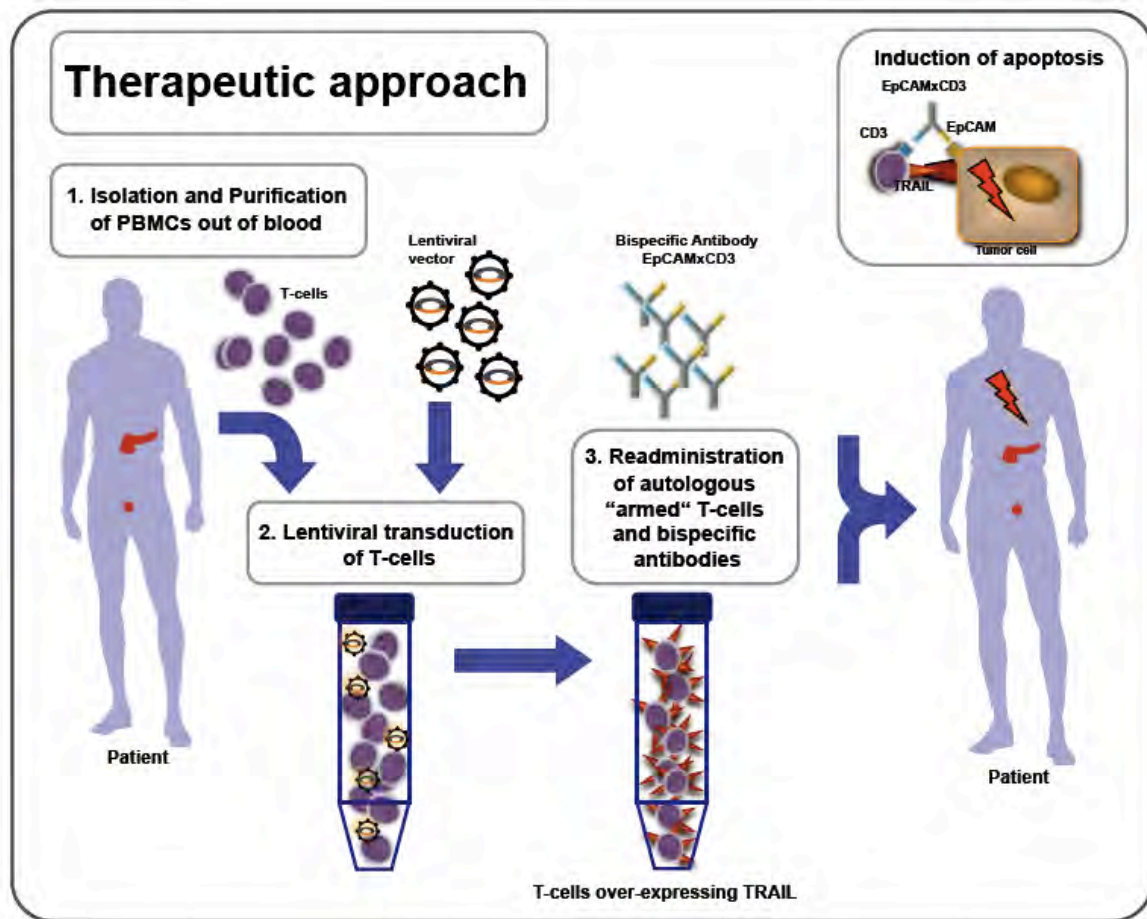
Fig 5 Scheme of the therapeutic approach

1.5.1 A novel therapy for pancreatic and prostate carcinoma combining TRAIL-over-expressing lymphocytes and bispecific antibody EpCAMxCD3

This work investigated the efficacy of a potential novel therapeutic approach This approach combines gene therapy with immunotherapy. The gene therapy part aims to use patient-derived lymphocytes, which are genetically manipulated to over-express TRAIL as an apoptosis-inducing ligand. In the immunotherapy part these manipulated lymphocytes are "armed" with EpCAMxCD3. Therefore, the induction of apoptosis would occur when manipulated T cells will be brought to a close contact with tumor cells by bispecific antibody (Fig 6). BsAb EpCAMxCD3 has a dual specificity for EpCAM, over-expressed by pancreatic and prostate tumor cells, and for the invariant CD3 signaling complex on lymphocytes. When these bsAb monovalently bind to the antigens they will bring the tumor cells and the T cells into a close contact and also active T cells to release cytotoxic molecules and thus to kill tumor cells. The gene therapy part allows the introduction of the effector protein TRAIL into lymphocytes. TRAIL is over-expressed on lymphocytes and has the ability to selectively

induce apoptosis in tumor cells. EpCAMxCD3 consequently can deliver these TRAIL-over-expressing lymphocytes to EpCAM over-expressing tumor cells. The monovalent binding of CD3 on lymphocytes and the close contact to the bsAb-linked tumor cells, induces a polyclonal T cell activation. This polyclonal activation consequently can mount all differentiated T cells of the CD8 as well as CD4 phenotype, without the need for an MHC class I dependent receptor recognition of antigen. Hence there is no requirement for tumor specific T cells. This close contact to the tumor cell enables a cytotoxic lysis by CD8$^+$ T cells, a stimulation of CD4$^+$ helper T cells or creates room for additional genetically introduced T cell functions such as TRAIL.

In a clinical setting, it could be possible to use patient's lymphocytes. These would be isolated from the patient's blood and transduced to over-express TRAIL ex vivo. These autologous "armed" lymphocytes would be re-administered back into the patient together with the bispecific antibodies. In the patient, the bsAb would recruit the TRAIL-over-expressing lymphocytes to the EpCAM-expressing tumor cells and eventually eradicate the tumor (Fig 5). In this work, this approach is tested with lymphocytes from healthy blood donors *in vitro* and *in vivo* in animal models for prostate and pancreatic carcinomas.
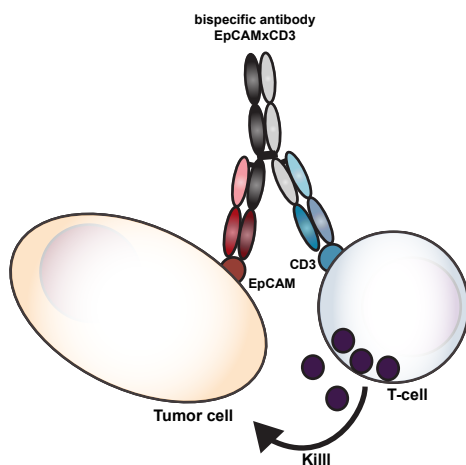
Fig 6 Scheme depicting the interaction of an EpCAM over-expressing tumor cells and a lymphocyte bridged by the bispecific antibody EpCAmxCD3

1.6 Aim of the study

The aim of this project was to test the efficacy of a novel therapeutic approach for cancer therapy. This approach combines immunotherapy with bsAb EpCAMxCD3 and gene therapy with TRAIL. The potential efficacy of this approach was tested in experimental models of pancreatic and prostate carcinoma.

Specific aims were i) to construct a lentiviral vector suitable for the transduction of human lymphocytes and the over-expression of TRAIL. The next aim was ii) to establish and to evaluate suitable xenograft models for the study of the chosen approach, iii) to test the efficacy and the anti-tumor potential of TRAIL-over-expressing lymphocytes and bsAb EpCAMxCD3 *in vivo* and iv) to elucidate the functional mechanisms underlying observed anti-tumor effects of TRAIL-over-expressing lymphocytes and bsAb EpCAMxCD3 *in vivo* and *in vitro*.

2   Results

2.1   Validation of tumor cell lines for *in vitro* and *in vivo* xenograft models

Finding a suitable model is essential for the analysis of potential anti-tumor effects of bsAb EpCAMxCD3 treatment together with TRAIL-over-expressing lymphocytes, which will be called TRAIL-L in the following. Several tumor cell lines were tested for their suitability in *in vivo* and *in vitro* models. The following parameters were analysed: the expression of EpCAM, growth kinetics of cell lines *in vivo* and the expression of TRAIL-receptors in tumor cells.

2.1.1   Expression of EpCAM in pancreatic and prostate tumor cell lines

The pancreatic tumor cell lines MIA-PaCa2, Colo357, AsPC-1 and BxPc-3 and the prostate tumor cell lines PC-3, LNCap and DU145 were analysed for the expression of EpCAM. All cell lines expressed EpCAM to approximately 100% on their cell surface, making them suitable candidates for an EpCAM-targeted treatment with EpCAMxCD3 bispecific antibody (data not shown).

2.1.2   Transplantation efficiency and growth kinetics of tumor cell lines

The tumor cell lines were tested for the transplantation efficiency and the growth kinetics of the tumor xenografts *in vivo*. BxPc-3, Mia-PaCa, PC-3 and LNCap were tested and a cell number of $1x10^6$, $2.5x10^6$ and $5x10^6$ tumor cells were transplanted into NOD/SCID mice. The most optimal transplantation volume was $5x10^6$. For DU145, Colo357 and AsPC-1 experimental experience existed from collaborating groups. Based on these results (data not shown), the BxPc-3 and PC-3 tumor cell lines were chosen. Detectable tumors develop after one to two weeks and reach a maximal tolerable volume of 2 cm^3 after three to four weeks. This time frame was most optimal for our study. Both cells lines have moderate growth kinetics, which would allow us to study the therapy approach in a two to three week time frame.

2.1.3   Expression of TRAIL-receptors in BxPc-3 and PC-3 cell lines

For the induction of apoptosis by TRAIL in the target cells, BxPc-3 and PC-3 were analysed for the expression of TRAIL-R1 and TRAIL-R2. In PC-3 22.1% of the cells were positive for TRAIL-R1 and 29.4% expressed TRAIL-R2. In BxPc-3 60.2% of the cells expressed TRAIL-R1 and 18.8% expressed TRAIL-R2 (Fig 7). Based on EpCAM and TRAIL-R1 and –R2

expression and *in vivo* growth kinetics, the BxPc-3 and the PC-3 cell line, were chosen as the most optimal candidates for the model system.
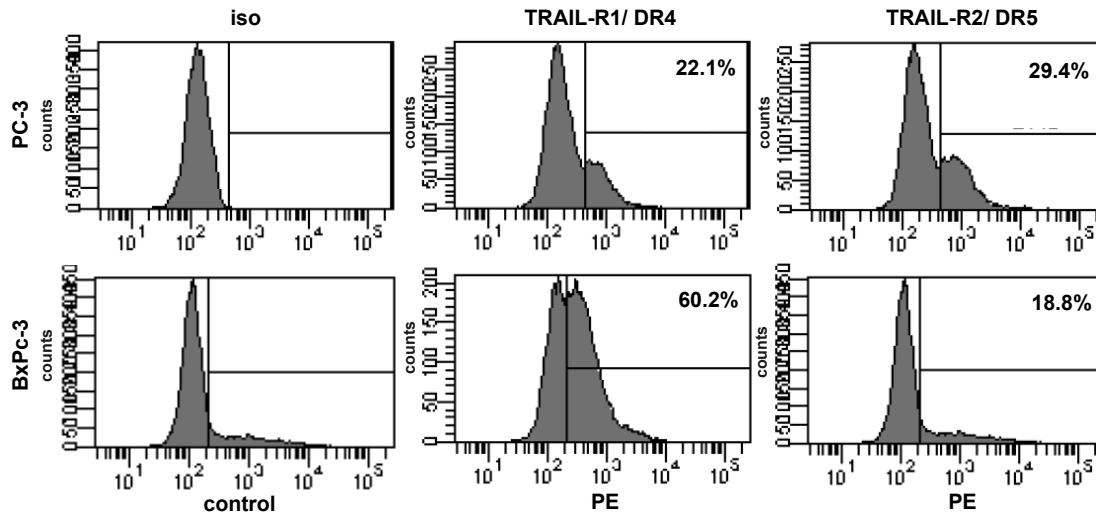
Fig 7 Expression of TRAIL-receptors on tumor cell lines *in vitro*

To verify the expression of TRAIL- receptors *in vitro*, pancreatic BxPc-3 and prostate PC-3 tumor cells were analysed for TRAIL-R1 and TRAIL-R2 by flow cytometry.

2.2 Over-expression of TRAIL in lymphocytes

2.2.1 Construction of an inducible lentiviral vector for the over-expression of TRAIL and EGFP in human lymphocytes

The lentiviral vector system based on HIV-1 was chosen for the transduction of lymphocytes. The original vector [129] was modified to over-express TRAIL. The following modifications were introduced: the human TRAIL gene, the marker gene EGFP linked by the picorna virus-derived peptide element P2A (2A element of porcine teschovirus) and the transactivator rtTA2-M2 were cloned into the original expression vector pd500Trip-CMVmin-WPRE. Binding of the rtTA2-M2 transactivator to the TRE upstream of the promoter activates transcription. The peptide linker allows an equivalent expression of both genes due to a "ribosomal skip" (described by Leisegang *et al.* [130]) compared to IRES elements. The final composition of the lentiviral vector pV3TP2AE is shown in (Fig 8). The final vector pV3TP2AE was verified for its identity and the correct configuration by sequencing. The pV3TP2AE vector consequently allows an inducible gene expression of TRAIL as well as an easy detection of transduced cells by EGFP.

Fig 8 Scheme of the lentiviral vector pV3TP2AE

The lentiviral vector pV3TP2AE (A) was created for the expression of human TRAIL and EGFP linked by a P2A element driven by a CMVmin promoter. The tet-on vector contains self-inactivating long terminal repeats from HIV-1 (LTR, SIN), the transactivator rtTA2-M2, a tet-responsive element (TRE) and the woodchuck hepatitis virus post-transcriptional regulatory element (WPRE).

2.2.2 Lentiviral transduction and TRAIL over-expression in human lymphocytes

Lentiviral particles were produced by co-transfection of the 293T producer cells with three plasmids: the vector pV3TP2AE, and the helper plasmids pMD2 and psPAX, encoding the essential viral proteins. The virus titer was quantified by FACS analysis of transduced 293T cells (confer M&M). The production titers ranged between $1x10^6$ and $1x10^8$, which was high enough to use unconcentrated supernatant in all experiments.

Peripheral blood mononuclear cells (PBMCs) were isolated from fresh heparinized blood of healthy donors via standard Ficoll gradient separation. To improve the efficiency of transduction, PBMCs were activated by IL-2 and anti-CD3 mAb (OKT3). The activation status was analysed five days later by FACS. The early activation marker CD69 and the late activation markers CD25 and CD95 were expressed (Fig 9 C).

The vector pV3TP2AE efficiently transduced lymphocytes compared to other vectors (data not shown). The transduction procedure was optimized for lymphocytes and the following method generated the best results. A multiplicity of infection (MOI) between 10-25 was applied, since higher MOI did not result in increased transduction efficiency (data not shown). Transduction was done on RetroNectin® coated dishes. RetroNectin®, a recombinant fibronectin, supports transduction by supplying a binding matrix for lymphocytes and virus particles in close proximity. The virus was centrifuged onto the dishes prior to addition of the cells, with repetition of the procedure on the consecutive day. This optimized protocol achieved an average transduction efficiency of 35-50% in lymphocytes. TRAIL was efficiently over-expressed in pV3TP2AE-transduced lymphocytes (TRAIL-L) compared to mock-transduced lymphocytes (MOCK-L). The transduction efficiency was 56.7% TRAIL expression compared to 59.8% EGFP fluorescence detected by flow cytometry (a representative experiment is shown in Fig 9 A).

2.2.3 Effect of lentiviral transduction of lymphocytes on their functions

The manipulation of the PBMCs by isolation, handling in cell culture and the transduction procedure could potentially affect the functions of lymphocytes. Therefore TRAIL-L, MOCK-L and lymphocytes (L), which had been in cell culture for the same period of time,

were subjected to an allogenic mixed lymphocyte reaction. Therefore, TRAIL-L, MOCK-L and L as effector cells were incubated with freshly isolated, irradiated PBMCs from an unrelated donor and used as stimulant cells to analyse proliferation upon allogenic recognition. TRAIL-L and MOCK-L exhibited a robust proliferation upon incubation with stimulant cells (Fig 9 B).

2.2.4 Effect of lentiviral transduction on CD4-CD8 T cell ratio

Among transduced lymphocytes, 18.8% of all cells (44.3% of transduced cells) were CD4- and 28.4% of all cells (67% of transduced cells) CD8-positive T cells lymphocytes (Fig 9 D), indicating proliferative selection for cytotoxic T cells by the viral transduction.
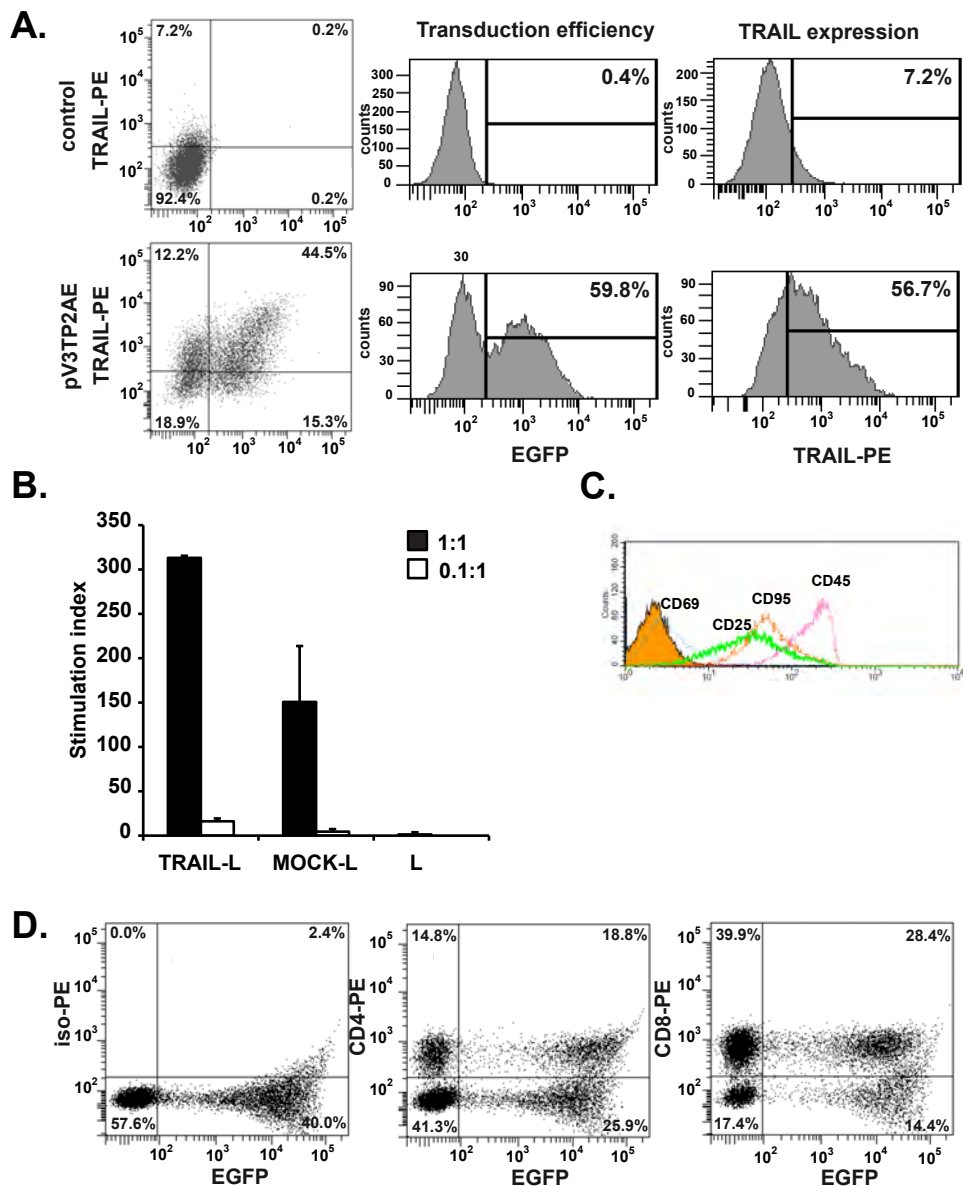
Fig 9 Efficiency of lentiviral transduction, functions and TRAIL over-expression in lymphocytes

(A) Activated lymphocytes were transduced with pV3TP2AE at MOI 10 as described in M&M: TRAIL over-expression and EGFP fluorescence related to transduction efficiency, were analyzed by FACS. Mock transduced lymphocytes served as a negative control. (B) Analysis of the proliferative functionality of TRAIL (TRAIL-L) and MOCK-transduced (MOCK-L) versus non-manipulated lymphocytes (L). The effector cells were stimulated by allogenic irradiated PBMCS (stimulant cells) in an allogenic mixed lymphocyte reaction. Proliferation was analysed by ^{3}H-thymidine incorporation. (C) Activation status was verified on day 5 after activation with OKT-3 and IL-2 by FACS. (D) The T cell subpopulations of pV3TP2AE transduced lymphocytes were analysed by FACS. Mock-tranduced lymphocytes served as control (MOCK).

2.2.5 Effect of lentiviral transduction on migratory properties of lymphocytes

The effects of transduction on lymphocyte locomotion, lymphocyte migration velocity and the percentage of migrating lymphocytes were determined in 3D collagen gels by time-lapse video microscopy. Lentiviral transduction did not influence lymphocyte velocity compared to non-transduced lymphocytes (data not shown).

2.2.6 Effect of lentiviral transduction on cytotoxic properties of lymphocytes

In a cytotoxicity assay, the abilities of TRAIL-L to target carcinoma cells was analysed. Apoptosis induced by TRAIL-L in carcinoma cells was compared to cell death upon co-incubation with MOCK-L. TRAIL-L were directly incubated with BxPc-3 cells in the ratios of: 1: 0.1, 1:1, 10:1 and 25:1. Apoptosis and cell death were analysed by staining of cells with annexinV-PE and propidiumiodide (PI) followed by flow cytometry (Fig 10). Within 4 hours of incubation, TRAIL-L and MOCK-L induced up to 25% cell death associated with DNA fragmentation. The addition of EpCAMxCD3 resulted in an up to 3-fold increase of PI$^+$ cancer cells for TRAIL-L and MOCK-L. AnnexinV levels were low in all groups (3 - 5%, data not shown) suggesting low exposure of phosphatidylserine by BxPc-3. TRAIL-L most efficiently induced apoptosis in combination with EpCAMxCD3, as seen by PI$^+$ cell death. The best results could be seen in a 1:10 target to effector cell ratio. Similar results were obtained for PC-3 cells (data not shown).

Taken together, TRAIL-L and MOCK-L efficiently lysed tumor cells *in vitro*. EpCAMxCD3 efficiently increased the induction of cancer cell death by TRAIL- and MOCK-L up to 3 fold.

Legend:
▲ BxPc-3 + MOCK-L
△ BxPc-3 + MOCK-L + EpCAMxCD3
■ BxPc-3 + TRAIL-L
□ BxPc-3 + TRAIL-L + EpCAMxCD3
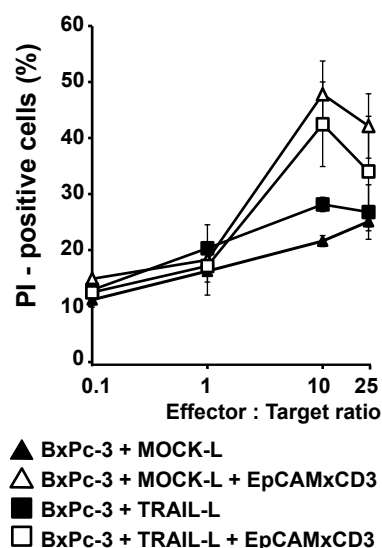
Fig 10 Effect of TRAIL-L and bsAb EpCAMxCD3 on cytotoxic lysis of BxPc-3 tumor cells *in vitro*

To test the cytotoxic efficacy of TRAIL-L on tumor cells, BxPc-3 cells were incubated with TRAIL- or MOCK-transduced lymphocytes in combination with EpCAMxCD3 at a dose of 10μg/ml for 4 hours as described in M&M. Cell death was analysed by PI incorporation into dead/dying cells. Data is shown as mean with standard deviation of individual experiments from different blood donors.

Summarized, lymphocytes could be successfully transduced to over-express TRAIL and EGFP by the lentiviral vector pV3TP2AE. Due to the comparable expression level of TRAIL and EGFP *in vitro*, the expression of EGFP can serve as a marker for transduction efficiency. Lentiviral transduction did not affect the lymphocyte activation status (CD25 or CD69 expression), proliferation (allogenic reaction), cytotoxic properties, migration in collagen gels and cytotoxic properties *in vitro*.

2.3 Pharmacokinetics of bispecific antibody EpCAMxCD3 *in vivo*

The pharmacokinetic properties of EpCAMxCD3 were analysed *in vivo*. Therefore, NOD/SCID mice were injected intraperitoneally (*i.p.*) with EpCAMxCD3 at a dose of 500 μg per mouse, followed by subsequent blood sampling at days 1, 2, 4, 7 and 14. The bsAb level in the blood was measured using an ELISA kit for human IgG. The EpCAMxCD3 serum concentration reached its maximum at day one after *i.p.* administration. The serum half-life ($T_{1/2}$) of EpCAMxCD3 was approximately seven days (Fig 11 A).

2.4 Efficiency of TRAIL-L and bsAb EpCAMxCD3 *in vivo* and *in vitro*

To investigate the effects of the TRAIL-L and the bispecific antibody EpCAMxCD3 different *in vivo* models were used as described in the following paragraphs.

In the first model (I) the suitability of co-transplantation of tumor cells together with lymphocytes was analysed.

In vivo model	Xenograft	Description
I.	BxPc-3	Transplantation of BxPc-3 *s.c.*
	PC-3	Transplantation of Pc-3 *s.c.*
	BxPc-3 + L	Transplantation of BxPc-3 mixed with pre-activated lymphocytes *s.c.*
	PC-3 + L	Transplantation of PC-3 mixed with pre-activated lymphocytes *s.c.*

In the second model (II) tumor cells were co-transplanted with pre-activated lymphocytes and the therapeutic effects of EpCAMxCD3 on xenograft tumor growth were analysed.

In vivo model	Xenograft	Description	Begin of treatment	Treatment
II.	BxPc-3 + L	Transplantation of BxPc-3 mixed with pre-activated lymphocytes *s.c.*	day 3 post cell transplantation	bispecific antibody EpCAMxCD3 - 10 mg/kg i.p. bispecific antibody EpCAMxCD3 - 1 mg/kg i.p. bispecific antibody EpCAMxCD3 - 0.1 mg/kg i.p. parental monoclonal antibody anti EpCAM and anti-CD3 1 mg/kg i.p. PBS i.p.
	PC-3 + L	Transplantation of PC-3 mixed with pre-activated lymphocytes *s.c.*	day 3 post cell transplantation	bispecific antibody EpCAMxCD3 - 10 mg/kg i.p. bispecific antibody EpCAMxCD3 - 1 mg/kg i.p. bispecific antibody EpCAMxCD3 - 0.1 mg/kg i.p. parental monoclonal antibody anti EpCAM and anti-CD3 1 mg/kg i.p. PBS i.p.

In the third model (III) tumor cells were co-transplanted with TRAIL-L to investigate whether TRAIL-L enhanced the therapeutic effects of EpCAMxCD3 treatment on xenograft tumor growth.

In vivo model	Xenograft	Description	Begin of treatment	Treatment
III.	BxPc-3 + TRAIL-L	Transplantation of BxPc-3 mixed with TRAIL-over-expressing lymphocytes *s.c.*	day 3 post cell transplantation	bispecific antibody EpCAMxCD3 - 1 mg/kg i.p. bispecific antibody EpCAMxCD3 - 0.1 mg/k gi.p. bispecific antibody EpCAMxCD3 - 0.01 mg/kg i.p. parental monoclonal antibody anti EpCAM and anti-CD3 - 1 mg/kg i.p. irrelevant bispecific antibody CD19xCD3 - 1mg/kg i.p. PBS i.p.
	PC-3 + TRAIL-L	Transplantation of PC-3 mixed with TRAIL-over-expressing lymphocytes *s.c.*	day 3 post cell transplantation	bispecific antibody EpCAMxCD3 - 1 mg/kg i.p. bispecific antibody EpCAMxCD3 - 0.1 mg/k gi.p. bispecific antibody EpCAMxCD3 - 0.01 mg/kg i.p. parental monoclonal antibody anti EpCAM and anti-CD3 - 1 mg/kg i.p. irrelevant bispecific antibody CD19xCD3 - 1mg/kg i.p. PBS i.p.

In the fourth model (IV) the combined effects of EpCAMxCD3 treatment in combination with TRAIL-L were analysed in developed xenograft tumors.

In vivo model	Xenograft	Description	Begin of treatment	Treatment
IV.	BxPc-3	Transplantation of BxPc-3 *s.c.*	day 12 post cell transplantation	bispecific antibody EpCAMxCD3 - 0.1 mg/kg i.p. + TRAIL-L s.c. bispecific antibody EpCAMxCD3 - 0.01 mg/kg i.p. + TRAIL-L s.c. TRAIL-L s.c. bispecific antibody EpCAMxCD3 - 0.1 mg/kg i.p. PBS i.p.

2.4.1 Establishment of pancreatic and prostate xenograft models with co-transplanted lymphocytes for the treatment with bsAb EpCAMxCD3

2.4.1.1 BxPc-3 + L and PC-3 + L xenograft morphology and growth kinetics

The possibility to subcutaneously (*s.c.*) co-transplant human pre-activated lymphocytes together with human pancreatic BxPc-3 *in vivo* was tested in model I.).

NOD/SCID mice were either injected *s.c.* with BxPc-3 tumor cells and were compared to mice injected with BxPc-3 tumor cells mixed in a 1:1 ratio with extra-corporally IL-2 and OKT3 pre-activated lymphocytes (BxPc-3 + L) (Fig 11 I.). The same model was used for PC-3 xenografts. Tumor engraftment (tumor take), tumor growth kinetics and tumor morphology were analysed at day 25 after cell implantation. Essentially, there was no difference in tumor incidence and tumor growth kinetics between BxPc-3 + L and BxPc-3 (data not shown). All animals developed tumors and tumor growth was independent of co-administration of pre-activated lymphocytes. Pre-activated lymphocytes did not influence BxPc-3 tumor stroma formation as seen by collagen distribution patterns and blood vessel morphology and density (Fig 11 C). Comparable results were obtained for PC-3 + L xenografts compared to PC-3 (data not shown).

2.4.1.2 Expression of EpCAM and TRAIL-receptors in BxPc-3 + L and PC-3 + L xenografts

The expression of EpCAM, which is the target antigen for bsAb, and TRAIL-receptors was analysed *in vivo* by flow cytometry. EpCAM was expressed by all tumor cells in BxPc-3 + L and PC-3 + L xenografts (Fig 11 C, data not shown). The majority of the cells in the tissue also expressed TRAIL-R1 and TRAIL-R2 (Fig 11 D).

2.4.1.3 Survival of co-injected lymphocytes in the xenograft tissue

Transplanted lymphocytes were detected by immunohistochemistry in BxPc-3 + L tumors 24 days after cell implantation (CD45$^+$) (Fig 11 B), suggesting that human lymphocytes survive for a long time in BxPc-3 xenografts in the mouse. Of these CD45$^+$ cells, almost all cells were CD4$^+$ and CD8$^+$ lymphocytes with only single CD16$^+$ NK cells (data not shown).

Taken together, the xenograft model of human tumor cells co-injected with lymphocytes showed a robust tumor engraftment and development. The lymphocytes survived for up to 24 days in the tumor tissue and their presence did not influence the tumor morphology and growth kinetics of the BxPc-3 and PC-3 xenografts *in vivo*. EpCAMxCD3 had a

pharmacologically long serum half life of approximately 7 days. Therefore, these models of BxPc-3 + L and PC-3 + L mixed xenografts were considered suitable for the *in vivo* analysis of the anti-tumor efficiency of bsAb EpCAMxCD3 treatment.
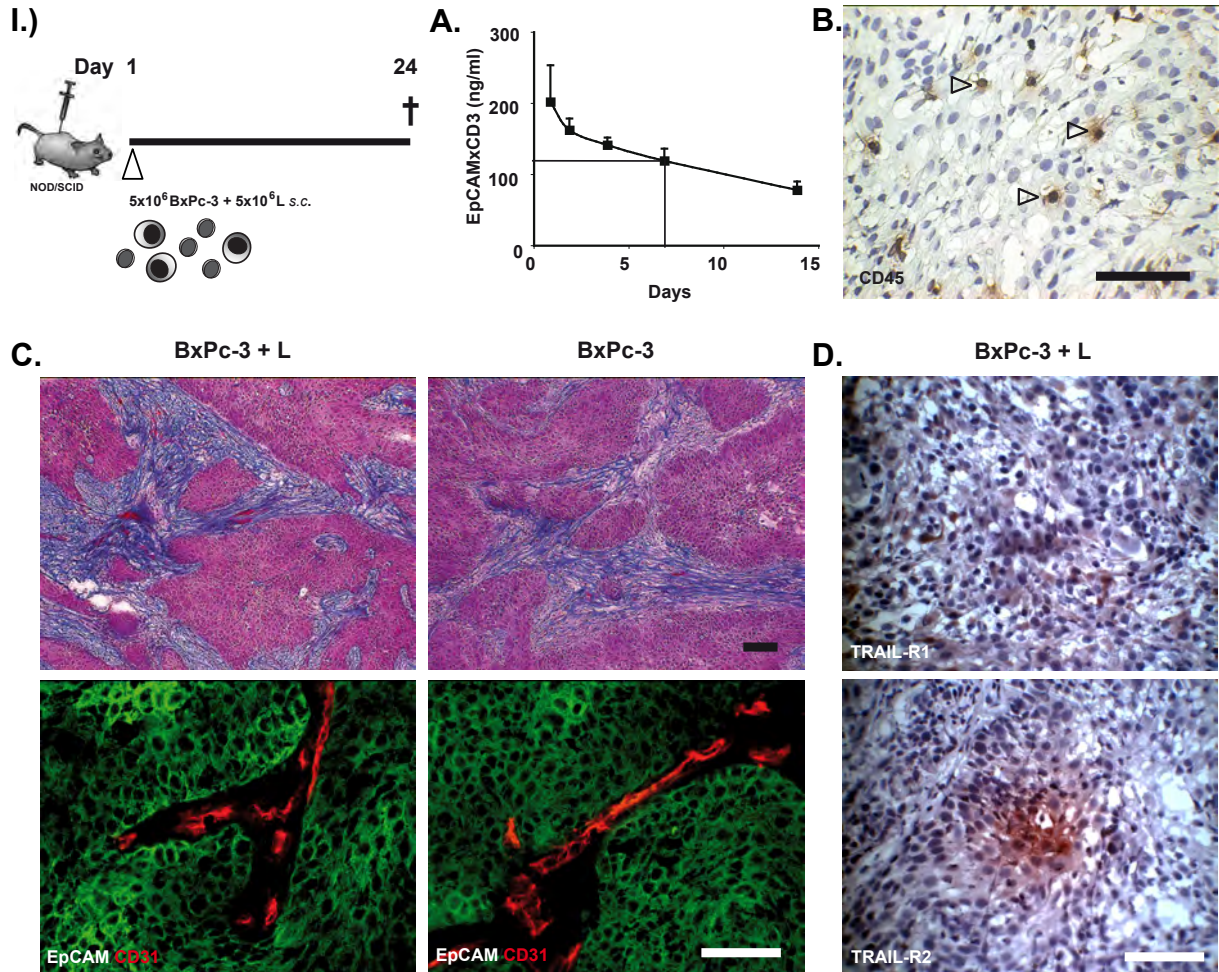
Fig 11 BsAb EpCAMxCD3 pharmacokinetics and validation of BxPc-3 + L pancreatic xenograft model

I.) Scheme of *in vivo* experiment. (A) NOD/SCID mice were *s.c.* transplanted with BxPc-3 pancreatic tumor cells ($5x10^6$) mixed with extra-corporally pre-activated human lymphocytes (L) ($5x10^6$) as described in M&M. NOD/SCID mice (n=5) received one *i.p.* injection of EpCAMxCD3 at a dose of 500 μg and peripheral blood was taken 1, 2, 4, 7, 14 days after the bsAb administration. BsAb EpCAMxCD3 concentration in the serum was determined by ELISA. (B) CD45^{+} cells were detected in tumor tissues by immunohistochemistry 24 days after the tumor cell/ lymphocyte implantation. 400x magnification. (C) Trichrome staining of tumor tissues was used to evaluate collagen distribution (blue) and stroma formation. Nuclei are colored in red. 100x magnification. Double immunofluorescence technique was used to detect EpCAM expression on tumor cells (green) and CD31^{+} blood vessels (red). (D) Immunohistochemistry was used to detect the expression of TRAIL-R1 and TRAIL-R2 in BxPc-3 + L tumors. 400x magnification. Bar = 100 μm.

2.4.2 EpCAMxCD3 treatment in BxPc-3 + L and PC-3 + L xenografts

2.4.2.1 Tumor engraftment and growth retardation of BxPc-3 + L and PC-3 + L xenografts by EpCAMxCD3

In the next model, BxPc-3 + L and PC-3 + L xenografts were injected with EpCAMxCD3 in treatment experiments. The anti-tumor efficacy of the bsAb and the ability of the bsAb to

deliver the lymphocytes to the tumor cells were analysed in these xenografts. The focus was on the optimal dose finding of EpCAMxCD3, which would allow the study of the TRAIL-L in the therapeutic approach.

In the pancreatic model NOD/SCID mice were *s.c.* transplanted with BxPc-3 tumor cells mixed with pre-activated lymphocytes BxPc-3 + L and in the prostate model with PC-3 cells mixed with lymphocytes PC-3 + L (Fig 12 II.). Three days after cell implantation animals received *i.p.* injections of bsAb EpCAMxCD3 at a dose of 0.1 mg/kg, 1 mg/kg, 10 mg/kg. The control groups received control parental bivalent anti-CD3 and anti-EpCAM mAbs or PBS. The treatment was repeated four times with a three day interval.

Repeated measurements of tumor growth during a period of 24 days, revealed a dose-dependent anti-tumor effect of EpCAMxCD3 in xenografts. In BxPc-3 + L xenografts, mice which had received the highest dose of EpCAMxCD3 (10 mg/kg) had dramatically reduced tumor take; only 50% (4/8) of the animals developed small tumors compared to 100% (8/8) of mice in the control Abs group. The highest dose of EpCAMxCD3 retarded the BxPc-3 + L tumor growth most efficiently, compared to the animals which had received control parental antibodies (Fig 12 A, B). Furthermore, the anti-tumor effect of EpCAMxCD3 at doses of 1 mg/kg and 0.1 mg/kg was considerable higher compared to control groups with PBS and control parental antibodies with a tumor take of 80% (4/5) in both control groups (Fig 12 C, D, A and E). The animals in the PBS control group also developed much larger tumors than in the EpCAMxCD3-treated groups. Overall, the treatment efficiency was dose-dependent compared to the groups of animals treated with PBS and parental control Abs (Fig 12 B - E). At day 24 the tumor weight was significantly reduced in all groups treated with EpCAMxCD3 compared to the controls (Fig 12 F). Similar results were obtained for PC-3 + L xenografts treated with EpCAMxCD3 (Fig 12 G – L).

Functionally available bsAb plasma level was 202 ± 45 ng/ml in BxPc-3 + L tumor-bearing mice treated with 10 mg/kg EpCAMxCD3 seven days after the last injection. The body weight of tumor-bearing mice was not affected by the EpCAMxCD3 treatment (data not shown), indicating an absence of severe toxic side effects. In addition, the formation of metastasis could not be detected by macroscopic inspection of organs and tissues and by immunohistochemistry with anti panCK Ab and by flow cytometry with anti-human MHC class I Ab (data not shown).
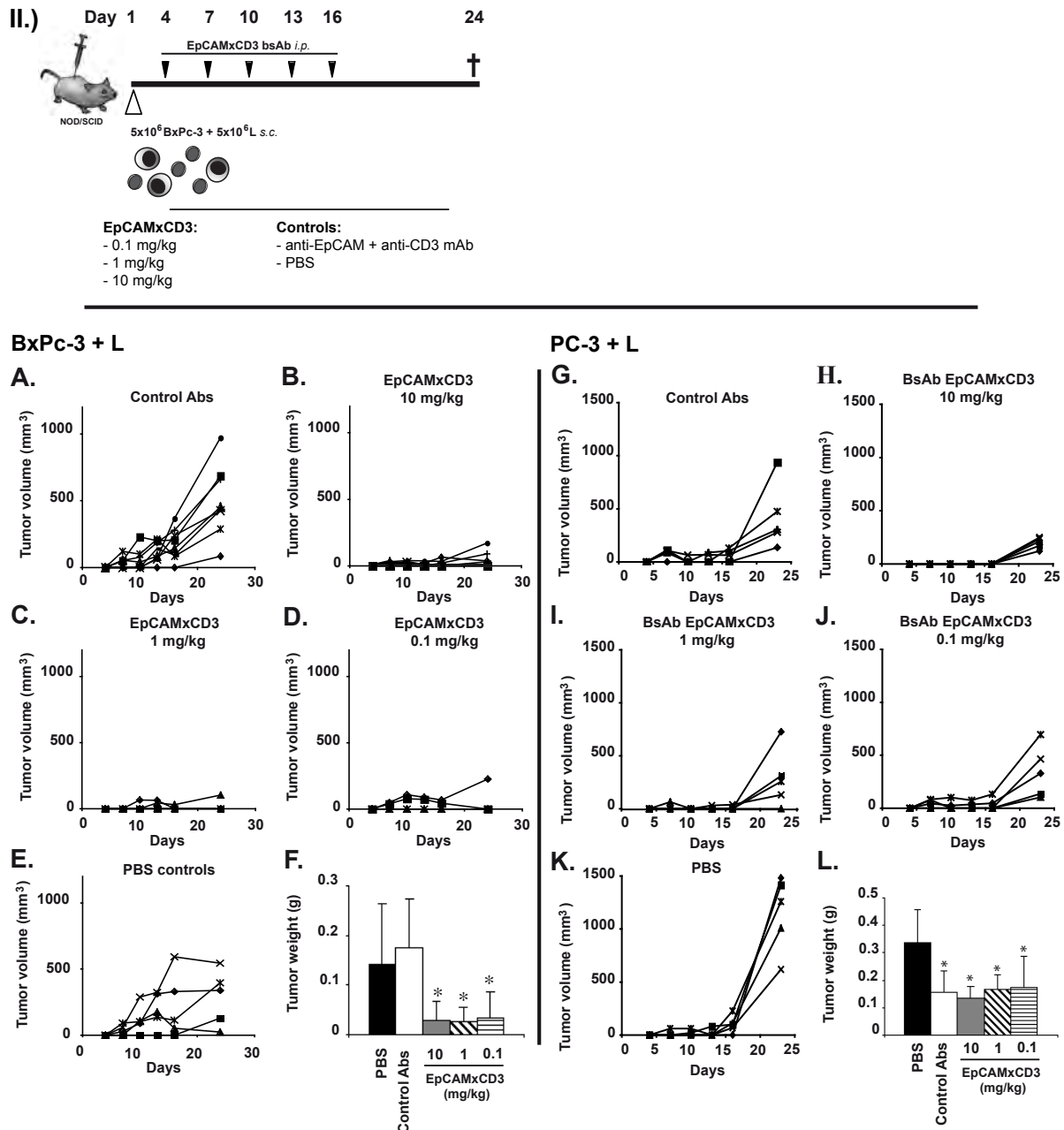
Fig 12 Efficiency of EpCAMxCD3 treatment in pancreatic BxPc-3 + L and prostate PC-3 + L tumor model

II.) Scheme of *in vivo* experiment. NOD/SCID mice were *s.c.* transplanted with pancreatic BxPc-3 or prostate PC-3 tumor cells ($5x10^6$) mixed with extra-corporally pre-activated human lymphocytes (L) ($5x10^6$). Three days later animals were randomized to 5 groups (n=5-8 per group) and received *i.p.* injections of bsAb EpCAMxCD3 or controls. Animals received either control parental bivalent EpCAM and anti-CD3 mAb at a dose of 1 mg/kg (A, G), EpCAMxCD3 at doses 10 mg/kg (B, H), 1 mg/kg (C, I), 0.1 mg/kg (D, J) or PBS (E, K). Treatment was repeated 4 times with a three-day interval as described in M&M. Tumor growth was measured every third day. Data is presented as growth kinetics of individual tumors. The weight of tumors is presented at the end-point of experiment at day 24 (F, L). ∗ $p<0.05$.

2.4.2.2 Apoptosis induction in BxPc-3 + L and PC-3 + L xenografts by bsAb EpCAMxCD3

The growth retardation of BxPc-3 and PC-3 tumors and the reduced tumor engraftment could be due to several mechanisms. First, the anti-tumor effects of EpCAMxCD3 treatment of

49

BxPc-3 + L and PC-3 + L tumors were analysed for the induction of apoptosis. Cryosections of tumors were subjected to TUNEL assay and to immunohistochemistry to detect active caspase 3. There was no difference in the density and in the percentage of active caspase 3-positive cells between EpCAMxCD3 treated tumors and controls (Fig 13). Analysis of TUNEL staining revealed similar results.

BxPc-3 + L
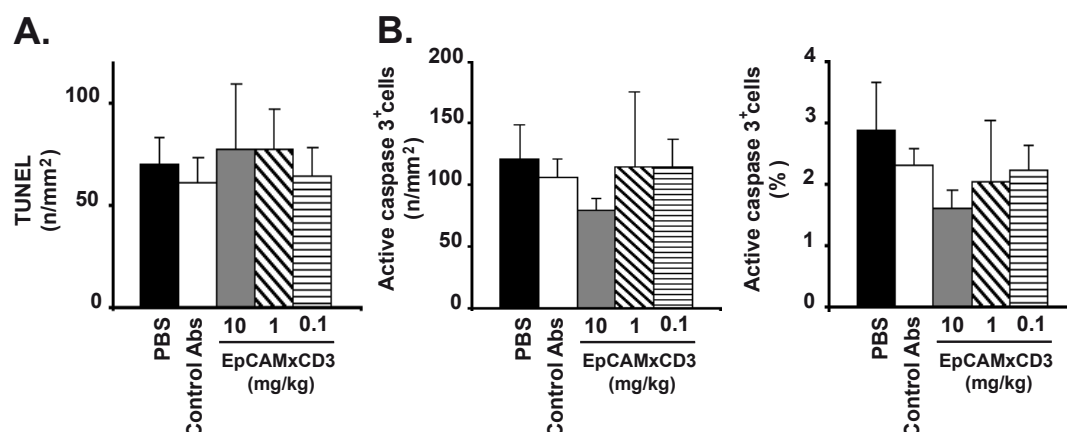
Fig 13 Effects of EpCAMxCD3 on apoptosis in BxPc-3 + L and PC-3 + L

To evaluate whether anti-tumor effects of EpCAMxCD3 and co-transplanted lymphocytes were due to apoptosis induction, BxPc-3 + L tumors were subjected to TUNEL assay and to immunohistochemistry to detect active caspase 3 (A). The density of apoptotic cells visualized by TUNEL staining and (B) the density and percentage of active caspase 3-positive cells in BxPc-3 + L tumor tissues (n=4 per group). * p<0.05.

2.4.2.3 Reduced Proliferation in BxPc-3 + L and PC-3 + L xenografts by bsAb EpCAMxCD3

Second, tumor tissues were immunohistochemically analysed for changes in tumor cell proliferation. In BxPc-3 + L and in PC-3 + L tumors, a significant reduction of Ki-67-positive cells could be detected in EpCAMxCD3 treated groups compared to controls (Fig 14).
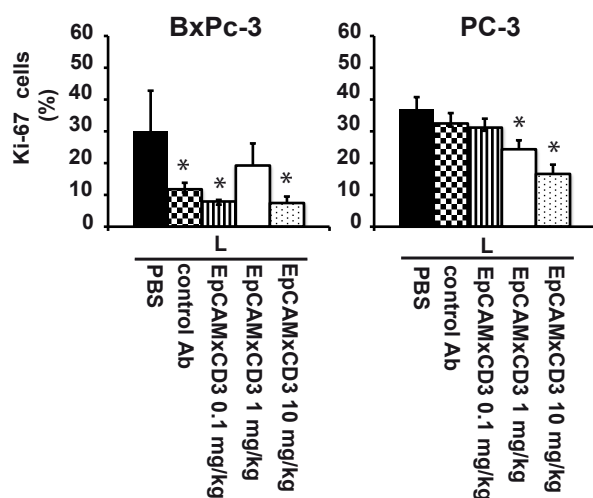
Fig 14 Effects of EpCAMxCD3 on apoptosis in BxPc-3 + L and PC-3 + L

To evaluate whether anti-tumor effects of EpCAMxCD3 and co-transplanted lymphocytes were due to proliferative changes, BxPc-3 + L and PC-3 + L tumors were subjected to immunohistochemistry to detect active Ki-67. ∗ p<0.05.

Summarized, EpCAMxCD3 treatment retarded the tumor growth and reduced the tumor engraftment in BxPc-3 + L and PC-3 + L xenografts. However, tumor growth retardation was not due to the induction of apoptosis at to the time of observation but a reduced number of proliferating cells could be detected. The tumor analysis at the endpoint of the treatment on day 24 after cell transplantation, is quite late and reactions of the tumor cells towards the treatment could have happened earlier.

2.4.3 Establishment of pancreatic and prostate xenograft models with co-transplanted TRAIL-L for the EpCAMxCD3 treatment

In the next *in vivo* model II, the question was, whether the anti-tumor effect of EpCAMxCD3 could be enhanced by using TRAIL-over-expressing lymphocytes (TRAIL-L). Based on the results from the BxPc-3 and PC-3 xenografts with co-injected human lymphocytes, the *in vivo* experiments were modified for TRAIL-L. The observation, that the 1 mg/kg and the 0.1 mg/kg dose of EpCAMxCD3 treatment was also very efficient, the dosage was further decreased. With lower doses of bsAb, the analysis of the contribution of the TRAIL-L is possible. To analyse the therapeutic effect of EpCAMxCD3 in combination with TRAIL-L, human pancreatic BxPc-3 cells were *s.c.* co-transplanted with human TRAIL-L (BxPc-3 +TRAIL-L) into NOD/SCID mice. The same model was established for human prostate PC-3 cell lines (PC-3 + TRAIL-L).

2.4.3.1 Activation of transgene expression by doxycycline *in vivo*

The lymphocytes were transduced with the inducible lentiviral vector pV3TP2AE. Therefore

it was necessary to analyse whether the transgene in transduced lymphocytes was efficiently "switched on" and to check a potential basal transgene expression *in vivo*. To exclude apoptotic effect of TRAIL *in vivo*, lymphocytes were transduced with a control vector to over-express the marker gene EGFP. NOD/SCID mice were *s.c.* transplanted with BxPc-3 cells mixed with EGFP-transduced lymphocytes and received doxycycline with the drinking water to induce the transgene expression. Animals (n=3) received doxycycline at a dose of 200 μg/ml or at a dose of 1 mg/ml with the drinking water. A control group of animals (n=3) received drinking water without doxycycline. Cryosections of tumor tissues from animals, which had received doxycycline, showed an efficient expression of the transgene EGFP in lymphocytes (Fig 15). However, the control group, which did not receive doxycycline in the drinking water, showed a basal expression of EGFP in the tissue, indicating that the CMVmin promoter is leaky in this lentiviral vector construction (data not shown).

Dox 200 μg/ml
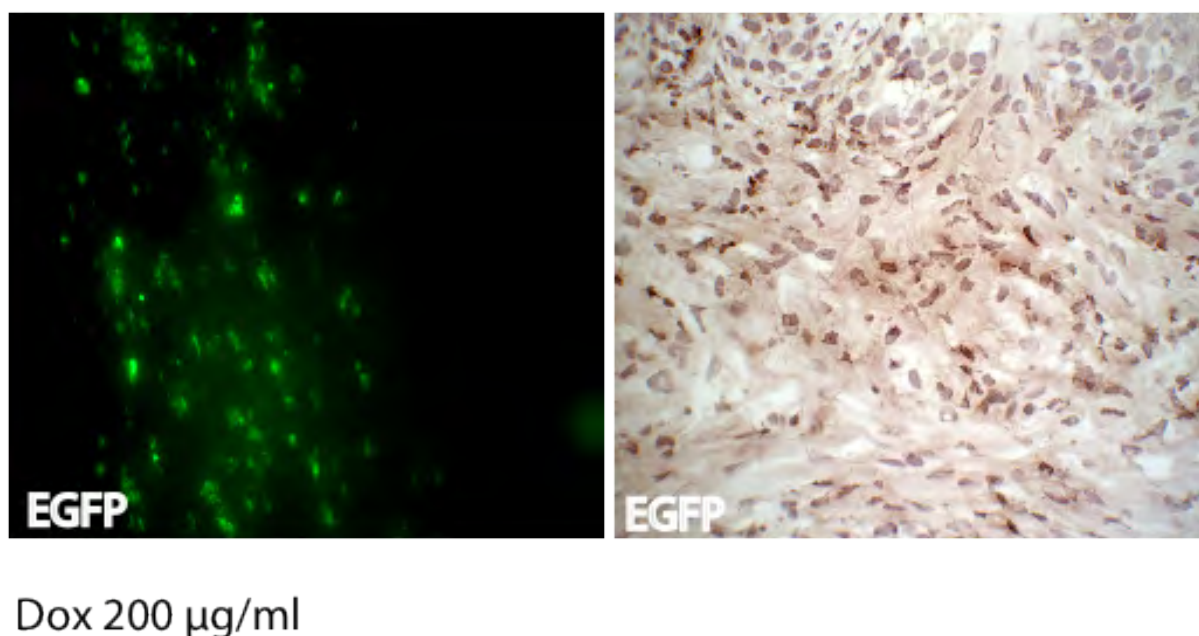
Fig 15 Induction of transgene expression in BxPc-3 + EGFP-L xenografts

NOD/SCID mice were *s.c.* transplanted with BxPc-3 pancreatic tumor cells (5x10^6) mixed with EGFP- transduced human lymphocytes (EGFP-L) (5x10^6). Animals received doxycycline in the drinking water (n=3 per group). To test whether the transgene was successfully switched on in the conditional tet-on vector, tumors were analysed for EGFP as a marker gene. Shown is a BxPc-3 + EGFP-L cryosection from animals treated with 200μg/ml doxycycline in the drinking water. Immunofluorescence and immunohistochemistry for EGFP were used to detect transduced and conditionally activated lymphocytes. 400x magnification.

2.4.4 BsAb EpCAMxCD3 treatment in BxPc-3 + TRAIL-L and PC-3 + TRAIL-L xenografts

2.4.4.1 Growth retardation of BxPc-3 + TRAIL-L and PC-3 + TRAIL-L xenografts by bsAb EpCAMxCD3

In EpCAMxCD3 treatment experiments, human pancreatic BxPc-3 cells were *s.c.* transplanted with human TRAIL-L (BxPc-3 + TRAIL-L) into NOC/SCID mice. (Fig 16 III.). Three days after cell implantation, animals received *i.p.* injections of bsAb EpCAMxCD3. The animal groups received EpCAMxCD3 at a dose of 0.01 mg/kg, 0.1 mg/kg and the treatment control groups received parental bivalent anti-CD3 and anti-EpCAM mAbs or PBS. The bsAb treatment was repeated four times with a three-day interval. Another control group received BxPc-3 co-transplanted with only pre-activated lymphocytes and PBS treatment BxPc-3 + L. This group served as a negative control for the use of TRAIL-L. The same model was used for the human prostate PC-3 cell lines: PC-3 + TRAIL-L and PC-3 + L.

In BxPc-3 + TRAIL-L and PC-3 + TRAIL-L xenografts, tumor take was 100% (6/6) in the PBS, the parental anti-CD3 and anti-EpCAM mAb, irrelevant bsAb CD19xCD3 and the BxPc-3 + L control group. The two groups treated with EpCAMxCD3 at a dose of 0.01 mg/kg and 0.1 mg/kg had a reduced tumor take of 83% (5/6) (Fig 16 C). Repeated measurements of tumor growth during a period of 23 days revealed, that the tumor growth of BxPc-3 + TRAIL-L xenografts was reduced in all groups compared to the BxPc-3 + L group with co-transplanted pre-activated lymphocytes, which developed the largest tumors.

The growth retardation was most significant between groups, which had received bsAb EpxCAMxCD3 at a dose of 0.1 mg/kg and 0.01 mg/kg, compared to the treatment control groups, which had received PBS, parental bivalent anti-CD3 and anti-EpCAM mAb or irrelevant bispecific CD19xCD3. Even very low doses of EpCAM (0.01 mg/kg) resulted in a reduced tumor volume (Fig 16 A). At day 23 the tumor weight was significantly reduced in the BxPc-3 + TRAIL-L groups treated with EpCAMxCD3 compared to controls (Fig 16 B). Similar results were obtained for PC-3 + TRAIL-L xenografts treated with EpCAMxCD3 (Fig 16 A, B). Surprisingly, a very low dose of EpCAMxCD3 (0.01 mg/kg) was the most effective dose in retarding PC-3 growth.

Interestingly, in BxPc-3 tumors, which had been co-transplanted with TRAIL-L, intra-tumoral liquid filled cysts could be observed. Cysts were detected in all BxPc-3 + TRAIL-L groups, but not in the BxPc-3 + L control group. This observation could not be made for PC-3 + TRAIL-L or the PC-3 + L xenografts. There was no apparent relationship between the cyst

formation and antibody treatment. However, the largest cysts were formed in the groups that received TRAIL-L lymphocytes and EpCAMxCD3. These cysts, which filled the BxPc-3 + TRAIL-L tumors, made the comparison of the volume and weight determination impossible (Fig 16 C).

The body weight of tumor-bearing mice was not affected by the EpCAMxCD3 treatment (data not shown). Furthermore, animals that received TRAIL-L did not develop metastasis I lungs, liver and spleen as analysed macroscopically and by immunohistochemistry anti panCK (human cytokeratins 4, 5, 6, 8, 10 and 18) and by flow cytometry anti-human MHC I (data not shown).

III.) Day 1 4 7 10 13 16 23

EpCAMxCD3 bsAb *i.p.*

NOD/SCID

5x10^6 BxPc-3 + 5x10^6 TRAIL-L *s.c.*

EpCAMxCD3:
- 0.01 mg/kg
- 0.1 mg/kg

Controls:
- anti-EpCAM + anti-CD3 mAb
- irrelevant bsAb CD19xCD3
- PBS

A.

BxPc-3

Tumor volume (cm^3)

Days

PC-3

Tumor volume (cm^3)

Days

B.

BxPc-3

PC-3

Tumor weight (g)

— L + PBS
— TRAIL-L + PBS
— TRAIL-L + EpCAM + CD3
— TRAIL-L + CD19xCD3
— TRAIL-L + EpCAMxCD3 0.1 mg/kg
— TRAIL-L + EpCAMxCD3 0.01 mg/kg

L + PBS
TRAIL-L + PBS
TRAIL-L + EpCAM + CD3
TRAIL-L + CD19xCD3
TRAIL-L + EpCAMxCD3 0.1 mg/kg
TRAIL-L + EpCAMxCD3 0.01 mg/kg

C.

Effector cell		L	TRAIL-L				
Treament		PBS	PBS	control Ab		bsAb EpCAMxCD3	
				EpCAM/ CD3 mAb	CD19xCD3 bsAb	0.1 mg/kg	0.01 mg/kg
PC-3	Tumor take	6/6	6/6	5/6	6/6	6/6	5/6
	Cyst formation	0/6	0/6	0/6	0/6	0/6	0/6
BxPc-3	Tumor take	6/6	6/6	6/6	6/6	5/6	6/6
	Cyst formation	0/6	5/6	5/6	1/6	3/6	6/6

Fig 16 Efficiency of bsAb EpCAMxCD3 treatment in pancreatic BxPc-3 + TRAIL-L and prostate PC-3 + TRAIL-L xenografts

III.) Scheme of *in vivo* experiment. NOD/SCID mice were *s.c.* transplanted with BxPc-3 pancreatic or PC-3 prostate tumor cells (5×10^6) mixed with TRAIL-transduced human lymphocytes (TRAIL-L) (5×10^6). Three days later animals were randomized to 6 groups (n=6) and received *i.p.* injections of bsAb EpCAMxCD3 or controls. Treatment was repeated 4 times with a three day interval as described in M&M. Animals received either bsAb EpCAMxCD3 at a dose of 0.1mg/kg or 0.01 mg/kg, control parental bivalent anti-human EpCAM and anti-CD3 mAbs or irrelevant bsAb CD19xCD3 at a dose of 1 mg/kg or PBS. An additional control group had received non-tranduced lymphocytes (L) co-injected with tumor cells and had been treated with PBS. (A) External tumor size was measured every third day. Data is presented as growth kinetics of mean of individual tumors with standard deviation. (B) The weight of tumors is shown at the end-point of the treatment at day 23. ∗ p<0.05. (C) The table shows the tumor take and cyst formation in pancreatic BxPc-3 and prostate PC-3 xenografts.

2.4.4.2 Apoptosis induction, proliferation and blood vessel density in BxPc-3 + TRAIL-L and PC-3 + TRAIL-L xenografts by bsAb EpCAMxCD3

The growth retardation of BxPc-3 + TRAIL-L and PC-3 + TRAIL-L tumors could be due to several mechanisms. First, BxPc-3 + TRAIL-L and PC-3 + TRAIL-L tumors were analysed for the induction of apoptosis. Cryosections of tumors were subjected to TUNEL assay and to immunohistochemistry to detect active caspase 3. There was no major difference in the density and in the percentage of active caspase 3 – positive cells between EpCAMxCD3 treated tumors and controls (Fig 17 A, B). Analysis of TUNEL staining revealed similar results. These results were comparable to those from BxPc-3 + L and PC-3 + L xenografts. Therefore, tumor growth retardation was not due to the induction of apoptosis at the time of observation.

The analysis of the tumor tissue at the endpoint of the bsAb treatment on day 23 could be critical in our treatment experiments. For an earlier time of observation, the experiment with BxPc-3 co-transplanted with TRAIL-L and subsequent treatment with EpCAMxCD3 was repeated as described and stopped on day 14 after cell transplantation. Nevertheless, immunohistological analysis revealed comparable numbers of apoptotic cells in the tumor tissue (data not shown).

Second, to understand the tumor growth retardation after the bsAb treatment, tumor tissue samples were analysed for changes in tumor cell proliferation and in the blood vessels. In BxPc-3 + TRAIL-L and PC-3 + TRAIL-L tumors, a significant reduction in the number of CD31$^+$ blood vessels could be observed. The density of CD31$^+$ blood vessels was decreased by around 30-40% in BxPc-3 and PC-3 tumors co-transplanted with TRAIL-L compared to control tumors with non-transduced lymphocytes. Also the number of Ki-67$^+$ cells was strongly decreased by around 40% in EpCAMxCD3 treated groups compared to the parental bivalent anti-CD3 and anti-EpCAM mAb, irrelevant bsAb CD19xCD3 control groups (Fig 17 C, D).

Summarized, low doses of EpCAMxCD3 were sufficient to retard the tumor growth in BxPc-3 + TRAIL-L and PC-3 + TRAIL-L xenografts. Co-transplanted TRAIL-L in BxPc-3 + TRAIL-L xenografts further retarded the tumor growth compared to the BxPc-3 + L group. In the EpCAMxCD3 treated tumor tissues, a significant reduction of CD31$^+$ blood vessel number and a reduced number of proliferating cells could be detected. However, the induction of apoptosis could not be detected at the time of observation. The repetition of the bsAb treatment experiment with a time of analysis on day 14 did not result in a different result. This result showed, that the analysis of time points earlier than 14 days is necessary for the explanation of the mechanisms underlying the growth retardation in xenografts.

However, earlier time points cannot be analysed in this *in vivo* model due to the small size of the xenografts and the availability of engrafted tumor material.
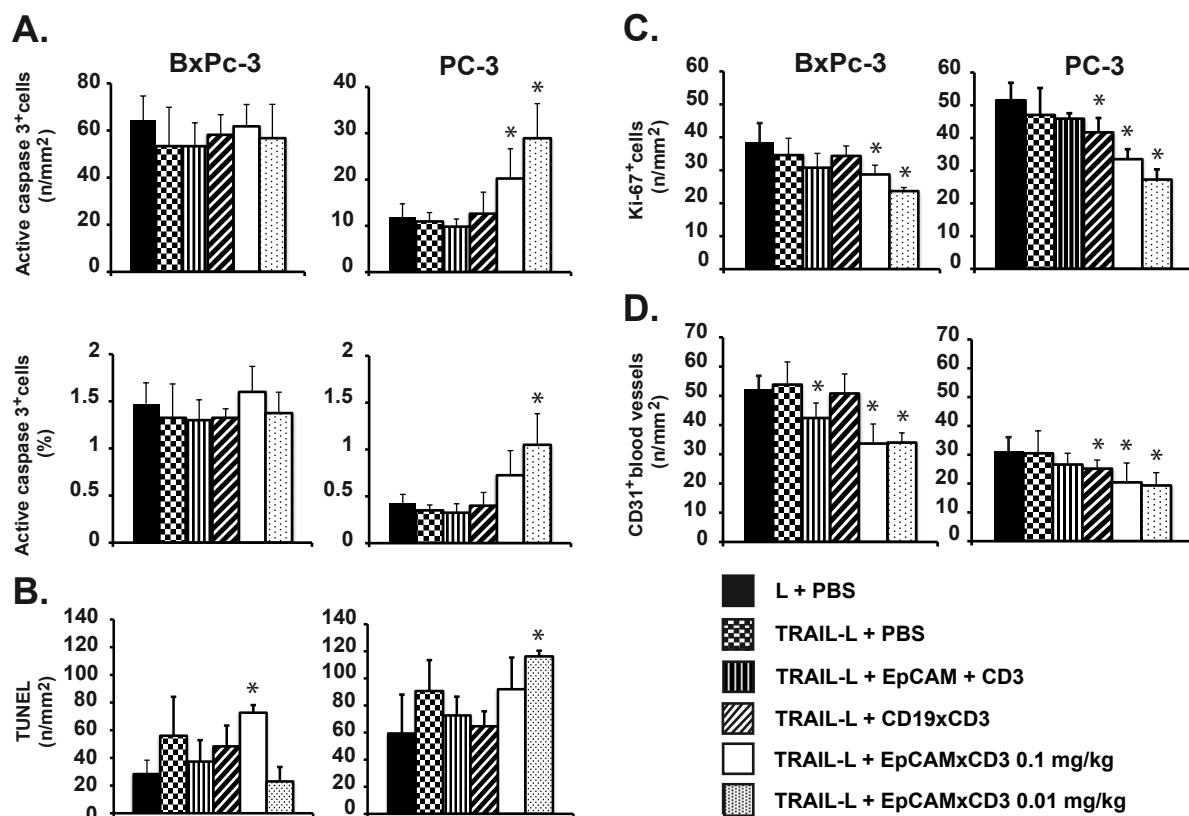
Fig 17 Effects of bsAb EpCAMxCD3 treatment on apoptosis induction, proliferation and blood vessel density in BxPc-3 + TRAIL-L and PC-3 + TRAIL-L xenografts

To evaluate whether the anti-tumor effects of TRAIL-L and EpCAMxCD3 were due to apoptosis induction, BxPc-3 and PC-3 tumor samples were subjected to TUNEL assay and to immunohistochemistry to detect active caspase 3. (A) Density and percentage of apoptotic cells stained for active caspase 3. (B) Density of apoptotic cells visualized by TUNEL staining. (C) To evaluate whether anti-tumor effects of TRAIL-L and EpCAMxCD3 influenced tumor cell proliferation, BxPc-3 and PC-3 tumors were subjected to immunohistochemistry to detect Ki-67 density. (D) To evaluate the impact on blood vessel density, tissue sections were stained for CD31 blood vessel density. $*$ p<0.05.

2.4.5   Efficiency of TRAIL-L and bsAb EpCAMxCD3 *in vitro*

2.4.5.1   Migration of lymphocytes and contacts duration of carcinoma cells and lymphocytes linked by bsAb EpCAMxCD3

The time of observation is critical for the explanation of the mechanism of the growth retardation in BxPc-3 and PC-3 xenografts co-transplanted with TRAIL-L and treated with EpCAMxCD3 *in vivo*. To understand these mechanisms and to analyse early events in the tumor cell and their interaction with lymphocytes following the bsAb treatment, *in vitro* experiments were set up.

Bispecific antibody EpCAMxCD3 has the dual specificity to target lymphocytes to tumor cells by binding to CD3 expressed on lymphocytes and by binding to EpCAM on tumor cells. EpCAMxCD3 together with either TRAIL-L or pre-activated lymphocytes had shown an anti-tumor effect *in vivo*. To analyse the ability of EpCAMxCD3 to bring lymphocytes in close contact with carcinoma cells, a collagen gel 3D tumor reconstruct system was utilized. BxPc-3 and human lymphocytes were co-cultivated in a collagen matrix, which closely resembles the tumor microenvironment. Lymphocytes are able to migrate freely in the gels. Dynamic cell-cell interactions were analysed using time-lapse video microscopy. Contact duration between lymphocytes and tumor cells was approximately three times longer in the presence of EpCAMxCD3 compared to control Abs (Fig 18 A). Pre-loading of lymphocytes with EpCAMxCD3 more efficiently increased the contact time with carcinoma cells. To delineate effects of EpCAMxCD3 on lymphocyte locomotion, lymphocyte migration velocity and the percentage of migrating lymphocytes in 3D collagen gels were determined. EpCAMxCD3 did not influence lymphocyte velocity (Fig 18 B). Lymphocyte migration velocity in 3D gels was as high as 60 times of that of tumor cells. Similar results were obtained for TRAIL-L (data not shown). The proportion of actively migrating lymphocytes was slightly decreased after the exposure to EpCAMxCD3 compared to controls (Fig 18 C).

A.

B.

C.

■ no Abs
□ EpCAM
▨ CD19xCD3
▧ EpCAMxCD3
▤ EpCAMxCD3
preload 2 h
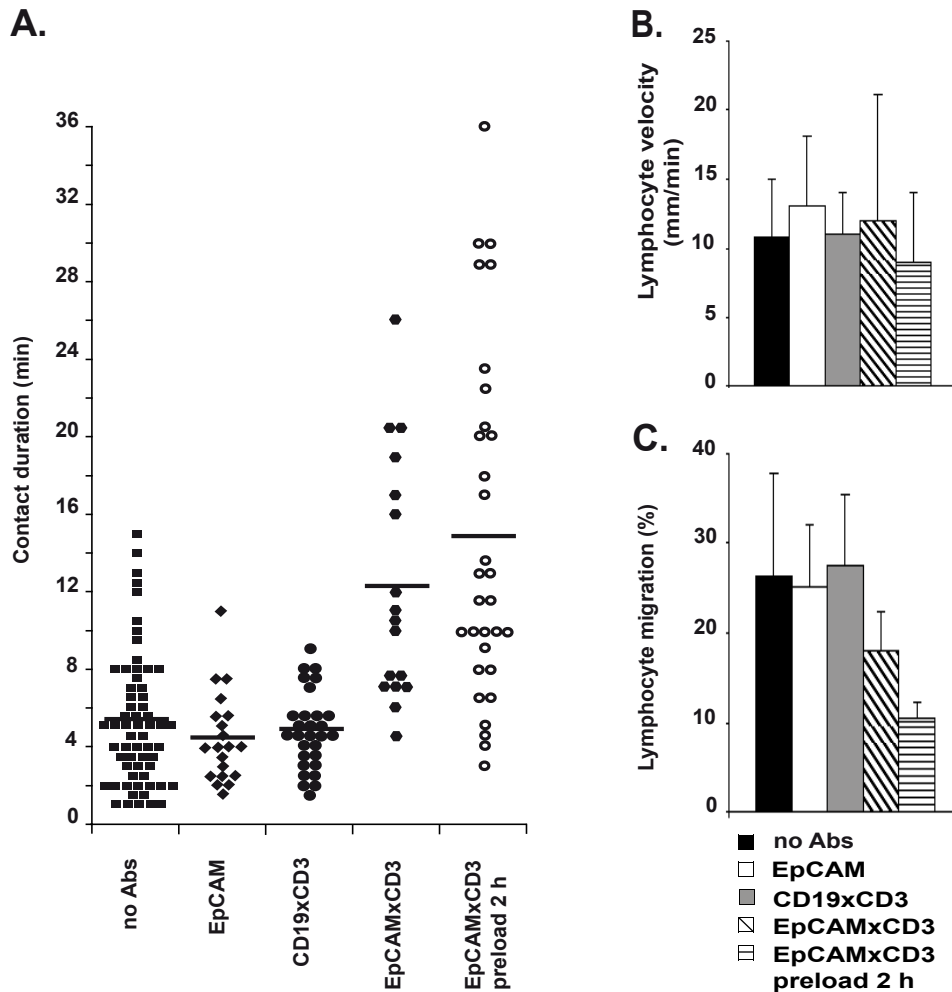
Fig 18 Effects of bsAb EpCAMXCD3 on migratory properties of lymphocytes and duration of contacts between lymphocytes and tumor cells

To evaluate the influence of EpCAMxCD3 on lymphocyte migration velocity and their interactions with tumor cells, the motility of pe-activated lymphocytes was monitored in 3D collagen gels using time-lapse microscopy. Lymphocytes and BxPc-3 cells were mixed at a concentration of $2x10^5$ cells per collagen gel. Lymphocytes were either pre-incubated with EpCAMxCD3 at 10 µg/ml or bsAb was added directly to the collagen solution prior to the 3D gel polymerization. Control irrelevant bsAb CD19xCD3 or control bivalent parental anti-human EpCAM mAb were added to the collagen solution prior to the 3D gel polymerization. Lymphocyte migration and their interactions with carcinoma cells were monitored for 1.5 hours. (A) Contact time of migrating lymphocytes and tumor cells. Contacts between a single lymphocyte and a single tumor cell were analysed using a „frame to frame" method in CapImage software as described in M&M. (B) Effects of EpCAMxCD3 on lymphocyte migration velocity and (C) the percentage of migrating lymphocytes in 3D collagen gels.

2.4.5.2 Apoptosis induction by bsAb EpCAMxCD3 in 3D tumor reconstructs

To further investigate the effects of EpCAMxCD3 *in vitro*, a collagen gel 3D tumor reconstruct system was utilized. These 3D gels mimic a tumor microenvironment and allow an easy and controlled setting for the study of tumor cell and lymphocyte interactions, cytokine production and apoptosis induction. 3D gels consist of a collagen matrix in which carcinoma cells are embedded with lymphocytes and incubated together with fibroblasts. Lymphocytes are able to freely migrate in these 3D gels. EpCAMxCD3 or control Abs were added to preformed gels to allow diffusion (Fig 19).

Collagen gel 3D tumor reconstruct
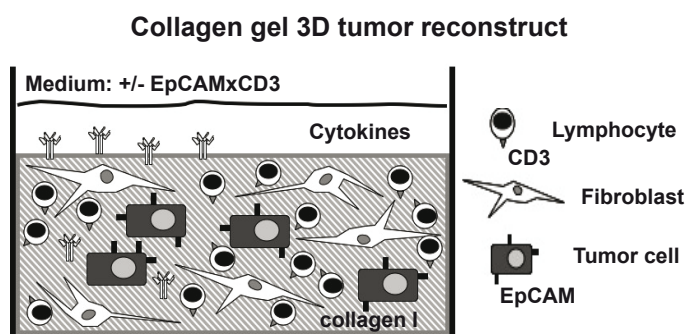
Fig 19 Scheme depicting the composition of collagen gel 3D tumor reconstructs

To analyse short-term effects of bsAb treatment, the induction of apoptosis was analysed in 3D tumor reconstructs. The effects of EpCAMxCD3 were analysed after 24 and 72 hours. A protein array system was utilized to detect the presence of apoptosis-related proteins. In 3D tumor reconstructs BxPc-3 or PC-3 tumor cells, human lymphocytes and fibroblasts were co-cultivated in the collagen matrix. In these 3D gels, the incubation of pre-activated lymphocytes with EpCAMxCD3 resulted in the production of cleaved caspase 3, catalase, cytochrome c and Hsp70. In control 3D reconstructs incubated with control irrelevant bsAb CD19xCD3 no apoptosis-related proteins could be detected (Fig 20 A), suggesting a contribution of bsAb EpCAMxCD3 to the apoptosis induction *in vitro*.

To investigate the question whether the effects of EpCAMxCD3 on apoptosis-induction could be enhanced by TRAIL-L, BxPc-3 or PC-3 tumor cells were mixed with TRAIL-L and fibroblasts in 3D tumor reconstructs. The presence of apoptosis-related proteins was detected (Fig 20 B). Compared to 3D reconstructs with pre-activated lymphocytes and tumor cells, apoptosis-related proteins were dramatically upregulated after 24 hour incubation and the presence of Bax, pro-caspase-3, cleaved caspase 3, catalase, claspin, cytochrome c, TRAIL-R2, FADD, Fas/TNFSF6, HIF-1a, HO1/HMOX1/Hsp32, Hsp27, Hsp60, Hsp70, HTRA2/Omi, p27/kip1, SMAC/Diablo, Survivin and XIAP was detected. There was no major difference in the expression level between BxPC3 and PC-3 3D tumor reconstructs. The analysis of the pixel density of the spots revealed that the addition of EpCAMxCD3 to the gels did not influence the expression of apoptosis-related proteins (Fig 20 C). Addition of EpCAMxCD3 to 3D tumor reconstructs did not influence the expression of apoptotic proteins after 24 hours.

Since the manipulation of lymphocytes by isolation, handling in cell culture and the transduction procedure could potentially affect the functions of lymphocytes, the 3D tumor reconstructs were repeated with TRAIL-L compared to mock-tranduced lymphocytes

(MOCK-L). Therefore, 3D reconstructs were prepared consisting of i) BxPc-3 mixed with TRAIL-L or ii) BxPc-3 mixed with TRAIL-L incubated with EpCAMxCD3 and were compared to 3D reconstructs consisting of iii) BxPc-3 mixed with control MOCK-L or iv) BxPc-3 mixed with MOCK-L incubated with EpCAMxCD3. The expression levels of apoptosis-related proteins were not significantly different between these groups. The protein expression result after 24 hour incubation was stronger compared to 72 hours. The panel of induced apoptosis-related proteins was the same as in the previous experiments shown in (Fig 20, data not shown)
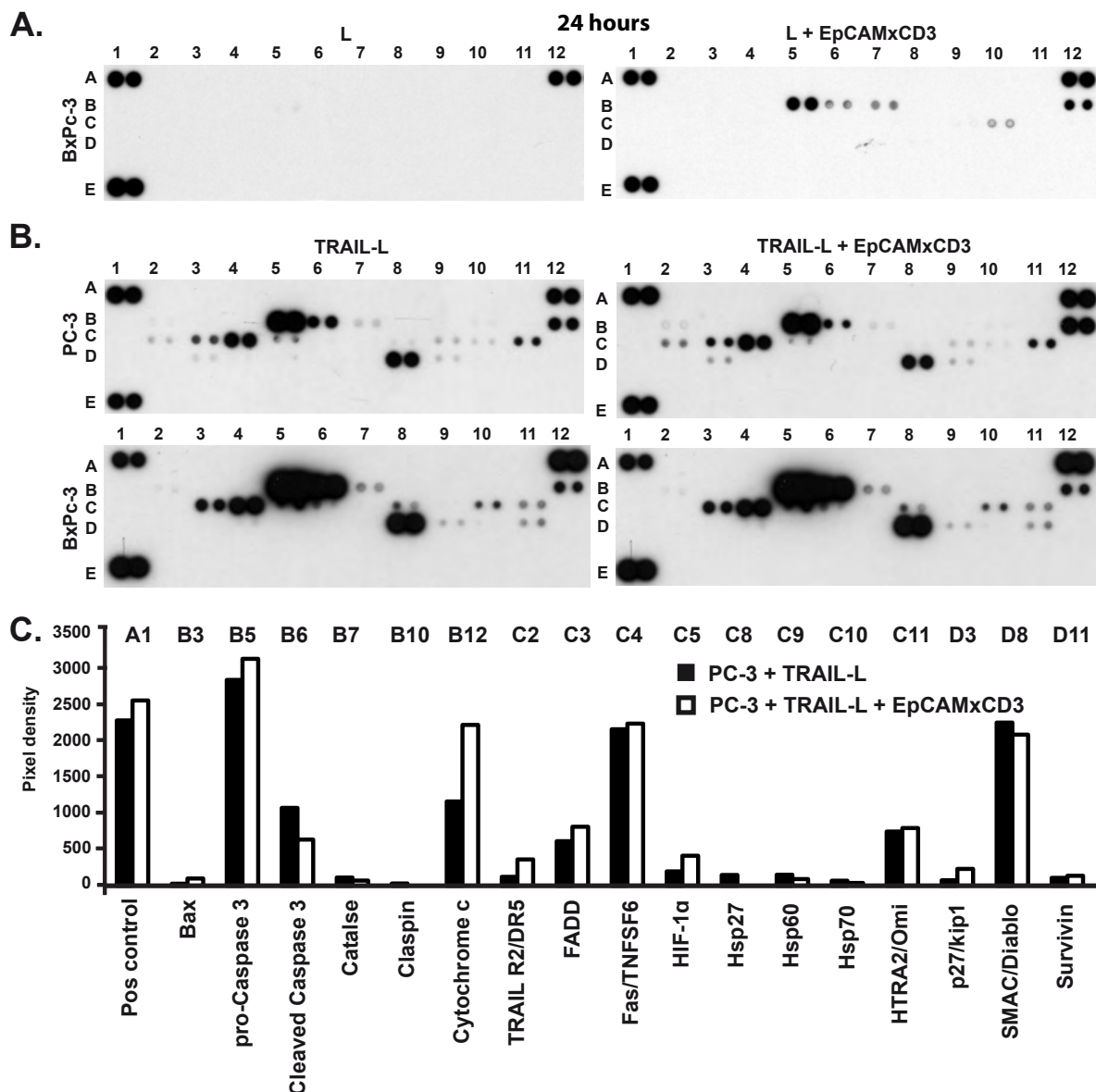
Fig 20 Effects of TRAIL-L and bsAb EpCAMxCD3 on apoptosis induction in 3D tumor reconstructs

The ability of TRAIL-L and EpCAMxCD3 to induce apoptosis-related proteins was analysed in 3D tumor reconstructs. Supernatants were collected after 24 hours and apoptosis-related proteins were detected with a human apoptosis antibody array kit. (A,B) X-ray film images of membranes with spots of apoptosis-related proteins from pooled supernatants (n=4) from 3D tumor reconstructs incubated for 24 hours with bsAb EpCAMxCD3 at a dose of 10μg/ml or with PBS as a control. Three pairs of positive control spots are located in the corner of each array. (A) X-ray films from gels consisting of BxPc-3 cells and pre-activated lymphocytes mixed with fibroblasts. The location of the protein spots on the membranes is indicated

by numerical (1-12) and literal (A-E) coordinates. The incubation of pre-activated lymphocytes with EpCAMxCD3 resulted in the detection of cleaved caspase 3(B6), catalase (B7), cytochrome c (B12) and Hsp70 (C10).

(B) X-ray films from gels consisting of BxPc-3 or PC-3 cells and TRAIL-L mixed with fibroblasts and incubated with EpCAMxCD3 or with PBS. The location of the protein spots on the membranes is indicated by numerical (1-12) and literal (A-E) coordinates. The presence of Bax (B2), pro-caspase-3 (B5), cleaved caspase 3 (B6), catalase (B7), claspin (B10), cytochrome c (B12), TRAIL-R2 (C2), FADD (C3), Fas/TNFSF6 (C4), HIF-1α (C5), HO1/HMOX1/Hsp32 (C6), Hsp27 (C8), Hsp60 (C9), Hsp70 (C10), HTRA2/Omi (C11), p27/kip1 (D3), SMAC/Diablo (D8), Survivin (D9) and XIAP (D11) was detected. (C) Analysis of the pixel density as the average signal of the duplicate spots representing each apoptosis-related protein quantified using ImageJ software. One representative analysis of 3D tumor reconstructs of PC-3 mixed with TRAIL-L with bsAb EpCAMxCD3 or with PBS is shown (upper B panel).

2.4.5.3 Production of TNF-α, IFN-γ, granzyme B and perforin induced by EpCAMxCD3 by pre-activated lymphocytes in 3D tumor reconstructs

To analyse the production of cytokines, pre-activated lymphocytes were mixed with carcinoma cells and incubated with fibroblasts. EpCAMxCD3, parental bivalent EpCAM mAb or irrelevant bsAb CD19xCD3 were added to the polymerized gels. EpCAMxCD3 was used at a dose of 10 μg/ml in 3D tumor reconstruct experiments, since this concentration had been found to be optimal in previous cytotoxic T cell assays [128]. The addition of EpCAMxCD3 to 3D tumor reconstructs with pre-activated lymphocytes significantly increased the production of IFN-γ and TNF-α compared to controls (Fig 21). Levels of IFN-γ and TNF-α were low in control 3D tumor reconstructs without any Abs or in gels without carcinoma cells (data not shown). The secretion of cytolytic granzyme B was not influenced by EpCAMxCD3 in 3D tumor reconstructs with pre-activated lymphocytes. However, perforin levels were increased under the influence of EpCAMxCD3 after 72h of incubation compared to controls (Fig 21). To investigate whether EpCAMxCD3 induces polyclonal activation of T cells including regulatory T cells, we analyzed secretion of inhibitory cytokines IL-10 and TGF-β1. Only trace amounts of IL-10 were detectable in 3D tumor reconstructs with pre-activated lymphocytes. The level of TGF-β1 was around 100-200 pg/ml and was not affected by EpCAMxCD3 (data not shown).

Fig 21 Effects of bsAb EpCAMxCD3 on the production of IFN-γ, TNF-α, granzyme B and perforin by pre-activated lymphocytes in 3D tumor reconstructs

The production of IFN-γ, TNF-α, granzyme B and perforin in collagen gel 3D tumor reconstructs was analysed. BxPc-3 carcinoma cells were mixed with non-activated or pre-activated human lymphocytes and fibroblasts and EpCAMxCD3, control parental anti-human EpCAM mAb, or irrelevant bsAb CD19xCD3, respectively, were added to 3D tumor reconstructs (n=4 per group) after the collagen gel polymerization. Supernatants from 3D tumor reconstructs were collected after 24 or 72 hours of incubation and analysed by ELISA. * $p<0.05$.

2.4.5.4 Activation of non-stimulated PBMCs by EpCAMxCD3 in the presence of carcinoma cells in 3D tumor reconstructs

To evaluate the ability of EpCAMxCD3 to activate PBMCs in the presence of carcinoma cells, 3D tumor reconstructs with non-stimulated PBMCs were used. Bivalent anti-CD3 mAb was used as a positive control and irrelevant bsAb CD19xCD3 or parental bivalent anti-EpCAM mAb as negative controls. Activation of PBMCs was analyzed by the production of the effector cytokines IFN-γ, TNF-α and IL-2. EpCAMxCD3 induced a strong production of IFN-γ, TNF-α and to a lesser extend IL-2 (Fig 22 A). EpCAMxCD3 was more efficient in stimulating IFN-γ and TNF-α in PBMCs than a bivalent anti-CD3 mAb administered at the same dose after 24 hours and TNF-α after 72 hours of incubation. Granzyme B levels were 50% higher in 3D tumor reconstructs after 24 hours compared to controls. There was no difference in granzyme B after 72 hours (Fig 22 B). The perforin level was increased after 24 hours, reaching an comparable level after 72 hours in all groups. Similarly, a loading of non-stimulated PBMCs with EpCAMxCD3 for 2 hours prior to 3D tumor reconstruct experiments resulted in an increased production of IFN-γ and TNF-α compared to an addition of EpCAMxCD3 to the 3D gels. Thus in 24 hours of incubation the level of IFN-γ increased by 45% and in 72 hours by 70%. In 24 hours of incubation the production of TNF-α was increased by 20%, compared with an about 8 times increase in TNF-α production in 72 hours (data not shown). In contrast to 3D tumor reconstructs with pre-activated lymphocytes, EpCAMxCD3 induced the production of the inhibitory cytokine IL-10 with non-stimulated lymphocytes. Production of TGF-β1 was between 50 and 100 pg/ml (Fig 22 C). Since

monocyte derived IL-1β can induce the TGF-β production by fibroblasts, its concentration was analysed in 3D tumor reconstructs. The IL-1β level was around 300 pg/ml in all 3D tumor reconstructs and EpCAMxCD3 did not influence IL-1β production. IL-10, IL-1β and TGF- β1 were not detectable in 3D tumor reconstructs without PBMCs.
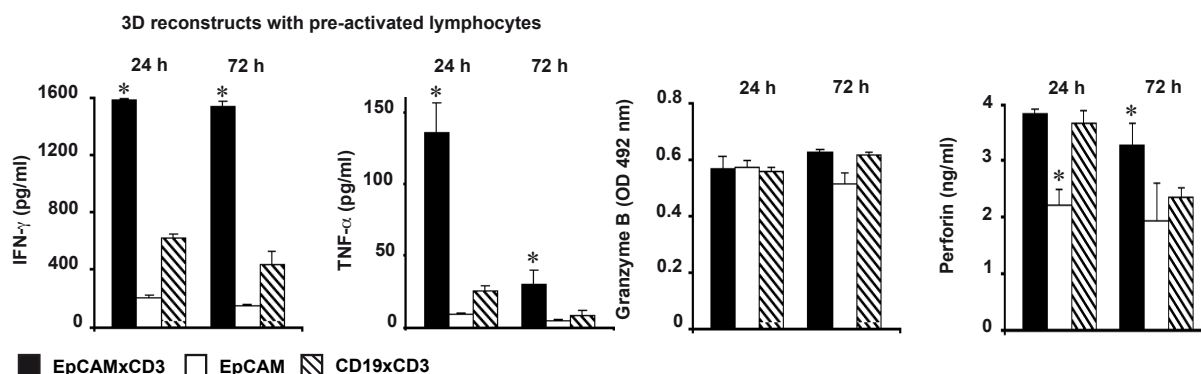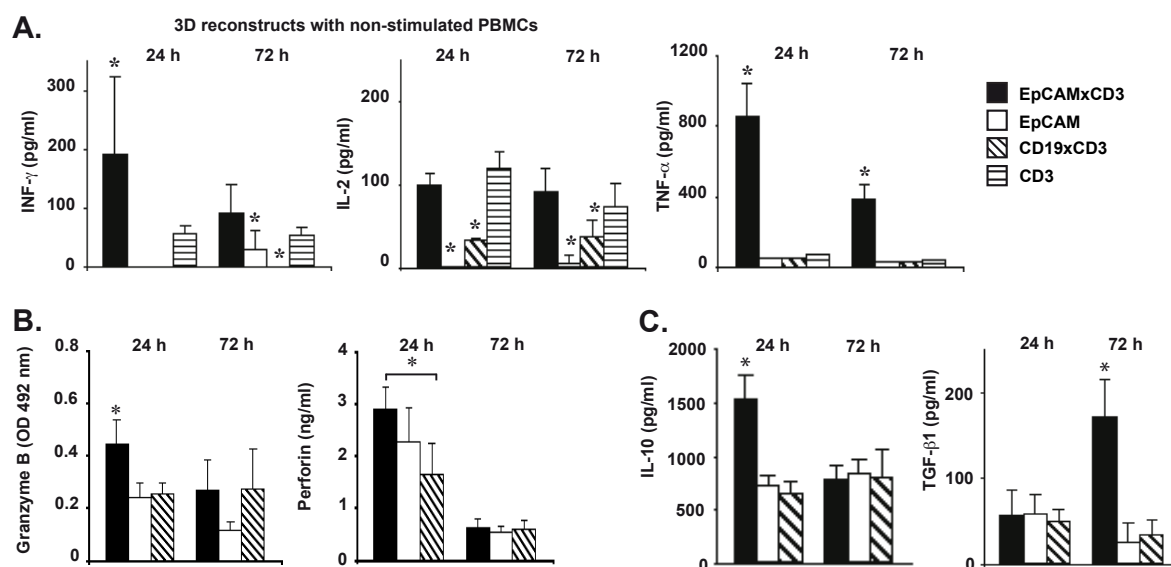

Fig 22 Effects of bsAb EpCAMxCD3 on the production of IFN-γ, TNF-α, IL-10, TGF-β1 granzyme B and perforin by non-stimulated PBMCs in 3D tumor reconstructs

The ability of EpCAMxCD3 to induce the effector cytokines IFN-γ, TNF-α and IL-2 by non-stimulated PBMCs was analysed in 3D tumor reconstructs (A). BxPc-3 carcinoma cells were mixed with non-stimulated PBMCs and fibroblasts and were incubated in 3D collagen gels for 24 or 72 hours (n=4). EpCAMxCD3, control parental anti-human EpCAM mAb, irrelevant bsAb CD19xCD3 or control bivalent anti-CD3 mAb, respectively, were added to 3D tumor reconstructs after the collagen gel polymerization. (C) The ability of EpCAMxCD3 to induce the production of IL-10 and TGF-β1 by non-activated PBMCs was analysed. (B) The levels of granzyme B and perforin in collagen gels were analysed. Cytokine levels in supernatants from 3D collagen gels were analysed by ELISA. ∗ $p < 0.05$.

2.4.5.5 Production of cytokines induced by bsAb EpCAMxCD3 by non-activated lymphocytes in 3D tumor reconstructs

Lymphocytes are able to produce a variety of cytokines upon activation apart from effector cytokines such as IFN-γ and TNF-α, which can shape the immune response *in vivo*. The production of cytokines by lymphocytes was analysed in 3D tumor reconstructs *in vitro* (Fig 21). 3D tumor reconstructs consisted of BxPc-3 mixed with non-stimulated lymphocytes and fibroblasts and were either incubated with EpCAMxCD3 or with control irrelevant bsAb CD19xCD3. Out of 36 analysed cytokines and chemokines, 16 molecules could bed detected (Fig 23). The expression of GROα, sICAM-1, IL-1α, IL-1β, IL-6, IL-8, MIF, MIP-1α, MIP-1β, Serpin E1 and RANTES was similar in 3D tumor reconstructs incubated with EpCAMxCD3 and in 3D reconstructs with CD19xCD3. However, IFN-γ was exclusively

detected in 3D reconstructs incubated with EpCAMxCD3. In addition in 3D reconstructs incubated with irrelevant bsAb CD19xCD3 G-CSF, GM-CSF, TNF-α, IP-10, I-TAC, IL-16 and IL-1ra (Fig 23).

These cytokines could be grouped into the effector cytokines IFN-γ and TNF-α, the acute phase cytokines IL-1α, IL-1β, IL-6 and the inflammatory sICAM-1, and the chemoattractants IL-8, MIF, MIP-1α, MIP-1β, Serpin E1, G-CSF, GM-CSF, GROα, IL-16, IP-10, I-TAC and RANTES.

3D tumor reconstructs
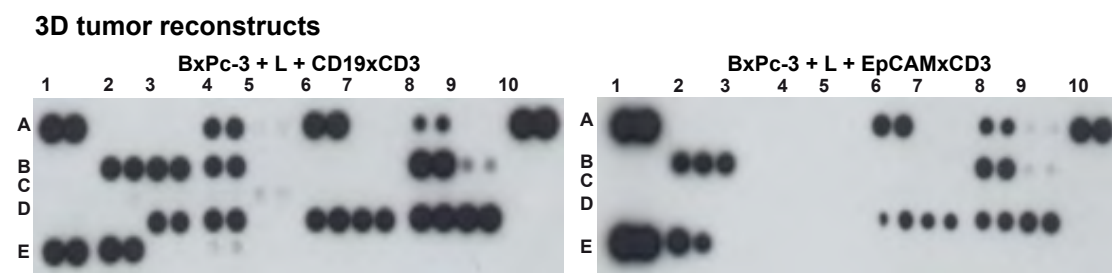
Fig 23 Effects of bsAb EpCAMxCD3 and lymphocytes on cytokine production in 3D tumor reconstructs and in tumor lysates

To analyse and compare the cytokine panels supernatants of 3D tumor reconstructs were collected after 24 hours and cytokines were detected using a human cytokine protein array kit. X-ray images of membranes with spots for cytokines in pooled supernatants from 3D tumor reconstructs consisting of BxPc-3 tumor cells, non-activated lymphocytes and fibroblasts incubated with bsAb EpCAMxCD3 at a dose of 10 µg/ml or with controls. Three pairs of positive control spot are located in the corner of each array. The location of the protein spots on the membranes is indicated by numerical (1-12) and literal (A-E) coordinates. The expression of CXCL-1/GROα (A6), sICAM-1 (A8), IL-1α (B2), IL-1β (B3), IL-6 (B8), IL-8 (B9), MIF (D6), MIP-1α (D7), MIP-1β (D8), Serpin E1 (D9) and RANTES (E2) was similar in 3D reconstructs incubated with EpCAMxCD3 or incubated with irrelevant bsAb CD19xCD3. INF-γ (A9) was exclusively detected in 3D reconstructs incubated with EpCAMxCD3. In addition, in 3D tumor reconstructs with irrelevant bsAb CD19xCD3 G-CSF (A4), GM-CSF (A5), TNF-α (E4), IP-10 (D3), I-TAC (D4), IL-16 (C5) and IL-1Ra (B4) were expressed.

Taken together, apoptosis could be detected in 3D tumor reconstructs by the induction of apoptosis-related proteins *in vitro*. In 3D tumor reconstructs of carcinoma cells mixed with pre-activated lymphocytes, addition of EpCAMxCD3 resulted in the induction of apoptosis-related proteins compared to no induction in control gels. The induction of specific proteins was the highest in 3D gels from cancer cells mixed with TRAIL-L. In these gels, the incubation with EpCAMxCD3 resulted in no difference compared to the control group, indicating a high contribution of TRAIL-L to the induced apoptosis *in vitro*. The ability of TRAIL-L or MOCK-L to induce apoptosis-related proteins *in vitro* was not further enhanced by EpCAMxCD3. It was demonstrated that EpCAMxCD3 potently stimulated pre-activated lymphocytes and non-stimulated PBMCs to secrete effector cytokines in 3D tumor reconstructs in the presence of EpCAM-expressing carcinoma cells. In 3D tumor reconstructs composed of carcinoma cells mixed with lymphocytes and fibroblasts, the addition of EpCAMxCD3 resulted in the increased production of the effector cytokines IFN-γ and TNF-α

and in the production of granzyme B and perforin by pre-activated lymphocytes. Experiments with non-stimulated PBMCs resulted in lower levels of these effector molecules. However, the inhibitory cytokines IL-10 and TGF-β1 could be detected after 24 hours. The levels of IL-10 and TGF-β1 decreased after 72 hours. EpCAMxCD3 was shown to monovalently activate non-stimulated PBMCs. Furthermore, *in vitro* experiments in collagen gels showed the ability of bsAb EpCAMxCD3 to target lymphocytes to the tumor cells. EpCAMxCD3 mediated a prolonged contact time without affecting the migratory proportion and velocity of lymphocytes.

2.4.6 Infiltration of BxPC3 + L and BxPc-3 + TRAIL-L xenografts with host macrophages

EpCAMxCD3 increased the anti-tumor efficiency of TRAIL-L and was effective in BxPc-3 + TRAIL-L xenografts. At the time of analysis, a significantly reduced number of proliferating cells and a diminished blood vessel density were observed after the treatment. However, the involvement of apoptosis as detected by immunohistochemistry can be excluded. In addition, necrotic areas could not be observed in the tumor tissues (data not shown).

With the observed production of cytokines by lymphocytes in 3D tumor reconstructs *in vitro*, the cytokine production was analysed in the tumor tissues. Tumor extracts from BxPc-3 + L xenografts treated with EpCAMxCD3 (1 mg/kg) were compared to tumor lysates from BxPc-3 + L xenografts treated with PBS for their local cytokine expression at the endpoint of the treatment at day 23 (Fig 24 A). Detectable levels of sIACM-1, IL-1α, IL-1β, IL-1ra, MIF and Serpin E1 could be found. The only difference between EpCAMxCD3 and PBS treated BxPc-3 + L xenografts, was the absence of sICAM-1 in bsAb treated mice. Compared to the *in vitro* cytokine levels, the detected cytokine levels were lower and less cytokines could be detected in the tumor.

The observation, that these cytokines were present in the tumor tissue, led to the question, whether these chemoattractants would affect immune cells of the mouse. Consequently, BxPc-3 and PC-3 tumor tissues were analysed for the infiltration with mouse immune cells. CD68^{+} - and F4/80^{+} - positive mouse macrophages and single Gr-1^{+} -positive granulocytes were detected in the xenografts. In all tumors, CD68^{+} and F4/80^{+} macrophages were found at the rim in the periphery of the tumor and inside the stroma. In BxPc-3 xenografts a clear difference could be detected between tumors, which had received co-injected TRAIL-L or pre-activated lymphocytes with EpCAMxCD3 treatment and tumors, which had received PBS. EpCAMxCD3 treatment of BxPc-3 tumors promoted the infiltration of tumor islets with

CD68$^+$ and F4/80$^+$ macrophages. In the PBS group, CD68$^+$ and F4/80$^+$ macrophages were detected at the rim and in the outer stroma of the tumors. In the EpCAMxCD3 treated groups, macrophages could be found to penetrate deeper into the tumor stroma and more single infiltrating cells could be detected inside the tumor islets (Fig 24, data not shown).

Also, the possibility of a local NF-κB mediated inflammation was analysed. Immunohistochemical analysis for NF-κB by staining for c-Rel and Rel A were negative (data not shown).

Summarized, the cytokine production by co-transplanted lymphocytes in the xenografts, attracted host CD68$^+$ and F4/80$^+$ macrophages into the tumor islets, without inducing a NF-κB mediated inflammation.
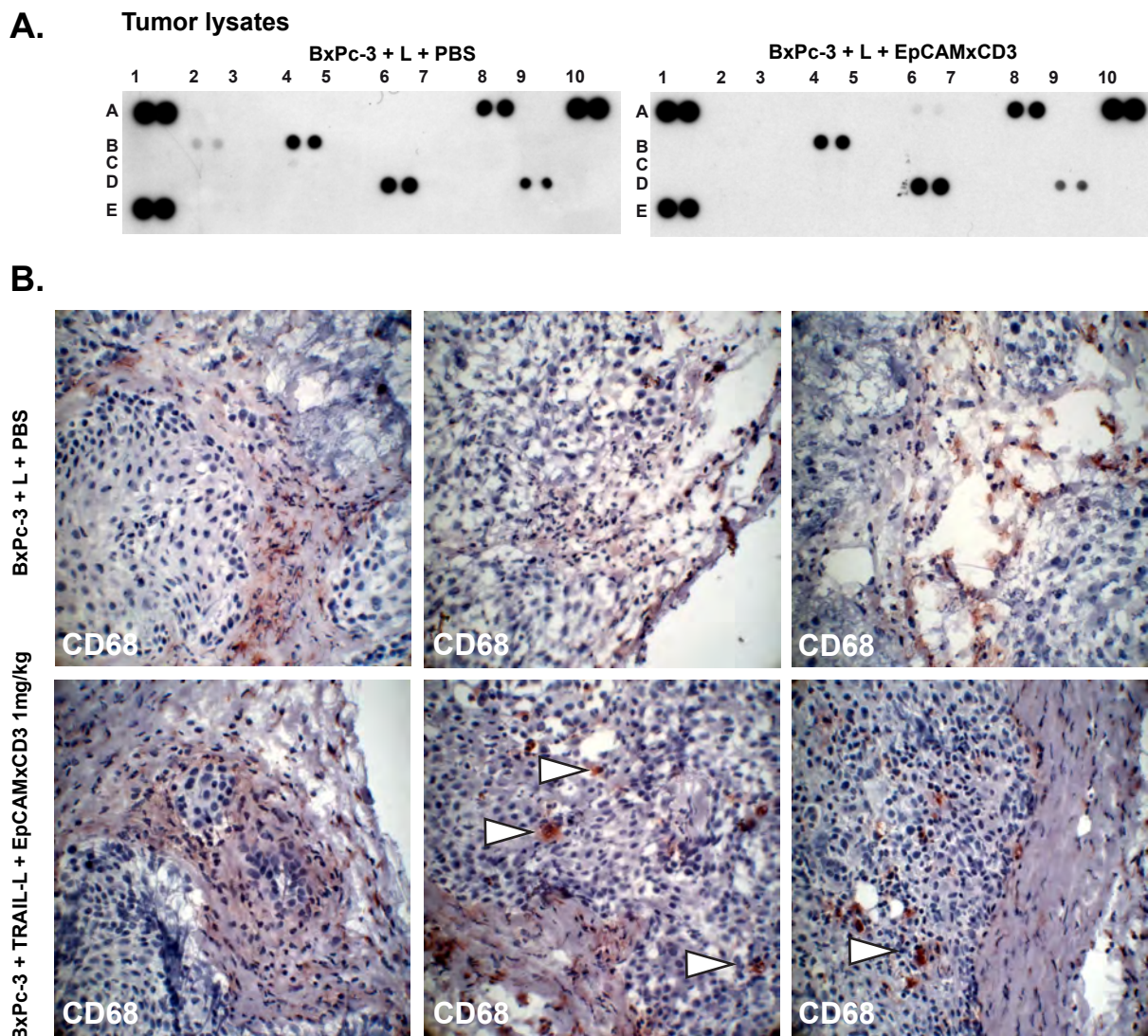
Fig 24 Effects of bsAb EpCAMxCD3 on cytokine production in tumor lysates and effects of bsAb EpCAMxCD3 and co-injected TRAIL-L on xenograft infiltration with host macrophages

(A) To analyse and compare the cytokine panels *in vivo*, tumor lysates were collected and cytokines were detected using a human cytokine protein array kit. X-ray images of membranes with spots for cytokines in pooled tumor lysates from of BxPc-3 + L xenografts treated with bsAb EpCAMxCD3 or with PBS. Three pairs of positive control spot are located in the

corner of each array. The location of the protein spots on the membranes is indicated by numerical (1-12) and literal (A-E) coordinates. MIF (D6), CXCL-1/GROα (A6), IL-1α (B2), IL-13 (C4), Serpin E1 (D9), IL-1Ra (B4) and sICAM-1 (A8) could be detected in tumor lysates at the EpCAMxCD3 or PBS treatment endpoint. (B) Cryosections of BxPc-3 xenografts were analysed for the infiltration with host immune cells by immunohistochemistry. Representative stainings from established BxPc-3 + L tumors treated PBS compared to BxPc-3 + TRAIL-L treated with EpCAMxCD3 at a dose of 1 mg/kg are show. Tumor tissues were stained for mouse CD68; arrows indicate infiltrating host cells. 400x magnification.

2.4.7 EpCAMxCD3 treatment in developed BxPc-3 xenografts

The transplantation of tumor cells mixed with effector cells is an experimental model, which is described in the literature. However, this co-injection does not reflect the clinical situation very well, when the cancer is already fully developed. To make the results more comparable to a clinical situation, another xenograft model was used. The pancreatic BxPc-3 cell line was chosen due to the greater sensitivity to EpCAMxCD3 treatment compared to prostate PC-3 cell line in the previous experiments.

2.4.7.1 Growth retardation of developed BxPc-3 xenografts by bsAb EpCAMxCD3 treatment and co-injection of TRAIL-L

In this model, NOD/SCID mice were *s.c.* transplanted with BxPc-3 tumor cells. At the time, when tumors reached an average size of 80 mm^3, TRAIL-L were *s.c.* injected in the periphery of the established tumor. EpCAMxCD3 treatment started at the time of TRAIL-L transplantation and was administered *i.p.* (Fig 25 IV.) The animals received i) *s.c.* TRAIL-L in combination with EpCAMxCD3 treatment at a dose of 0.1 mg/kg, ii) *s.c.* TRAIL-L in combination with EpCAMxCD3 treatment at a dose of 0.01 mg/kg and control groups received iii) *s.c.* TRAIL-L alone, iv) EpCAMxCD3 treatment alone at a dose of 0.1 mg/kg or v) PBS. The treatment was repeated three times with a three-day interval.

Tumor measurements were started with the begin of the EpCAMxCD3 treatment on day twelve. Repeated measurement of tumor growth over a period of ten days revealed no significant difference in tumor volume and tumor weight, due to massive intra-tumoral cysts in the groups, which had received TRAIL-L alone or in combination with EpCAMxCD3 groups (Fig 25 A). The PBS treated control group did not have detectable cysts (data not shown). Therefore, the tumor were analysed with ImageJ software for their vital tissue areas. Hematoxylin and eosin stainings of cross-tumor cryo sections were analysed for their viable tumor area. The groups that had received TRAIL-L alone, EpCAMxCD3 treatment alone and TRAIL-L in combination with EpCAMxCD3 treatment showed an approximately 40% reduced viable tumor area compared to the cyst-free PBS control group (Fig 25 C, D). The

largest cyst were found in the group that received TRAIL-L and EpCAMxCD3 at a dose of 0.1 mg/kg.

To evaluate the short term effect of the EpCAMxCD3 treatment and the transplanted TRAIL-L, a group of animals was analysed at an early time point after three days (after the begin of the bsAb treatment). Ina ll groups, which had received TRAIL-L alone or in combination with EpCAMxCD3 intratumoral cysts were detected as early as 3 days after the initiation of the treatment on day 12 (Fig 25 D). The PBS treated control group did not have detectable cysts.

2.4.7.2 Proliferation, blood vessel density and apoptosis induction in developed BxPc-3 xenografts treated by bsAb EpCAMxCD3 and transplanted with TRAIL-L

The tumor tissues were analysed for changes in proliferation, blood vessel density and apoptosis induction. The CD31$^+$ blood vessel density was significantly reduced in all groups, which had received TRAIL-L alone or in combination with EpCAMxCD3, compared to the PBS control group. The density and percentage of active caspase 3 and TUNEL staining revealed no significant difference between the groups (Fig 25 B).

Examples of immunohistochemical stainings from BxPc-3 xenografts treated with PBS compared with BxPc-3 xenografts with *s.c.* injected TRAIL-L in combination with 0.1 mg/kg EpCAMxCD3 treatment are shown in (Fig 26).
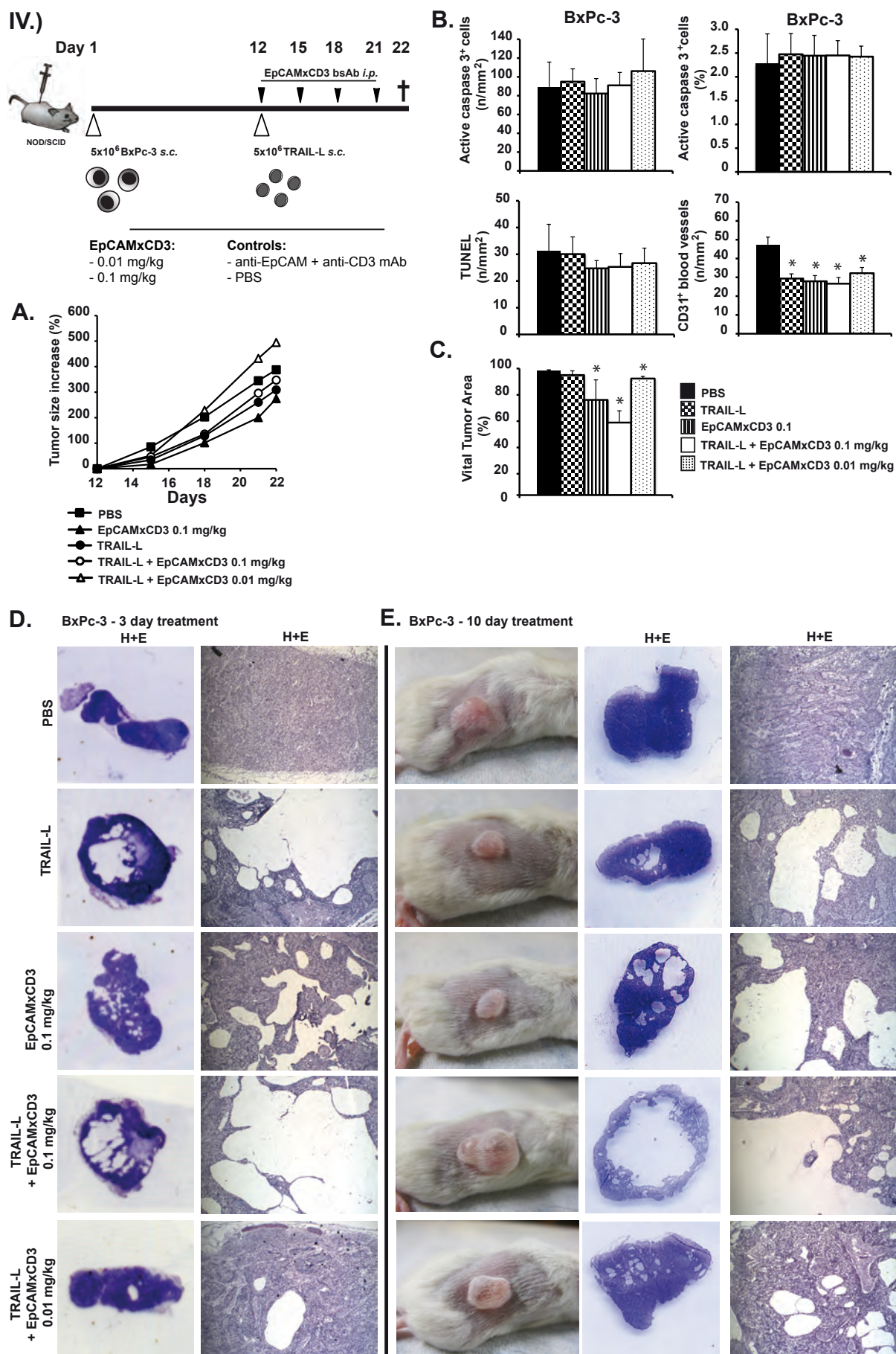
Fig 25 Efficiency of bsAb EpCAMxCD3 treatment and *s.c.* injection of TRAIL-L in developed BxPc-3 xenografts

(V.) Scheme of *in vivo* experiment. NOD/SCID mice were *s.c.* injected with BxPc-3 pancreatic tumor cells ($5x10^6$). TRAIL-L were *s.c.* injected in combination with EpCAMxCD3 treatment when tumors reached a size 80 mm^3 at day 12. On this day animals (n=5 per group) were *s.c.* injected with TRAIL-L ($5x10^6$) around the tumor. The treatment with bsAb EpCAMxCD3 or controls was administered to the animals the same day by *i.p.* injections. Treatment was repeated 3 times with a three day interval as described in M&M. Animals either received *s.c.* TRAIL-L in combination with EpCAMxCD3 treatment at a dose of 0.1 mg/kg, *s.c.* TRAIL-L in combination with EpCAMxCD3 treatment at a dose of 0.01 mg/kg, control groups received *s.c.* TRAIL-L alone, EpCAMxCD3 treatment alone at a dose of 0.1 mg/kg or PBS. (A) Relative size increase of the tumors is shown from day 12. (B, C) To evaluate whether the anti-tumor effects of TRAIL-L and EpCAMxCD3 were due to apoptosis induction, BxPc-3 tumor samples were subjected to TUNEL analysis and to immunohistochemistry to detect active caspase 3. Density and percentage of apoptotic cells in stained for active caspase 3 and tissue samples subjected to TUNEL assay. Changes in blood vessel density were analysed by immunohistochemistry stained for CD31. (D, E) One group of animals was sacrificed 3 days after the start of the treatment. Tumor morphology and intra-tumoral cyst occurrence was analysed in tumor cross sections. BxPc-3 xenografts treated for 10 days and tumors treated for 3 days were analysed by hematoxylin and eosin stainings (HE). Pictures of treated animals and HE stainings as cross sections. 100x magnification. (B) Analysis of full tumor cross sections for vital tumor area analysed by ImageJ software. $*$ p<0.05.
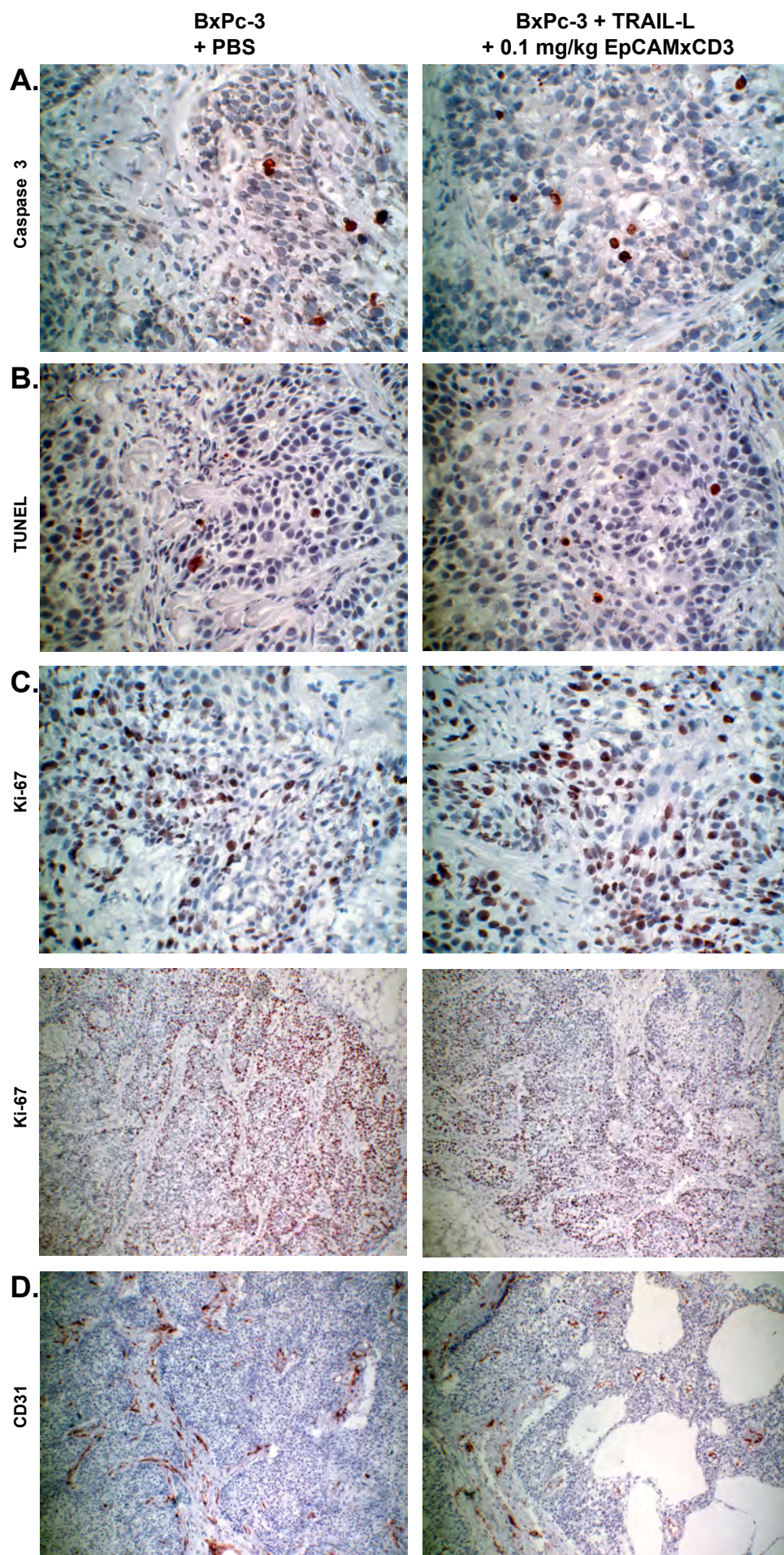
Fig 26 Immunohistochemistry of developed BxPc-3 xenografts after bsAb EpCAMxCD3 treatment and injection of TRAIL-L

Representative sample picture of cryosections of developed BxPc-3 xenografts stained and analysed for active caspase 3, TUNEL, Ki-67 and CD31 by immunohistochemistry. Pictures from control BxPc-3 tumors with PBS and BxPc-3 tumors after injection of TRAIL-L and EpCAMxCD3 treatment at a dose of 0.1 mg/kg are shown. (A, B) Apoptosis induction (active caspase 3 and TUNEL). 400x magnification. (C) Proliferation (Ki-67) upper panel: 400x magnification, lower panel: 100x magnification. And (D) blood vessel density (CD31) 250x magnification.

2.4.7.3 Infiltration of BxPc-3 xenografts with host macrophages

Many of the cytokines detected in 3D tumor reconstructs and in the tumor lysates of BxPc-3 + L and BxPc-3 + TRAIL-L xenografts were chemokines. Therefore, BxPc-3 tumor tissues were analysed for potential infiltrating host cells. Cryosections were stained for CD68$^+$ and F4/80$^+$ host macrophages. Mouse cells positive for CD68 and F4/80 were detected at the rim and to a different extend inside the stroma in all animals. In BxPc-3 xenografts with transplanted TRAIL-L alone, with EpCAMxCD3 treatment alone or with transplanted TRAIL-L in combination with EpCAMxCD3 treatment single infiltrating CD68$^+$ and F4/80$^+$ host cells could be detected inside the tumor islets. In the PBS treated control group, no single infiltrating cells could be detected. A comparison between the xenograft models revealed further differences. In BxPc-3 derived xenografts with co-injected lymphocytes: BxPc-3 + L and BxPc-3 +TRAIL-L, single infiltrating F4/80$^+$ host cells could be detected inside BxPc-3 + TRAIL-L tumors treated with EpCAMxCD3 at day 23 after cell transplantation (= 20 days after start of the bsAb treatment) (Fig 27 A). Compared to these observations, even more F4/80$^+$ host cells could be detected inside developed BxPc-3 tumors after 10 days (Fig 27 B) and after 3 days of treatment with EpCAMxCD3 (Fig 27 C).

Taken together, in the mouse model with developed BxPc-3 xenografts, EpCAMxCD3 treatment was most effective in combination with *s.c.* transplanted TRAIL-L. The tumor tissue revealed a significant reduction of CD31+ blood vessel density and a reduced number of proliferating cells in tumors, which had been treated with EpCAMxCD3 transplanted with TRAIL-L. The data indicates that apoptosis induction was not the major mechanism for the observed reduced vital tumor area in BxPc-3 xenografts after EpCAMxCD3 treatment at the time of the tumor tissue analysis. This verified the anti-tumor effects of EpCAMxCD3 son the growth retardation in the BxPc-3 + L and the BxPc-3 + TRAIL-L xenografts. The EpCAMxCD3 effects were independent of the application of the lymphocytes. The presence and increased infiltration with mouse macrophages suggests a contribution of these host cells to the induced anti-tumor effects by EpCAMxCD3 and TRAIL-L.

A

BxPc-3 + L
23 day treatment

PBS

F4/80

F4/80

BxPc-3 + TRAIL-L
23 day treatment

EpCAMxCD3 0.1 mg/kg

F4/80

F4/

B

BxPc-3
10 day treatment

EpCAMxCD3 0.1 mg/kg

F4/80

F4/80

C

BxPc-3
3 day treatment

EpCAMxCD3 0.1 mg/kg

F4/80

F4/80
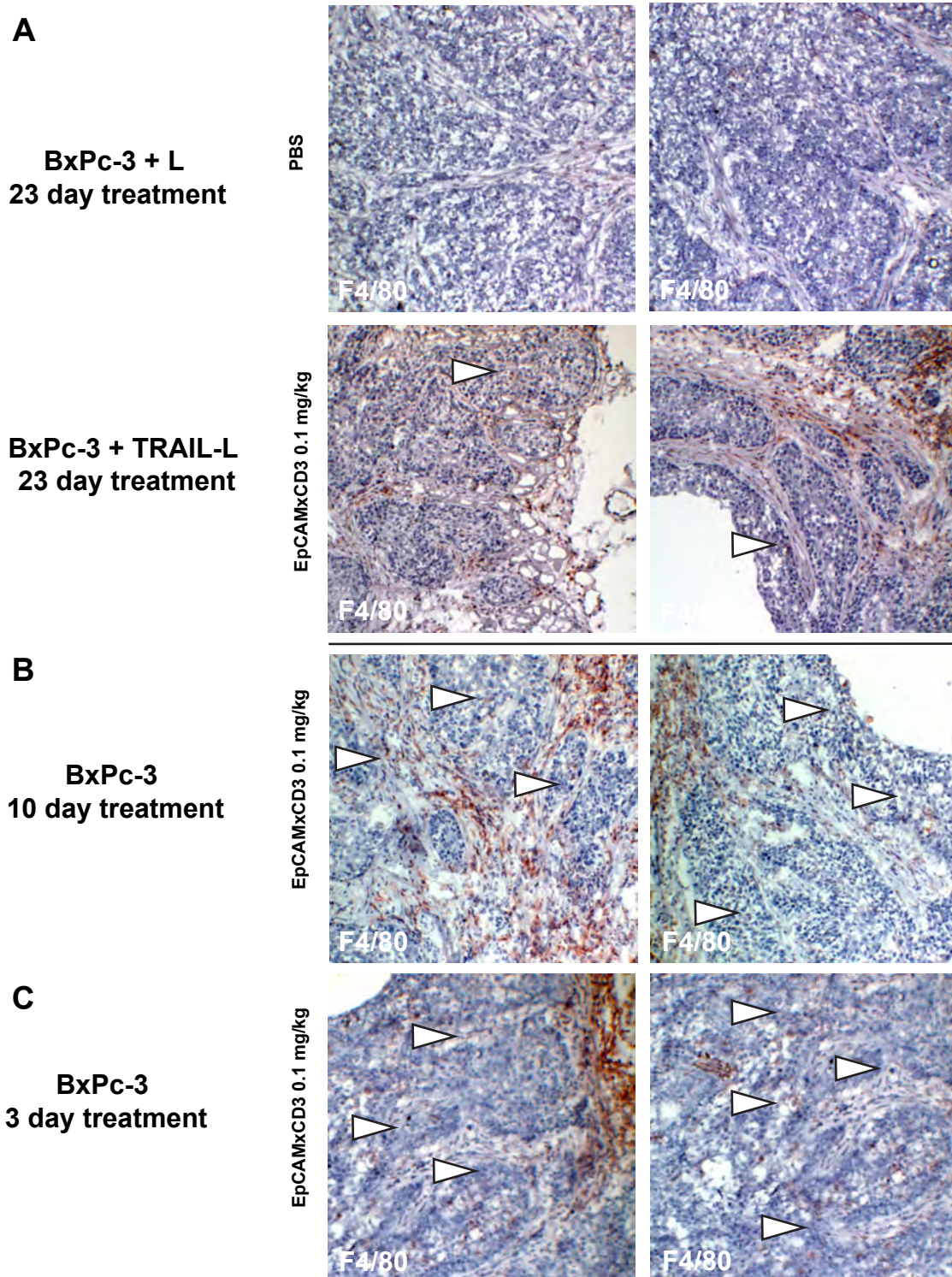
Fig 27 Effects of bsAb EpCAMxCD3 treatment and co-injection of TRAIL-L on xenograft infiltration with host macrophages

Cryosections of BxPc-3, BxPc-3 + L and BxPc-3 + TRAIL-L xenografts were analysed for the infiltration with host immune cells by immunohistochemistry. (A) Representative stainings from BxPc-3 + L tumors treated with PBS compared to BxPc-3 + TRAIL-L treated with EpCAMxCD3 at a dose of 0.1 mg/kg are show at day 23 after cell transplantation and 20 days after begin of the bsAb treatment. (B) Representative stainings from developed BxPc-3 tumors treated with EpCAMxCD3 at a dose of 0.1 mg/kg are show at day 22 after cell transplantation and 10 days after begin of the bsAb treatment. (C) Representative stainings from established BxPc-3 tumors treated with EpCAMxCD3 at a dose of 0.1 mg/kg are show at day 15 after cell transplantation and 3 days after begin of the bsAb treatment. Tumor tissues were stained for mouse F4/80, arrows indicate infiltrating cells. 250x magnification.

3   Materials and Methods

3.1   Materials

3.1.1   Equipment and consumables

Analytic balance scale (Mettler P220)	Mettler Toledo, Gießen
Autoradiography film (Amersham HyperfilmTM ECL)	GE Healthcare Ltd, Pollards Wood, UK
Caliper	
Cell culture dishes	TPP, Trasadingen, Switzerland
Cell culture flasks	TPP, Trasadingen, Switzerland
Cell culture plates	TPP, Trasadingen, Switzerland
Centrifuge	
- Biofuge 15 R	Heraeus, Hanau
- Varifuge 3.0 R	Heraeus, Hanau
Centrifuge tubes (15 ml and 50 ml)	TPP, Trasadingen, Switzerland
Chamber slides	Nunc, Rochester, NY, USA
CO2 -incubator (Sanyo MCO-20AIC)	MS Laborgeräte, Wiesloch
CO2 incubator	
Coverslips	Knittelgläser, Braunschweig
Cryostat (CM 3050)	Leica Microsystems, Wetzlar
Cryotubes	Nunc, Wiesbaden
Electrophoresis power supply (Phero-Stab. 500V)	Biotec Fisher, Reiskirchen
Electrophoresis unit (Horizon 11-14)	Life, Karlsruhe
Embedding molds	Labonord, Mönchengladbach
FACS LSRII	Becton Dickinson, Heidelberg
Gel documentation system (E-Box)	Vilber Lourmat, Switzerland
Gloves	VWR, Bruchsal
Hemacytometer glasses	Fisher Scientific, Nidderau
Ice maschine (AF 80)	Scotsman (Enodis), Herborn
Laminar flow hood	Heraeus, Hanau

Light microscope	Leica, Wetzlar
Magnetic stirring hot plate (MR 3001)	Heidolph, Schwabach
Microcentrifuge (Biofuge 15R)	Heraeus, Hanau
Microcentrifuge tubes (1,5 ml and 2 ml)	Eppendorf, Hamburg
Microscope slides (Superfrost plus)	Menzel, Braunschweig
Microwave (HMT 843C)	Bosch-Siemens, München
NanoDrop® ND-1000 spectrophotometer	NanoDrop Technologies, Wilmington, USA
Neubauer hemacytometer	Sigma, Taufkirchen
Parafilm M	Neolab, Heidelberg
Pasteur pipettes	Buddenberg, Mannheim
pH-meter (pH 538)	WTW, Weilheim
Pipette controller	pipetus Integra, Fernwald
Pipette tips (20 µL, 200 µL, 1000 µL)	Starlab, Ahrensburg
Pipettes	Gilson, Middleton, WI, USA
Power supply (Phero-Stab.500)	Biotech Fischer, Reiskirchen
Reagent tubes (1,5 ml, 2 ml)	Sarstedt, Nümbrecht
Repeat pipettor, multistep	Eppendorf, Hamburg
Shaker (Unimax 2010)	Heidolph, Schwabach
Spectrophotometer (Smart Spec 3000)	Biorad, München
Stericup-Filter (0,22 µm)	Millipore, Eschborn
Thermomixer	Eppendorf, Hamburg
Vortexer (REAX 2000)	Heidolph, Schwabach
Waterbath	Kottermann, Hänsingen
Weighing dishes	Neolab, Heidelberg

3.1.2   Media, supplements and reagents for cell culture

DMSO (Dimethylsulfoxide, >99%)	AppliChem, Darmstadt
Albumin (fractionV)	Serva, Heidelberg, Germany
Biocoll	Biochrom, Berlin
Calcium chloride	Sigma, Steinheim

Chloroquine	Sigma, Steinheim
Collagen	
Disodiumhydrogenphosphate	Roth, Karlsruhe
DMEM (Dulbecco's Modified Eagle Medium, high glucose)	PAA, Cölbe
Doxycycline	Sigma, Steinheim
Dulbecco's phosphate buffered saline	Invitrogen, Karlsruhe
FBS (Fetal Bovine Serum)	Sigma, Steinheim
HBSS, Hank's buffered salt solution (10x)	Sigma, Steinheim
HEPES	PAA, Cölbe
Human AB serum	Sigma, Steinheim
Human AB Serum	Invitrogen, Karlsruhe, Germany
IL-2	Biosource, Camarillo, CA, USA
L-glutamine	PAA, Cölbe
PBS (Phosphate buffered saline)	Gibco/Invitrogen, Karlsruhe
Penicillin-Streptomycin	PAA, Cölbe
Polybrene	Sigma, Steinheim
Protamine sulfate	Sigma, Steinheim
Retronectin	Takara, Saint-Germain-en-Laye, France
RPMI1640 Medium	PAA, Cölbe
Sodium azide	Roth, Karlsruhe
Sodium chloride	Roth, Karlsruhe
Trypanblue	Biozol, Eching
Trypsin-EDTA	PAA, Cölbe
Water (Aqua ad injectabilia)	Braun, Melsungen
x-vivo	Cambrex, Charles City, USA

3.1.3   Kits

DAB Kit	Invitrogen, Karlsruhe, Germany
Human apoptosis antibody array kit (Proteome	R&D Systems, Abingdon, UK

Profiler)

Human cytokine antibody array kit (Proteome Profiler)	R&D Systems, Abingdon, UK
IFN-γ ELISA Kit	Cell Sciences, Canton, MA, USA
TNF-α ELISA Kit	R&D Systems, Abingdon, UK
TUNEL (TACS TdT in situ apoptosis detection kit)	R&D Systems, Abingdon, UK
Vectastain ABC Elite Kit	Linaris, Wertheim-Bettingen, Germany

3.1.4   Chemicals and biochemicals

7AAD	Sigma, Steinheim
Acetone	J.T.Baker, Deventer, NL
Agar-Agar	AppliChem, Darmstadt
Agarose	Life Technologies, Karlsruhe
Ampicilline	Roth, Karlsruhe
Avidin D: Texas Red	Vector, Burlingame, CA, USA
Avidin-Biotin Blocking Kit	Vector, Burlingame, CA, USA
Biocoll	Inno-Train Diagnostics Gmbh, Kronberg, Germany
Bovine serum albumin (BSA)	New England Biolabs, Frankfurt
Citric acid	Sigma, Steinheim
DAPI (4',6-Diamidino-2-phenylindol Dihydrochlorid)	Sigma, Steinheim
Di-sodium hydrogen phosphate	Merck, Darmstadt
Diaminobenzidine (DAB) Kit	Invitrogen, Karlsruhe
DMSO (Dimethylsulphoxide)	Roth, Karlsruhe
DNA Isolation Kit (DNeasy™ Tissue Kit)	Qiagen, Hilden
DNA Ladder (Mass ruler DNA ladder mix)	Fermentas, St. Leon-Rot
EDTA-disodium	Sigma, Steinheim
embedding medium for cryo-sections, O.C.T.	Engelbrecht, Edermünde

Entellan (mounting medium)	VWR, Bruchsal
Ethanol	Roth, Karlsruhe
Ethidium bromide	Applichem, Darmstadt
Fluoromount G	Biozol, Eching
Gel extraction and PCR Purification Kit	Qiagen, Hilden
Gel extraction Kit (QIAquick™)	Qiagen, Hilden
Glycerine	Roth, Karlsruhe
Goat serum	Alexis, Grünberg
Hematoxylin solution, (Mayer's)	Sigma, Steinheim
Heparin	StemCell Technologies Inc., Vancouver, BC, Canada
Hydrochloric acid	J.T.Baker, Deventer, NL
Iodoacetic acid	Sigma, Steinheim
Isopropanol	Roth, Karlsruhe
Kanamycin	Roth, Karlsruhe
Klenow fragment	Fermentas, St. Leon-Rot
Manganese chloride	Roth, Karlsruhe
Methanol	Roth, Karlsruhe
MOPS	Sigma, Steinheim
Mung bean nuclease	Fermentas, St. Leon-Rot
Paraformaldehyde (37%)	Merck, Darmstadt
Pfu Polymerase	Roche, Basel, Switzerland
PI	Sigma, Steinheim
Plasmid Maxipreparation Kit	Qiagen, Hilden
Plasmid Minipreparation Kit	Qiagen, Hilden
Potassium chloride	Riedel- de Haën, Seelze
Potassium dihydrogenphosphate	Merck, Darmstadt
Pwo Polymerase	Roche, Basel, Switzerland
Restriction enzymes	NEB
Rubidium chloride	Sigma, Steinheim

Sodium acetate	Fluka, Buchs, CH
Sodium chloride	Merck, Darmstadt
Sodium citrate	Riedel- de Haën, Seelze
T4-DNA-ligase	Fermentas, St. Leon-Rot
Tris Base	Sigma, Steinheim
Triton X-100	Sigma, Steinheim
Trypton	Life Technologies, Karlsruhe
Tween-20	Serva, Heidelberg
Xylene	Merck, Darmstadt
Xylene-Cyanol	Sigma, Steinheim
Yeast Extract	Life Technologies, Karlsruhe
ZytoChem-Plus HRP polymer Kit	Zytomed Systems, Berlin

3.1.5 Antibodies

3.1.5.1 Antibodies *in vivo*

EpCAMxCD3 (HEA125xOKT3) and CD19xCD3 (HD37xOKT3) bsAb were produced by hybrid-hybridoma technique and purified by affinity chromatography over protein A-Sepharose CL-4B (Amersham Pharmacia Biotech, Freiburg, Germany) followed by HPLC purification on a Bakerbond ABx column (J.T. Baker, Phillipsburg, NJ) as described [128]. Parental anti-human EpCAM hybridoma (HEA125, IgG_1) was raised in the laboratory of G. Moldenhauer [106, 131]. Hybridoma OKT3 (IgG_{2A}) directed against the ε-chain of the CD3 molecule was purchased from the ATCC. Both parental mAb were purified by affinity chromatography.

3.1.5.2 Antibodies for FACS

goat anti mouse	Jackson Immunoresearch
goat anti mouse –PE	Alexis (Enzo), Farmingdale, NY, USA
iso-type control – FITC	Jackson Immunoresearch, West Grove, PA, USA
iso-type control – PE	Jackson Immunoresearch, West Grove, PA,

USA

Mouse anti human MHC-class I (HLA-A,B,C) mAb	BD Pharmingen, Heidelberg, Germany
Mouse anti human MHC-class I mAb	W6/32 hybridoma, own production
mouse anti human TRAIL (2E5) mAb	Alexis (Enzo), Farmingdale, NY, USA
mouse anti human CD25 mAb	BD Pharmingen, Heidelberg, Germany
mouse anti human CD4 mAb	BD Pharmingen, Heidelberg, Germany
mouse anti human CD45 mAb	BD Pharmingen, Heidelberg, Germany
mouse anti human CD69 mAb	BD Pharmingen, Heidelberg, Germany
mouse anti human CD8 mAb	BD Pharmingen, Heidelberg, Germany
mouse anti human CD95 mAb	BD Pharmingen, Heidelberg, Germany
mouse anti human EpCAM mAb (HEA125)	homemade
mouse anti human TRAIL-R1 mAb	ProSci, Poway, CA, USA
mouse anti human TRAIL-R2 mAb	ProSci, Poway, CA, USA

3.1.5.3 Antibodies for immunohistochemistry

rat anti mouse F4/80 mAb	Acris Antibodies, herford, Germany
mouse anti human CD45 mAb	BD Pharmingen, Heidelberg, Germany
mouse anti human CD16 mAb	BD Pharmingen, Heidelberg, Germany
mouse anti human CD4 mAb	BD Pharmingen, Heidelberg, Germany
mouse anti humam CD8 mAb	BD Pharmingen, Heidelberg, Germany
rat anti mouse CD31 mAb	BD Pharmingen, Heidelberg, Germany
rat anti mouse Gr-1 (Ly-6g/Ly-6C) mAb	BioLegend, San Diego, CA, USA
mouse anti human c-rel mAb	Cell Signaling, Danvers, MA, USA

mouse anti human Rel A mAb	Cell Signaling, Danvers, MA, USA
mouse anti GFP (JL-8) mAb	Clontech, Montain View, CA, USA
mouse anti human EpCAM mAb (HEA125)	Homemade
goat anti rat Alexei Fluor 594 IgG	Molecular Probes, Eugene, USA
goat anti mouse Alexa Fluor 488 IgG	Molecular Probes, Eugene, USA
rabbit anti human TRAIL-R1 mAb	ProSci, Poway, CA, USA
rabbit anti human TRAIL-R2	ProSci, Poway, CA, USA
rabbit anti human active caspase 3 pAb	R&D Systems, Abingdon, UK
rabbit anti humanactive caspase 3 pAb	R&D Systems, Abingdon, UK
rat anti mouse CD68 mAb	Serotec, Oxford, UK
rabbit anti human Ki-67 mAb	Thermo Scientific, Rockford, IL, USA
goat anti mouse IgG biotynilated	Vector, Burlingame, CA, USA
rabbit anti rat IgG biotynilated	Vector, Burlingame, CA, USA
panCK	Sigma Aldrich

3.1.6 Primers

Primer for the cloning of the peptide linker P2A between the two genes TRAIL and EGFP into the pV3TP2AE vector.

Nucleic acid sequence P2A:

5'-gga agc ggc gcc acg aac ttc tct ctg tta aag caa gca gga gac gtg gaa gaa aac ccc ggt ccc-3'

5' primer TRAIL in and P2A (1)

5'-ttc cac gtc tcc tgc ttg ctt taa cag aga gaa gtt cgt ggc gcc gct tcc gcc aac taa aaa ggc ccc gaa aaa act gg-3'

3' primer EGFP in and P2A (2)

5'-aac ttc tct ctg tta aag caa gca gga gac gtg gaa gaa aac ccc ggt ccc atg gcc aca acc atg gtg agc aag ggc gag ga-3'

<u>5' primer TRAIL out with SpeI site (3)</u>

5'-cag act agt cac cat ggc tat gat gga ggt ccg-3'

<u>3' primer EGFP out with BamHI site (4)</u>

5'-cct gga tcc tca ctt gta cag ctc gtc cat gcc-3'

3.1.7 Lentiviral plasmids and vectors

All plasmids for production of lentiviral particles contain a SV40 origin of replication and an ampicilline resistance gene.

<u>pV3TP2AE</u>

The vector was originally created by Vogel *et al.* [129] and modified for the expression of human TRAIL and EGFP (short: pV3TP2AE) by standard cloning techniques. The binary vector is a second generation self-inactivating SIN vector that allows a conditional expression of the transgene under the control of a tet-responsive promotor element (TRE) in the presence of doxycycline (Tet-on). Binding of this rtTA2-M2 transactivator to 3 copies upstream of a minimal cytamegalovirus (CMVmin) promoter activates transcription. The TRAIL and EGFP genes were combined by the Picorna virus-derived peptide elements P2A (2A element of porcine teschovirus) as described by Leisegang *et al.* 2008 [130]). The pV3TP2AE construct contains the HIV-1 5'-LTR consisting of the truncated unique sequence 3 (SIN U3), the unique sequence 5 (U5) and the redundant sequence R. The rtTA2M2 reverse transactivator is under the control of the phosphoglycerate kinase (pPGK) promotor and is followed by the bovine growth hormone polyadenylationsignal (BGH polyA). Further elements are the central DNA flap sequence (TRIP) and the woodchuck hepatitis virus post-transcriptional regulatory element (WPRE).

<u>pV3E</u>

The vector pV3E, served as control vector for pV3TP2AE and was cloned accordingly just with the insertion of the EGFP gene.

psPAX2 (kindly provided by L. Naldini, Turino, Italy)

CMVenh | Gag / Pro | Pol | dV | tat/rev | RRE | pA

The psPAX2 packaging construct is coding for the proteins needed for packaging of the viral vector in the producer cell. It carries the gag, pol, tat and rev genes which express the HIV-1 proteins for the capsid/nucleocapsid (gag), the polymerase/reverse transcriptase/integrase (pol), transcription transactivating protein Tat (tat) and expression regulating protein Rev (rev).

pMD2.G (kindly provided by L. Naldini, Turino, Italy)

CMV | βG-Intron | VSV.G | pA

The pMD2.VSV-G envelope construct contains the Vesicular Stomatitis Virus Glycoprotein (VSV-G) and the first intron of the human β-globine gene (β G-Intron) [132]. The VSV-G is used to pseudotype the viral envelope in order to transduce a broad host range.

3.1.8 Bacterial strains

For all transformation experiments *E. coli* K12 were made chemo-competent as described in (Hanahan, 1983). For lentiviral vectors only *recA*-negative strains HB101 (from Life Technologies, Rockville, MD, USA) and TOP10 (Topo-TA cloning Kit; Invitrogen, Karlsruhe) were used to prevent inter- and intramolecular recombination.

HB101

Genotype: F$^-$ *mcr*B *mrr hsd*S20 (r$_B^-$, m$_B^-$) *rec*A13 *sup*E44 *ara*14 *gal*K2 *lac*Y1 *pro*A2

*rps*L20(Sm^r) *xy*15 λ$^-$ *leu mtl*1

TOP10

Genotype: F$^-$ *mcr*A Δ(*mrr-hsd*RMS-*mcr*BC) φ80 *lac*ZΔM15 Δ *lac*X74 *rec*A1 *ara*D139 Δ(*araleu*) 7697 *gal*U *gal*K *rps*L (Str^R) *end*A1 *nup*G

3.1.9 Commercial cell lines

Primary skin fibroblasts were provided by Dr. H.-J. Stark (DKFZ, Heidelberg, Germany).

The packaging cell lines human epithelial kidney HEK-293T cell line was obtained from American Type Culture Collection (Manassas, VA, USA). Pancreatic cancer cell lines AsPC-1, BxPc-3, Colo357 and MIA-PaCa2, and prostate cell lines PC-3, DU-145 and LNCap were obtained from the American Type Culture Collection (Manassas, VA, USA). Fibroblasts, 293T and pancreatic cell lines were cultured in DMEM medium supplemented with 10% FCS and 10 mM HEPES and prostate cell lines in RPMI medium supplemented with 10% FCS and 10 mM HEPES.

3.1.10 Animals

Four-to five-week-old female NOD/SCID mice (NOD.CB17-$Prkdc^{scid}$/NcrCrl), were purchased from Charles River Laboratories (L'Arbresle, France) and were house at the animal facility of the DKFZ.

3.2 Molecular methods

3.2.1 Production of competent bacteria

For production of competent bacteria, that can be transformed with DNA, the following protocol was used (Dagert and Ehrlich, 1979). Bacteria were placed on a LB-agar dish and incubated over night at 37°C. One single bacterial colony was taken up in 5 ml LB- medium and was placed over night on a shaker at 37°C. Two hundred fifty millilitre of prewarmed LB-medium were inoculated with 1 ml of this bacterial culture. The suspension was incubated at 37°C on a shaker until the bacterial suspension reached an OD_{590} value of 0.5. Then bacterial suspension was cooled on ice. All following steps were performed on ice and solutions were precooled at 4°C. Bacteria were centrifuged at 2900 g for 10 min at 4°C and pellet was mixed with 15 ml of buffer A (10 mM calcium chloride, 30 mM potassium acetate, 100 mM rubidium chloride, 79 mM mangan(II) chloride, 15% glycerine [v/v], pH 5,8). Following incubation for 2 h on ice, cells were sedimented at 1250 g for 10 min, 4°C and were mixed with 4 ml of buffer B (10 mM MOPS, 10 mM rubidium chloride, 75 mM calcium chloride, 15% glycerine [v/v], pH 7). One hundred microliter aliquots were snap frozen in liquid nitrogen and stored at -80°C.

3.2.2   Media for bacterial cell culture

<u>LB- Liquid medium</u>

For production of 5x LB-medium, 50 g Trypton, 25 g yeast extract and 25 g NaCl were diluted in 1L dH2O and autoclaved. Prior usage medium was diluted 1:5 with sterile dH2O. Ampicilline was mixed in the final medium to a concentration of 50 µg/ml.

<u>LB agar</u>

Thirty two grams of LB-agar were mixed in 1 L 1x LB-medium and autoclaved. Upon cooling down at 40°C, ampicilline (end concentration: 50 µg/ ml) was added and agar was placed in Petri dishes. Dishes were stored up to one month at 4°C.

3.2.3   Cloning of the lentiviral vector pV3TP2AE

The HIV-1-based Tet-on lentiviral vector which was used in all lymphocyte transduction experiments. The vector was originally created by Vogel *et al.* [129] and modified for the expression of human TRAIL and EGFP (short: pV3T2AE) by standard cloning techniques. The binary vector is a second generation self-inactivating SIN vector that allows a conditional expression of the transgene under the control of a tet-responsive promotor element (TRE) in the presence of doxycycline (Tet-on). Binding of this rtTA2-M2 transactivator to 3 copies upstream of a minimal cytamegalovirus (CMVmin) promoter activates transcription. The TRAIL and EGFP genes were combined by the Picorna virus-derived peptide elements P2A (2A element of porcine teschovirus) as described by Leisegang *et al.* 2008 [130]). The pV3T2AE construct was verified by sequencing.
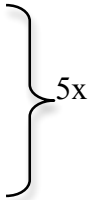
The TRAIL and the EGFP gene were amplified and linked by the P2A peptide linker. Therefore, the TRAIL and the EGFP gene were amplified each from the pHRPS-CMV-TRAIL-IRES-EGFP-WPRE plasmid (Till Wenger (44) modified from the original Tronoplasmid pWPTS-GFP and Clontech pIRES2-EGFP (4)) by a touch down PCR with primers pairs also encoding the P2A amino acid sequence.

Touch-down PCR

with the primer pairs (1) and (3) for the TRAIL gene and (2) and (4) for the EGFP gene (in 3.1.6).
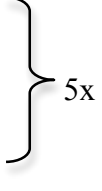
94°C 5'

94°C 30''

60°C 30''   } 5x
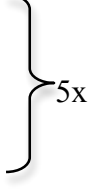
72°C 30''
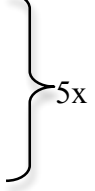
94°C 30'

57.5°C 30''   } 5x

72°C 30''
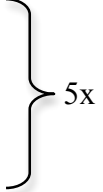
94°C 30''

55°C 30''   } 5x

72°C 30''

94°C 30''

52.5°C 30''   } 5x

72°C 30''

94°C 30''

50°C 30''   } 5x

72°C 30''

72°C 7'

cool

The resulting fragments (TRAIL-P2Apart and P2Apart-EGFP) were annealed first without primers in another touch down PCR

94°C 40''
-1°C/ 6'' } 5x
72°C 2'

and then the full length fragment (TRAIL-P2A-EGFP) amplified with the primers (3) and (4) in a standard PCR :

94°C 30''

94°C 30''
56°C 30'' } 30x
72°C 2'

72°C 7'

cool

The original lentiviral vector pd500Trip-CMVmin-WPRE (pV3) (by Vogel *et al.* [129]) was opened by restriction digest with SpeI and BamHI. The full length fragment (TRAIL-P2A-E) was also digested with SpeI and BamHI, ligated into pV3 and HB101 bacteria were transformed. Positive clones were picked by Colony PCR and amplified in HB101. The resulting plasmid was opened with SalI and NheI and the rtTA2-M2 transactivator from the plasmid pd500-PGK-rtTA2M2-BGHpolya (pV7) (by Vogel *et al.*) was ligated into the plasmid and amplified in HB101. The resulting vector pd500-BGHpolyA-rtTA2M2-BGHpolya-TRIP-CMVmin-TRAIL-P2A-EGFP-WPRE (pV3TP2AE) was verified by sequencing (Eurofins MWG Operon).

3.2.4 Transformation of bacteria

Chemically competent bacteria are able to uptake plasmids following a heat shock at 42°C. In detail, 50 µl of competent bacteria were thawed on ice and were incubated with up to 200 ng plasmid-DNA in a maximum of 10 µl dH$_2$O. Following incubation on ice for 30 min a heat

shock at 42°C was performed for 90 sec. Subsequently, the bacteria-plasmid mixture was incubated for 2 min on ice and then was mixed with 500 µl of pre-warmed LB-medium and incubated for 40 min at 37°C. Bacteria were subsequently plated on pre-warmed LB-agar dishes and incubated for 15-18 h for selection of ampicilline resistant clones.

3.2.5 Plasmid mini preparation

Following transformation, single bacterial colonies were picked and incubated over night in 5 ml LB medium (supplemented with 50 µg/ml ampicilline) on a shaker (200 rpm) at 37°C. Subsequently, bacterial cells were sedimented for 5 min at 6000rpm. The bacterial pellet was lysed and the plasmid DNA was isolated and purified according to the manufacturers recommendations (Qiagen).

3.2.6 Plasmid maxi preparation

The plasmid maxi-preparation serves for isolation of large amounts (over 100 µg) of highly purified plasmid DNA. The maxi-preparation was performed with the Plasmid Maxi preparation Kit (Qiagen) provided with DNA binding columns with silica membranes. Two hundred milliliter of bacterial over night culture were seimented for 15 min at 6000 rpm at 4°C. The bacterial pellet was lysed and the plasmid DNA was isolated and purified according to the manufacturers recommendations (Qiagen). The plasmid was purified by a subsequent ethanol precipitation.

3.2.7 Analysis of DNA purity

DNA samples were diluted in dH_2O and DNA concentration as well as DNA purity was measured spectrometrically by NanoDrop at 260 and 280 nm. An extinction of 1 at 260 nm corresponds to 50 µg/ml DNA and protein contamination is detected at 280 nm. The quotient of extinction at 260 and 280 nm (E_{260}/E_{280}) determines purity and should have a value between 1.8 and 2.

3.3 Cell biological methods

3.3.1 Culture of cell lines

Cells were cultured in an incubator at 37°C and 5% CO_2. Media were supplemented, if not indicated differently, with 10% [v/v] FCS and 10 mM HEPES (pH 7.4). Media were pre-warmed at 37°C prior use. FCS was heat-inactivated for 30 min at 56°C. For determination of

the number of viable cells, cell suspension was diluted 1:1 in Trypan blue solution (0.125%). Cells were counted using an improved Neubauer counting chamber.

3.3.2 Passaging of adherent cell lines

Media from 80-90% confluent cell cultures were aspirated and cells were washed once with 5-10 ml PBS. After aspirating PBS, 1 ml 1xTrypsin was added and cells were incubated at 37°C and 5% CO_2 until they were completely detached. Trypsin was inactivated by addition of supplemented culture medium. Cells were thoroughly resuspended followed by determination of cell concentration and split ratio.

3.3.3 Cryostorage of eukaryotic cell lines

Established cell lines were frozen at -80 °C long term storage. Cells were pelleted at 1500 rpm for 2 min. Aliquots of $5x10^6$-$1x10^7$ cells were resuspended in heat-inactivated FCS and 10% (v/v) DMSO in a total volume of 1 ml in cryotubes. To allow a constant decrease in the temperature at a rate of 1 °C per minute, cryotubes were placed in a freezing container filled with isopropanol. Subsequently, cryotubes were immediately transferred to the -80 °C freezer.

3.3.4 Thawing of cells

To avoid the toxic side effects of DMSO in freezing medium, thawing of cells was performed as fast as possible. Cryotubes were placed in the warm waterbath at 37°C until a little piece of ice clot was still visible in the cryotube. Cell suspension was transfered to 10 ml of pre-warmed supplemented cell culture medium. After centrifugation at 1500 rpm for 1 min, supernatant was removed and pellet was carefully resuspended in fresh medium in a new culture flask. Media were changed 24 h later, in order to dispose the rest of toxic DMSO. Cells were passaged after 1-2 days depending on cell growth rate.

3.3.5 Isolation of PBMCs

PBMC were isolated from peripheral blood of healthy donors by a Biocoll gradient. Donor material was obtained following the University of Heidelberg Ethical Committee approval. Fresh, heparinized blood was diluted 1:2 in ice-cold PBS supplemented with 2mM EDTA. A layer of 35ml of diluted cell suspension was added to 15ml Bicoll and was centrifuged at 400 g for 45 min at RT (without acceleration and without brakes). The interphase with the mononuclear cellswas gently aspirated, resuspended in PBS/EDTA and centrifuged at 300 g for 15 minutes. The cell pellet was resuspended in PBS/EDTA and and centrifuged at 200 g

for 10 minutes to remove platelets. This step was repeated with PBS. The PBMCs were then resuspended in X-Vivo medium supplemented with 5% [v/v] AB Serum, 4 mM L-Glutamin, 300 U/ml IL-2 and 50 ng/ml OKT3 and plated at a density of 3×10^6 cells/ml. Monocytes were removed by plastic adherence.

3.3.6 Culture of lymphocytes

The isolated PBMCs were activated for 3 days with 300 U/ml IL-2 and 50 ng/ml OKT3 and after that the medium was supplemented with 100 U/ml IL-2. IL-2 and OKT3 were supplemented to the medium every 3 days and the cells were adjusted to a density of 3×10^6 cells/ml every few days. For all experiments with pre-activated cells, lymphocytes were cultivated for five days and used on day five. For the transduction of lymphocytes, the lymphocytes were activated with 300 U/ml IL-2 and 50 ng/ml OKT3 for one day and transduced with fresh medium supplemented with 300 U/ml IL-2 and 50 ng/ml OKT3 on day two and three. After that, the medium was supplemented with 100 U/ml IL-2. IL-2 and OKT3. The transduced cells were used on day five, since they could be considered safety level S1 on that day.

3.3.7 Production of lentiviral particles

Lentiviral particles were produced in HEK-293T cells, which were transfected with lentiviral vector plasmids (3.1.7). The cell line HEK-293T (293T) derives from human embryonic kidney cells that were transformed with Typ 5-Adenovirus-DNA (Graham and van der Eb, 1973). They are also stably transfected with the T-antigen from SV40, which enables amplification of plasmids with an SV40-Replication origin (DuBridge et al., 1987). For the production of lentiviral particles 293T have to be kept in low passages (passage < 20) and subconfluent in cell culture. The calcium phosphate method was used for a transient transfection with the lentiviral plasmids. The mixture of DNA and a calcium chloride solution in a phosphate buffer leads to the formation of a DNA-calcium phosphate co- precipitate that is taken up by 293T cells through phagocytosis. From the endosomes the DNA molecule reaches the nucleus where its transient transcription takes place. Addition of chloroquine to 293T cells enhances the transfection efficiency. Chloroquine decreases acidification in the lysosomes and results in a higher stability of DNA through inhibition of lysosomal DNAses and/or swelling and displosion of endosomes (Guy et al., 1995). The plasmids required for virus production (3.1.7) contain an SV40 replication origin and thus are replicated upon transfection in 293T cells. As a result an increased number of viral transcripts and proteins

within a transfected 293T cell and thus an increased number of released viral particles is achieved. Twenty four hours prior transfection, 293T cells were cultured in 10 cm cell culture dishes. The cells should have 50 -70% confluence on the day of transduction. One hour prior to transfection the media were removed and replaced by fresh media. Immediately prior to transfection chloroquine was added to cell culture dish at an end concentration of 25 μM. 20μg transfer-vector (pV3TP2AE), 14 μg packaging construct psPAX2 (enabling expression of HIV gag, pol, rev and tat) and 7 μg packaging construct pMD.2-VSVG (enabling expression VSV-G) were diluted up to 500 μl water (Aqua ad injectabilia) followed by addition of 50 μL 2.5 M calcium chloride. The solution was thoroughly mixed by "bubbling" with a pipet and 500 μL 2 x HBS- buffer (281 mM NaCl, 100 mM HEPES, 1.5 mM Na_2HPO_4 [pH 7.12 ± 0.01]) was added carefully. The precipitates were allowed to form for approximately 10 min. Subsequently, the precipitate was added drop by drop to cells and mixed gently by shaking the dish. After 8-10 hours the medium containing the precipitate was replaced by fresh medium. After 15-18 hours of incubation, the first supernatant was discarded and the medium was replaced with fresh medium. 24 hours later (day 2) supernatant containing viral particles was collected, while fresh medium was added to the transfected cells. 24 hours later (day 3) supernatant was collected again. Directly after the collection, viral particle containing supernatants (day 2 and 3) were centrifuged to remove cell debris and supernatant was filtrated through 0.22 μm-filters. Virus containing supernatant was aliquoted and stored at -20°C.

3.3.8 Quantification of lentiviral vector titers

For determination of the viral titer, 293T cells were transduced with serial dilutions of the viral supernatant (thawed from -20 °C stock). The titer is indicated in TU/ml (293T Transducing Units) and determined indirectly through the percentage of cells expressing EGFP, which is included in all lentiviral vectors. The titer was calculated using the following formula: Titer (TU/ml) = (number of seeded 293T cells) x (percentage of transduced cells) x dilution factor. 293T cells were seeded to an approximate confluence of 80% on the day of transduction in 1 ml medium in a 24- well plate. Twenty four hours later, medium was exchanged with fresh medium followed by addition of the poly-cation polybrene (5 μg/ml), which acts as a bridge between negatively charged virus particles and cells and thus enhances transfection efficiency. Serial 10x-fold dilutions of concentrated viral supernatant were added to 293T cells (10^1 - 10^3). Immediately prior transduction, cell numbers were determined in

three separated wells. 293T cell were trypsinized 72 h after transduction and prepared for FACS analysis to determine EGFP-expression.

3.3.9 Transduction of lymphocytes

Following an IL-2 and OKT3 activation of lymphocytes for 24 h the cells were transduced. Transduction was done based on centrifugation of the virus onto coated plates and subsequent addition of the lymphocytes in 2 cycles on the 2 consecutive days. Transduction was done on Retronectin®-coated plates (TaKaRa, Saint-Germain-en-Laye France). The 24-well plates were pre-coated with Retronectin (20μg/ml) at 4°C over night, blocked for 30 min with 5% BSA/ PBS (fraction V, Serva, Heidelberg, Germany). The coated plates were then loaded with viral supernatants (SN). Therefore viral SN was diluted to the required MOI in volume of 400 µl/ well in PBS and 8 µg/ml protaminesulfate (Sigma, St. Louis, MO, USA) and was then spun down onto the 24-well plates at 3000 rpm at 4°C for 30 min. This step was repeated 3 times until the final MOI 10-20 was reached. 24h -pre-activated lymphocytes were seeded in the plates ($2,5*10^5$ cells/ 24-well) over night at 37°C in a 5% CO2 incubator. The same procedure was repeated in a second cycle of transduction after 24 h and the lymphocytes were transferred to the second virus-coated plate.

3.3.10 Flow cytometry

Activation marker expression of activated lymphocytes were analysed by flow cytometry using the BD LSR II machine (Becton–Dickinson, Heidelberg, Germany). Lymphocytes were stained with fluoresceinisothiocyanate (FITC)-conjugated or phycoerythrin (PE)-conjugated anti-CD25, anti-CD69 and anti-CD95 mAbs (BD Biosciences, Heidelberg, Germany). EpCAM expression on carcinoma cells was evaluated using unconjugated anti-epithelial specific antigen (HEA125) mAb (homemade). Expression of TRAIL-receptors 1 and 2 (DR4 and DR5, respectively) on tumor cell lines was verified. (Biolegend, San Diego, CA, USA; Sigma, St. Louis, USA; ProSci, San Diego, CA, USA). Expression of CD4 and CD8 on lymphocytes was analysed by mAB anti human CD4 and anti human CD8 (BD Pharmingen, Heidelberg, Germany). Organs and tumors of transplanted animals were stained for micrometastasis by staining for anti human MHC class I (   ). Expression of TRAIL on lymphocytes was detected using anti human TRAIL (2E5) mAb. As secondary Ab we used PE-labelled anti mouse IgG1 pAb (Human & Mouse Ig adsorbed) (R-PE) (Alexis, Farmingdale, USA). Briefly, $1x10^6$ cells were incubated with Gammunex® (Talecris Biotherapeutics, Frankfurt, Germany) at 4°C for 10 min to inhibit unspecific binding of

antibodies. After washing with PBS/ 5% FCS, the cells were incubated with the desired primary antibody. PE-conjugated goat anti-mouse IgG (BD Pharmingen, Heidelberg, Germany) or FITC-conjugated goat anti-mouse IgG (Jackson ImmunoResearch, Birmingham, AL, USA) were used as secondary Ab and cells were incubated at 4°C for 30 min. After washing with, cells were respuspended in PBS/ 5% FCS and analysed by flow cytometry. The data was analyzed using BD FACS Diva software (Becton–Dickinson, Heidelberg, Germany). PE- or FITC-labeled mouse IgG (BD Pharmingen, Heidelberg, Germany) served as isotype controls. Dead cells were excluded by 7-Aminoactinomycin D (7AAD) staining.

3.3.11 Detection of cytokines

Supernatants of 3D tumor reconstructs were collected after 24 and 72 hours of incubation with EpcAMxCD3 or control Ab. TNF-α and IFN-γ levels in the supernatants of collagen gel 3D tumor reconstructs were measured by ELISA (R&D Systems, Abingdon, UK), (Cell Sciences, Canton, MA, USA) and Abcam (Cambridge, UK). Analyses were performed according to the manufacturer's recommendations.

Relative levels of cytokines and chemokines in tumor lysates and in supernatants form 3D tumor reconstructs were evaluated using a human cytokines antibody array kit (Proteome Profiler, R&D Systems, Abingdon, UK). Tumor lysates were obtained at the endpoint of the bsAb treatment experiment. The presence of the following 36 cytokines and chemokines ws evulated: C5a, CD40 ligand (CD154), G-CSF, GROα (CXCL1), I-309 (CCL1), sICAM-1 (CD54), IFN-γ, IL-1α, IL-1β, IL-1ra, IL-2, IL-4, IL-5, IL-6, IL-8, IL-10, IL-12p70, IL-13, IL-16, IL-17, IL-17E, IL-23, IL-27, IL-32a, IP-10 (CXCL10), I-TAC (CXCL11), MCP-1 (CCL2), MIF, MIP-1α (CCL3), MIP-1β (CCL4), Serpin E1 (PAI-1), RANTES (CCL5), SDF-1 (CXCL12), TNF-α and sTREM-1.

3.3.12 Migration

To evaluate the effects of EpCAMxCD3 on the migratory properties of lymphocytes in 3D collagen gels, 2×10^5 activated lymphocytes and 2×10^5 BxPc-3 cells were mixed in a collagen type I solution. EpCAMxCD3 and control bivalent anti-EpCAM mAb or irrelevant bsAb CD19xCD3 were added to the collagen solution at a dose of 10 μg/ml. In one set of experiments lymphocytes were pre-incubated with EpCAMxCD3 for 2 hours prior to the migration experiments. A POCmini microscope chamber (LaCon GbR, Ulm, Germany) was filled with the mixture of lymphocytes and tumor cells in a collagen solution. This mixture

formed a polymerized collagen gel after 15 min of incubation at 37°C in a CO_2 incubator. The POCmini chamber with the polymerized 3D collagen gel was then placed on the heating plate (36.6°C, LaCon, Ulm, Germany) under the microscope (Leitz, Wetzlar, Germany). Cells in 3D collagen gels were focused under 40x magnification. Images were recorded using a Kappa digital videocamera (DX2, Kappa GmbH, Gleichen, Germany) and were taken consequently with a 30 second interval during a period of 1.5 hours. Sequential TIFF images were transferred into the AVI-video format using Animation Shop software. The analyses of cell movements were performed with CapImage 8.4 software (Dr. Zeintl Biomedical Engineering, Heidelberg, Germany). Interactions between cells were analyzed under 2:1 zoom using a "frame to frame" method. Percentage of migrating lymphocytes, lymphocyte velocity and duration of contacts between lymphocytes and carcinoma cells were evaluated. Only duration of contacts between carcinoma cells and actively moving lymphocytes with its clear onset and termination of interaction was calculated.

3.3.13 3D tumor reconstructs

To create 3D tumour reconstructs and to mimic tumour microenvironment BxPc-3 cells, lymphocytes and fibroblasts were cultured in a collagen type I gel on chamber slides (Nunc, Rochester, NY). The collagen type I gel was prepared as described previously [116]. Briefly, to prepare the working collagen solution, 5.1 ml from a stock of 3 mg/ml of collagen type I (PureColTM, Inamed Biomaterials, Fremont, CA) were added to 798 µl of DMEM medium with 5% FCS and 330 µl of 0.34 M NaOH. Cancer cells (10^6 cells per ml) (BxPc-3 or PC-3)

Were mixed with lymphocytes (10^7 cells per ml) (pre-activated lymphocytes, TRAIL-transduced or MOCK-transduced lymphocytes) and fibroblasts (10^4 cells per ml) were mixed in the collagen solution and were seeded in 8-well chamber slides in a volume of 0.5 ml. This mixture formed a polymerized collagen gel after incubation at 37°C in a CO_2 incubator for 1.5 hrs. A volume of 250 µl of medium containing 10 µg/ml EpCAMxCD3 bsAb, 50 U/ml IL-2 and 5 µg/ml doxycycline was added on top of 3D tumour reconstructs. Gels and supernatants were harvested after 24 or 72 hrs of incubation at 37°C in the CO_2 incubator.

3.3.14 Apoptosis detection in 3D tumor reconstructs

Apoptotic proteins in supernatants of collagen gel 3D tumor reconstructs were detected using a human apoptosis antibody array kit (Proteome ProfilerTM, R&D Systems, Abingdon, UK) according to themanufacturers recommendations. Pooled supernatants (n=4) of 3D tumor reconstructs with TRAIL- or MOCK-transduced lymphocytes were collected after 24 h or 72

h of incubation with bsAb EpCAMxCD3 or control Ab (10μg/ml). The presence of the following 35 apoptosis-related proteins was evaluated: Bad (B1), bax (B2), Bcl-2 (B3), Bcl-x (B4), pro-caspase 3 (B5), cleaved caspase 3 (B6), catalase (B7), cIAP-1 (B8), cIAP (B9), claspin (B10), clusterin (B11), cytochrome c (B12), TRAIL R1/ DR4 (C1), TRAIL R2/DR5 (C2), FADD (C3), Fas/TNFSF6 (C4), HIF 1α (C5), HO-1/HMOX1/Hsp32 (C6), HO-2/HMOX2 (C7), Hsp27 (C8), Hsp60 (C9), Hsp70 (C10), HTRA1/Omi (C11), Livin (C12), PON2 (D1), p21/CIP1/CDNK1A (D2), p27/Kip1 (D3), Phospho-p53(S15) (D4), Phospho-p53(S46) (D5), Phospho-p53(S392) (D6), Phospho-p53(S635) (D7), SMAC/Diablo (D8), survivin (D9), TNF R1/TNFRSF1A (D10) and XIAP (D11). The numbers in brackets confer to the description in the figure. Three pairs of positive control spots are located in the corners of each array. Xray films and positive spots were quantified by pixel density in each spot using ImageJ 1.42 software.

3.3.15 *In vitro* cytotoxicity assay

To test cytotoxic activity of TRAIL-transduced lymphocytes, BxPc-3 or PC-3 tumor cells were incubated with TRAIL- or MOCK-transduced lymphocytes. Briefly, BxPc-3 or PC-3 cells were pre-labelled with anti MHC class I- APC mAb (BD Pharmingen, Heidelberg, Germany). TRAIL- and MOCK-transduced lymphocytes were pre-loaded with bsAb EpCAMxCD3 (10 μg/ ml) for 1h on ice. Tumor cells and lymphocytes were mixed and incubated in a CO_2 incubator at 37°C for 4 h. The following target : effector cell ratios of 1:0.1, 1:1, 1:5 and 1:10 were evaluated. Cytotoxic activity of lymphocytes and apoptosis induction in tumor cells were analysed by FACS analysis using AnnexinV-PE and PI (Sigma, St. Louis, CA, USA) staining. Mixed cells were gated on MHC class I –APC positive cells.

3.3.16 Allogenic mixed lymphocyte reaction

Fresh allogenic stimulant lymohocytes were obtained from several donors unrelated to the effector lymphocyte donors and were seeded at a concentration of 10^5 cells/well in dublicates in 96 round bottom well plates. TRAIL- or MOCK-transduced effector lymphocytes (10^5) were incubated with irradiated stimulant lymphocytes (30 Gy) in a 1:1 or 1:10 ratio. Stimulant and IL-2 and anti-CD3 mAb pre-activates effector lymphocytes cultured alone served as controls. Plates were incubated at 37 °C in a humidified atmosphere with 5% CO_2 for 3 days and then 1 μCi/well of tritiated (^{3}H) thymidine (Amersham Bioscience) was added and incubated over night. Cells, incubated in 96 well plates, were harvested (Inotec Biosytsmes, Rockville, MS, USA) onto glass fibre filter mats (Inotec Biosytems, Rockville, MS, USA)..

Filter mats were allowed to dry at 56 °C for 30 min and sealed in sample bags containing 4 ml scintillation fluid (Betaplate Scint). Filter mats were analysed on a Microbeta 1450™ liquid scintillation counter to determine ^{3}H-thymidine uptake by cells. The stimulation index was calculated as ^{3}H-thymidine uptake in the test wells divided by the ^{3}H-thymidine uptake in the control wells with stimulant cells.

3.3.17 Immunohistochemistry

Immunohistochemistry was performed on 6 μm frozen tumortissue sections using the standard avidin-biotin technique with a Vectastain ABC Elite kit from Linaris (Wertheim-Bettingen, Germany). Briefly, tissue samples were fixed in aceton followed by incubation with 20% normal goat or rabbit serum in PBS to block unspecific binding of Abs. After incubation with primary mAb and PBS washing steps, tissue samples were incubated with biotinylated secondary Ab. DAB (Invitrogen, Karlsruhe, Germany) was used as a chromogen. The following primary Abs were used: rat anti-mouse CD31 mAb detecting endothelial cells and mouse anti-human CD45 mAb detecting lymphocytes both from BD Pharmingen (Heidelberg, Germany), rabbit anti human TRAIL-R1 (DR4) and TRAIL-R2 (DR5) Ab (ProSci, Poway, CA, USA), rat anti mouse F4/80 Ab detecting mouse macrophages (acris Antibody, Herford, Germany), rat anti mouse Gr-1 (Ly-6G/Ly-6C) Ab detecting granulocytes (Biolegend, San Diego, CA, USA), rat anti mouse CD68 AB (Serotec, Oxford, UK) and rabbit anti human Ki-67 (Thermo Scientific, Rockford, IL, USA). Homemade mouse anti-human EpCAM (HEA125) mAbs were purified from hybridoma supernatants. Biotinylated goat anti-mouse IgG and biotinylated rabbit anti-rat IgG from Vector (Burlingame, CA, USA) were employed as secondary Abs. For double immunofluorescence staining goat anti-rat Alexa Fluor 594 IgG and goat anti-mouse Alexa Fluor 488 IgG (Molecular Probes, Eugene, USA) were used as secondary Abs. Omission of primary Ab was used as a negative control. Proliferation was detected using Ki67 rabbit anti human Ab (Thermo Fisher Scientific, Waltham, MA, USA). Apoptosis was detected by active caspase 3 staining (rabbit anti-human pAb, R&D Systems, Abingdon,UK) and by TUNEL assay (TACS TdT in situ apoptosis detection kit (R&D Systems, Abingdon, UK) performed according to the manufacturer's recommendations and modified by signal enhancement using a Vectastain ABC Elite kit and color development using a DAB kit. Tissue stainings were examined using a Leica DMRB microscope. Images were captured using a SPOT Flex digital color camera (Diagnostics Instruments Inc., Sterling Height, MI, USA) and analysed with SPOT Advanced software 4.6.

Hematoxylin and eosin stainings of cross tumor sections were analysed for vital tumor area by Image J software version 1.42.

3.4 Animal experiments

All animal experiments were approved by the Ethical Committee of the Regierungspräsidium, Karlsruhe, Germany.

3.4.1 Subcutaneous pancreatic and prostate xenograft models

I. To validate a xenograft tumor model, BxPc-3 cells were transplanted *s.c.* either alone or with pre-activated human lymphocytes mixed in a 1:1 ratio. Animals were randomized to four groups and received (i) BxPc-3 cells ($5x10^6$), (ii) BxPc-3 cells ($5x10^6$) mixed with pre-activated lymphocytes ($5x10^6$), BxPc-3 cells ($2.5x10^6$) mixed with pre-activated lymphocytes ($2.5x10^6$) or (iii) BxPc-3 cells ($1x10^6$) mixed with pre-activated lymphocytes ($1x10^6$). Tumor take (engrafment, outgrowth) and size were monitored for 24 days after cell implantation. On day 25 tumors were dissected, weighed, embedded in OCT, snap frozen and stored at -80°C for further analysis.

II. In EpCAMxCD3 treatment experiments, BxPc-3 or PC-3 tumor cells ($5x10^6$) were mixed with pre-activated lymphocytes ($5x10^6$) in PBS and were transplanted *s.c.* to the right flank of NOD/SCID mice in a volume of 100µl. Three days later, animals were randomized to three groups and received *i.p.* injections of EpCAMxCD3 (i) at a dose of 0.1 mg/kg, (ii) 1 mg/kg or (iii) 10 mg/kg. Control tumor bearing mice received (iv) parental bivalent anti-human CD3 (OKT3) and anti-human EpCAM (HEA125) mAbs at a dose of 1 mg/kg or (v) PBS.. Animals received five injections of EpCAMxCD3 or control Abs administered *i.p.* every third day. Tumor size was measured externally every third day using a caliper. Animals were sacrificed at day 24 after tumor cell implantation. Tumors were dissected, weighed, embedded in OCT, snap frozen and stored at -80°C for further analysis. Tumor size was measured externally every third day using a caliper. Tumor volume was calculated according to the formula: $V =\pi/6*a_2*b$, where *a* is the shortest diameter and *b* is the longest diameter.

III. In TRAIL experiments, BxPc-3 or PC-3 tumor cells ($5x10^6$) were mixed with TRAIL-transduced lymphocytes ($5x10^6$) in PBS and were transplanted *s.c.* to the right flank of the mice in a volume of 100µl. Three days later, nimals were randomized to five groups and received *i.p.* injections of EpCAMxCD3 at a dose of (i) 0.01 mg/kg, (ii) 0.1 mg/kg, (iii) irrelevant bsAb CD19xCD3, (iv) parental bivalent anti human CD3 (OKT3) and anti human

EpCAM (HEA125) mAbs at a dose of 1 mg/kg or (v) PBS. Control mice (vi) were transplanted with a mixture of non-rtnasduced pre-activated human lymphocytes and tumor cells, and received PBS. All animals received 1 mg/ml doxycycline and 5% glucose in the drinking water. Animals received five injections of EpCAMxCD3 or control Abs administered *i.p.* every third day. Tumor size was measured externally every third day using a caliper. Animals were sacrificed at day 23 after tumor cell implantation. Tumors were dissected, weighed, embedded in OCT, snap frozen and stored at -80°C for further analysis. Tumor volume was calculated according to the formula: $V = \pi/4*a2*b$, where *a* is the shortest diameter and *b* is the longest diameter.

IV. To evaluate the effects of TRAIL-transduced lymphocytes and bsAb EpCAMxCD3 on the growth of developed tumors, NOD/SCID mice were engrafted *s.c.* with BxPc-3 tumor cells. Twelve days later, BxPc-3 tumors reached a volume of 30-40 mm^3 and the treatment was initiated. TRAIL-transduced lymphocytes (5×10^6) were pre-loaded with bsAb EpCAMxCD3 (1µg/ml) for 1 h and then transplanted *s.c.* around the tumor. Animals were randomized to three groups and received *i.p.* injections of bsAb EpCAMxCD3 at a dose of (i) 0.01 mg/kg or (ii) 0.1 mg/kg or (iii) PBS. Control BxPc-3 tumor bearing mice received only (iv) bsAb EpCAMxCD3 at a dose of 0.1 mg/kg or (v) PBS. bsAb EpCAMxCD3 treatment was repeated 3 times with a 3 day interval. All animals received 1 mg/ml doxycycline and 5% glucose in the drinking water. Tumor size was measured externally every third day using a caliper. Tumors Animals were sacrificed on day 22 after tumor cell implantation. were dissected, weighed, embedded in O.C.T. Tissue -Tek (Sakura, Japan), snap frozen and stored at -80°C for further analysis. Tumor volume was calculated according to the formula: $V = \pi*a*b*h$, where a is the shortest diameter, b is the longest diameter and h the height of the xenograft.

3.4.2 Analysis of metastasis formation

The occurrence of metastasis in BxPc-3 + EGFP-L engrafted mice was evaluated on the day of sacrifice. Briefly: after isolation, liver, lungs and spleen were treated with collagenase I (Sigma, St. louis, MO, USA) filtered, washed and stained with anti human MHC class I mAb (W6/32 hybridoma, own production) and samples were analysed by flow cytometry. In addition, cryosections of BxPc-3 + EGFP-L tumors and organs were stained anti human panCk, to detect single metastatic cells.

3.5 Statistical analysis

Data is presented as mean of with standard deviation. Student's t-test was used to evaluate the

differences between the groups. The growth kinetics was evaluated using variance analysis (variance analysis with repeated measurement and Post-Hoc-Test for comparison of groups after Dunnett) over time with $* = p < 0.05$ considered statistically significant.

4   Discussion

The over-all aim of this project was to test whether a combination of TRAIL-L with bsAb EpCAMxCD3 would effectively eliminate pancreatic and prostate tumors *in vitro* and in xenograft models. Pre-activated lymphocytes and EpCAMxCD3 effectively retarded the tumor growth of BxPc-3 pancreatic and PC-3 prostate xenografts. The combination with TRAIL-L strongly enhanced this efficacy, resulting in the need of much lower doses of EpCAMxCD3. Tumor growth retardation was associated with a reduced tumor cell proliferation and with a reduced blood vessel density. In 3D *in vitro* tumor reconstructs, TRAIL-L dramatically increased the expression of apoptosis-related proteins, which may contribute to the cytotoxic effects induced by pre-activate lymphocytes and EpCAMxCD3 by upregulation of the effector cytokines IFN-γ and TNF-α. In addition, EpCAMxCD3 stimulated the expression of multiple chemokines in 3D tumor reconstructs. These chemokines may potentially contribute to the observed increased infiltration of the tumor xeongraft tissues with CD68^{+} and F4/80^{+} macrophages.

4.1   Establishment and evaluation of suitable xenograft models to study the efficacy of TRAIL-L and EpCAMxCD3

The pancreatic tumor cell line BxPc-3 and the prostate tumor cell line PC-3 were chosen for the xenograft tumor models based on the transplantation efficiency and the *s.c.* tumor growth kinetics on NOD/SCID mice. EpCAM used as target antigen for the bsAb EpCAMxCD3 treatment was expressed by both cell lines *in vitro* and in derived xenografts *in vivo*. This was expected since several publications show that EpCAM is commonly expressed at a high level and with high frequency on differentiated cancer cells of the adenocarcinoma of the prostate and of the pancreas [107, 133, 134]. Interestingly, a number of studies has recently used anti-EpCAM antibodies for isolation of cancer stem cells i.e. from human pancreas and prostate tumor tissues [135-137], since EpCAM was identified as a cancer stem cell marker in pancreatic and prostate cancer. Therefore, the present approach may target not only the majority of normal cancer cells, but also highly aggressive EpCAM-over-expressing cancer stem cells.

The death ligand TRAIL was used as therapeutical gene. TRAIL has the unique characteristic to selectively induce apoptosis in malignant cells and not in normal cells, which akes it an ideal tool for cancer therapy. However, the sensitivity of tumor cells towards TRAIL is

crucial for the success of a treatment with TRAIL. Despite TRAIL's ability to induce apoptosis in a wide variety of human tumor cell lines, there are many reports describing the resistance of tumor cells towards TRAIL. Since an underlying reason for TRAIL resistance may be an abundant receptor expression, the expression of the apoptosis-inducing TRAIL-receptors (TRAIL-R1 and -R2) was verified for the BxPc-3 and PC-3 cell lines and derived xenografts. Both cell lines expressed TRAIL-R1 and -R2 *in vitro* and *in vivo*. Sensitivity to TRAIL *in vitro* has been shown for both BxPc-3 and PC-3 cell lines in our group by Kallifatidis *et al.* [138] and by others [139-144]. Upon addition of recombinant TRAIL the viability of BxPc-3 was decreased to approx. 20% and the viability of PC-3 was decreased to 60% [138]. The higher TRAIL sensitivity of the cell line BxPc-3 could be the reason for the observed more efficient tumor growth retardation in BxPc-3 xenografts by TRAIL-L than in PC-3 xenografts, as discussed in detail later.

The efficiency of the combined TRAIL-L and EpCAMxCD3 treatment was studied in tumor xenograft models. Carcinoma cells were mixed with lymphocytes and subsequently engrafted *s.c.* into NOD/SCID mice. This approach of co-transplanted cell is preferable to *s.c.* engraftment of tumor cells followed by an *i.v.* administration of lymphocytes due to the potential redistribution of lymphocytes and their removal from the circulation in mouse organs. A similar *in vivo* tumor model was used by Schlereth *et al.* [115] and Brischwein *et al.* [122] studying the therapeutic effects of the single-chain bsAb EpCAMxCD3 constructs MT102 and MT110 in xenograft SW480 colon tumors. A lymphocyte to tumor cell ratio of 1:1 was used to mimic the situation within human tumors. In the studies presented here xenografts were formed despite the presence of the lymphocytes demonstrating that the administration of a mixture of pre-activated lymphocytes and tumor cells does not affect xenograft PC-3 or BxPc-3 tumor growth and its morphology. Both xneografted tumor entities established a robust blood vessel network and a collagen containing stroma. Similar results were obtained upon co-transplantation of TRAIL-L together with tumor cells. Our findings that pre-activated lymphocytes survive in BxPc-3 tumors for more than 24 days further underline that the xenograft model is well suited for the suggested gene-immunotherapy.

4.2 TRAIL delivery by human lymphocytes

Human lymphocytes of healthy donors were used as vehicles for the delivery of TRAIL as an apoptosis-inducing agent to tumor cells. Although the delivery of TRAIL as a therapeutic protein is widely explored by other groups, its delivery by lymphocytes has not been described before.

TRAIL has already been delivered to tumors by cellular carriers such as mesenchymal stem cells (MSCs), which have tumor targeting properties [70-73]. However, the use of T cells as vehicles is advantageous to the delivery of TRAIL by MSCs, since T cells as effector cells of the immune system have a variety of anti-tumor properties. Among them is the ability to lyse tumor cells by perforin, granzyme B, or the production of the multifunctional effector cytokines IFN-γ and TNF-α. Therefore, the over-expression of TRAIL in lymphocytes may enhance the anti-tumorigenic action of these immune cells.

Additional methods to deliver TRAIL to tumor cells have been used, such as the viral transduction of the TRAIL coding sequence directly in tumor cells or by a systemic application. The direct gene delivery with adenoviral vectors has been the most abundantly studied [74-83], while also other vectors were tested for their suitability [84-87]. However, the delivery of TRAIL by lentiviral vectors has rarely been described for this application [88-90].

The lentiviral transduction of lymphocytes with TRAIL has not been described before. However, lymphocytes have been transduced with other genes i.e. antigen-specific receptors. These receptors, which typically recognize native cell-surface antigens e.g. human leukocyte antigen-restricted, heterodimeric T cell antigen receptor, or chimeric antigen receptors CARs (reviewed in [145], [146]) help to artificially retarget T cells. The present approach does not follow this receptor-recognition based concept to target cancer cells. It relies on the hypothesis that bsAb EpCAMxCD3 efficiently targets TRAIL-L to the tumor cells and enables a close cell-cell contact by the dual specificity for the tumor associated antigen EpCAM and CD3 expressed on lymphocytes.

In the actual work, the lentiviral vector system was used to achieve the over-expression of the apoptosis-inducing ligand TRAIL in human lymphocytes. Lentivirus-derived vectors are very efficient for gene transfer due to their stable integration into the genome of dividing and non-dividing cells. Also they are less susceptible to gene silencing by host restriction factors. However, it should be clearly mentioned, that the retroviral integration into the host genome has been associated with the risk for insertional mutagenesis [147-149]. Thus, in a clinical gene therapy trial attempting to treat ten children with X-linked severe combined immunodeficiency (SCID-X1) disease using gammaretroviral-based vectors [150, 151]. Four patients developed secondary leukemia after an initially successful therapy. This was due to cellular proto-oncogene activation by the retrovirus [152-154]. This risk of secondary cancer may be specifically due to retrovirus based vectors like the MLV-based vectors since these

express viral oncogenes. They have the ability to integrate nearby cellular proto-oncogenes both in animal models and in human gene therapy trials [152, 155-161]. The use of lentiviral vectors for gene therapy could solve this concern about insertional mutagenesis of retroviral vectors. Whereas gammaretroviruses preferentially integrate around transcription start sites and CpG islands, consistent with host gene promoter features, lentiviruses integrate preferentially in active transcription units, with no bias along the transcript, nor for introns or exons [149], thereby minimizing the risk for insertional mutagenesis. Additional advantages of the lentiviral vector system are the efficient preparation and production of vectors with very high titers, the transduction of target cells independently of their cell cycle phase and a stable long term expression of the transgene.

In the present study, the lentiviral vector pV3TP2AE, a SIN vector of the second generation was used. This vector was constructed for a tetracycline induced transgene expression under the control of the CMVmin promoter. Human TRAIL and the marker gene EGFP were expressed as a single transgene linked by the P2A peptide linker. Peptide-linkers, such as P2A are superior to bicystronic systems using an IRES element and circumvent cross-inhibition of two promoters on one vector [130]. With the pV3TP2AE vector we were able to successfully transduce human lymphocytes to express TRAIL on the cell surface with an average efficiency of 40-60% and to express the marker gene EGFP in equivalent percentage. Increasing the MOI 10 up to MOI 300 did not further improve the transduction efficiency (data not shown). Thus, MOI above 100 resulted in an integration of the vector but not in expression of the transgene (data not shown). To avoid interference with neighboring genes or insertional mutagenesis, all experiments were conducted with MOI 10.

The majority of the transduced lymphocytes were cytotoxic CD8$^+$ T cells. Why the lentiviral vector seems to have a preference for CD8$^+$ T cells is not clear. A reason may be the favor of lentiviruses for the integration in active transcription units, dependent on chromatin accessibility, cell cycle effects and tethering proteins [162-165]. The preference for CD8$^+$ T cells, is probably related to an activation of the antiviral functions of CD8$^+$ T cell by viral antigens during the transduction procedure.

The isolation and subsequent transduction procedure with pV3TP2AE did not affect the lymphocyte's function to proliferate upon an allogenic stimulus. Moreover, transduction did not influence the ability of lymphocytes to migrate in 3D gels or to lyse tumor cells in *in vitro* cytotoxicity assay. Thus, transduced lymphocytes may be well suited as carriers for the delivery of TRAIL to tumor cells.

The successful application of gene therapy requires the development of vectors that can provide a regulatory control of therapeutic gene expression i.e. during embryonal development or expression of cytotoxic genes. The "Tet-on" system in pV3TP2AE allows the conditional expression of both TRAIL and EGFP after stimulation by doxycycline as demonstrate din our *in vitro* experiments. The pV3TP2AE vector was only induced when doxycycline was added. However, the promoter proved to be leaky *in vivo* since without the addition of doxycycline into the drinking water, a basal expression of the marker gene EGFP in transduced cells was detected in xenograft tissues. This leakiness may be attributed to the fact that rtTA retains some affinity for tetO sequences even without doxycycline and to the unwanted residual activity of the tetO CMV responder even when the active rtTA is absent [166]. This phenomenon has been described and could potentially be repaired by the addition of an additional insulator element [166, 167]. However, the leak in this Tet-based systems was acceptable since this therapeutic approach is based on the direct transplantation of TRAIL-L with a desired direct effect of the implanted cells.

The TRAIL-R system is controversially described for its role as a metastasis suppressor or as a promoter of metastasis [168]. TRAIL has a physiological role in tumor surveillance, tumor development and tumor protection. TRAIL knockout mice are more susceptible to experimental and spontaneous tumor metastasis [169] suggesting that TRAIL suppresses metastasis. Similarly, TRAIL-R deficient mice appear to develop fewer primary tumors [170]. These data are confirmed by Grosse-Wilde *et al*. where TRAIL suppressed metastasis formation, although an effect on growth rates of primary tumors were not observed in this particular study [171]. The transplantation of TRAIL-sensitive tumor cells into syngeneic TRAIL-deficient mice led to an increased subcutaneous tumor growth and experimental liver metastasis [169, 172] supporting an anti-tumorigenic action of TRAIL. There seems to be a strong tissue dependence of TRAIL-mediated tumor immune surveillance [169, 173, 174]. However, autochthonous mouse tumor models using TRAIL and TRAIL-R-deficient mice revealed a strong tissue dependency of tumor suppression by TRAIL and TRAIL-R. Some tumor tissues resist TRAIL-induced apoptosis and rather start to metastasize. This is related to the induction of NF-κB by TRAIL [175-178]. However, in our experiments, the activation of NF-κB (c-Rel, RelA) could not be detected in xenografts with co-transplanted TRAIL-L at the endpoint of the experiment on day 23 (data not shown), suggesting that the death-inducing properties are fully active in our model. In addition, in BxPc-3 and PC-3 tumor models, metastasis could not be detected, which indicates a safe application of TRAIL in our experiments. This is in contrast to a recent report from Trauzold *et al.* [168], who reported

that TRAIL promotes invasion and metastasis in an apoptosis resistant orthotopically xenograft of Colo357 pancreatic ductal adenocarcinoma. The difference between the finding of the present work and the results of Trauzold *et al.* may be due the choice of the *s.c.* xenograft model over the orthotopic xenograft model.

Taken together, the delivery of TRAIL by over-expression in human lymphocytes is described for the first time in the present study. TRAIL-L are functional and the TRAIL delivery by lymphocytes was safe without detectable side effects in animal models.

4.3 Targeting EpCAM on tumor cells and CD3 on lymphocytes by bsAb EpCAMxCD3

EpCAMxCD3 has a long half-life in mouse serum ($t_{1/2} \sim 7$ days) and was detectable in blood even seven days after the last administration. EpCAMxCD3 was abundantly distributed in the tumor tissues with a decreasing gradient with more distance from the blood vessels (data not shown). This is of great advantage for the proposed gene-immunotherapy since it suggests long-term effectivity. In comparison, the single-chain bsAb EpCAMxCD3 used by Schlereth *et al.*, MT102, reduced the tumor growth of experimental SW480 colon tumors, but had to be administered daily due to its terminal elimination half-time of around 5.3 hours [115]. Also the hybrid rat/mouse bsAb EpCAMxCD3 (Removab, Catumaxomab) by Lindhofer *et al.* had a terminal elimination half-life of only 2.5 days in patients (Fresenius/ TRION pharma). The increased serum half-life of our recombinant bsAb EpCAMxCD3 may provide a considerable clinical advantage over single-chain bsAb constructs.

The contact time between migrating lymphocytes and tumor cells was three times longer in the presence of EpCAMxCD3 compared to control antibodies in 3D *in vitro* tumor reconstructs. The increased time of a direct contact between target and effector cells indicates that EpCAMxCD3 facilitates interactions between lymphocytes and tumor cells regardless of T cell receptor specificity. This is in agreement with Zeidler *et al.* [128], who showed that EpCAMxCD3 brings T cells and tumor cells into close contact, redirecting T cells to kill carcinoma cells. This finding is further supported by our data demonstrating an increased cytotoxicity upon addition of EpCAMxCD3 *in vitro*. Apoptosis and cell death after incubation of tumor cells with TRAIL-L or MOCK-L lymphocytes was significantly increased in the presence of EpCAMxCD3, demonstrating the high potency of this bispecific antibody. These findings indicate that EpCAMxCD3 can potentiate the anti-tumor efficacy of lymphocytes, which may be applied for the site-specific delivery of anti-cancer agents such as TRAIL. Unfortunately, the experimental setting in 3D tumor reconstructs did not allow for the

monitoring of the fate of tumor cells following lymphocyte contact. In this regard it would have been interesting to know after which time lymphocytes would eliminate the tumor cells and whether this elimination would have been complete.

Most importantly, the binding of EpCAMxCD3 to CD3 molecules on lymphocytes did not influence the migratory properties of lymphocytes. Our results on lymphocyte velocity are in agreement with Niggemann *et al.* [179] showing a similar migration percentage and velocity of T cells in 3D collagen gels.

After the binding to CD3 molecules on lymphocytes with one arm and to EpCAM antigen on tumor cells with the other arm, bsAb lead to the activation of lymphocytes in an antigen-independent manner in 3D reconstructs. There was an induction of IL-2 production. Furthermore, EpCAMxCD3-induced activation of lymphocytes which leads to the production of effector cytokines and cytolytic substances including TNF-α, IFN-γ, perforin and granzyme B. In agreement with these results presented here, Wimberger *et al.* [118] comfirmed that tumor resident T cells following treatment with a single chain bsAb EpCAMxCD3 efficiently lysed malignant cells *in vitro*. Also, EpCAMxCD3 efficiently retarded BxPc-3 and PC-3 tumor growth *in vivo*. The treatment was not associated with therapy-related toxic side effects in tumor-bearing mice. This indicates a local production of effector cytokines and an absence of TNF-α and IFN-γ in the systemic circulation. BsAb EpCAMxCD3 is composed of mouse IgG$_1$ and IgG$_{2A}$ constant heavy chain regions and has low affinity to human Fc receptors. This property of EpCAMxCD3 would also reduce Fc-mediated side effects. By contrast, the therapeutic efficacy of other bsAb constructs greatly relies on the Fc portion, for instance, in case of mixed rat/mouse heavy chains [102, 180].

We identified several potential mechanism for the anti-tumor efficacy of EpCAMxCD3. In the 3D tumor reconstruct model, EpCAMxCD3 potently increased the production of granzyme B and perforin, suggesting a contribution of these lytic molecules to tumor cell killing. This finding corresponds to other *in vitro* models, which used other recombinant bsAb EpCAMxCD3. In these studies the bsAb potently increased the cytotoxic action of T cells by perforin and granzyme B-mediated lysis of the tumors cells within 1-3 days which was associated with the induction of apoptosis [118, 181, 182]. In comparison, the mechanism of action of the human bispecific EpCAMxCD3 antibody Catumaxomab mainly relies on antibody-dependent cellular (ADCC) and complement-dependent cytotoxicity (CDC) [102].

Taken together, EpCAMxCD3 has a long half-life *in vivo*, which would be beneficial for a clinical application. The increased contact time between tumor cells and lymphocytes can

facilitate the reaction of TRAIL-L with the tumor cells. EpCAMxCD3 potently activated lymphocytes, and induced the production of granzyme B and perforin, which can have cytotoxic abilities on tumor cells.

4.4   Combination therapy with TRAIL-L and EpCAMxCD3

EpCAMxCD3 very efficiently reduced tumor engraftment and retarded tumor growth in BxPc-3 and PC-3 xenografts with pre-activated lymphocytes *in vivo*. Tumor take was decreased by EpCAMxCD3 in a dose-dependent manner, without any detectable side effects of the bsAb. In the highest dose of EpCAMxCD3 (10 mg/kg) tumor take was only 50% and the growing tumors were smaller compared to control groups. Lower doses of EpCAMxCD3 (1 mg/kg and the 0.1 mg/kg) had a similar efficiency, arguing for the reduction in bsAb doses. Therefore, we decided to use lower EpCAMxC3 concentrations for combination experiments with TRAIL-L to circumvent potential cytotoxic side effects. In this regard, Amann *et al.* reported severe side effects of high dose of the anti murine EpCAMxCD3 bsAb in immunodeficient mice due to the rapid release of inflammatory cytokines. High doses of this recombinant bsAb were even lethal in mice [110].

As expected, in presence of TRAIL-L very low doses of EpCAMxCD3 efficiently retarded the tumor growth of xenografts. To minimize the effect of blood donor variation, individual animals per group received lymphocytes from different donors. Compared to the experiments with pre-activated lymphocytes, only very low doses of EpCAMxCD3 were necessary to achieve a pronounced anti-tumor effect and to efficiently retarded tumor growth. The delivery of TRAIL by lymphocytes was safe since no obvious side effects were detectable. This is in contrast to mouse experiments of other laboratories, in which the application of recombinant TRAIL for the elimination of glioma induced hemiparesis and weight loss at high doses of TRAIL [64]. Such side effects were not observed in the present study, which might be due to the short half life of applied high doses of recombinant TRAIL and its rapid clearance [183]. In addition, the delivery of TRAIL by lymphocytes may be involved in reduction of the suggested liver toxicity of this death ligand.

In BxPc-3 xenografts intra-tumoral cysts were observed after the treatment. Furthermore, cysts could be detected as early as three days after initiation of the treatment, suggesting that the effective mechanism behind this phenomenon is a specific early reaction to the treatment.Since cyst could only be detected in xenografts with transplanted TRAIL-L that had received EpCAMxCD3, received TRAIL-L or EpCAMxCD3 alone, the formation of cyst could be a potential treatment result. There are several potential explanations for the cysts.

We ruled out that the cyst formation was due to hemorrhage or necrosis since no blood or necrotic tissue areas were detectable. The liquid was clear, free of cells, fibrin clots or deposits and often filling the whole tumor. A potential explanation for the cysts could be the formation of a transsudate, via changed intra-tumoral vascular permeability. Blood vessels can be stimulated by a local cytokine production and consequently cell-free liquids accumulate. Cysts are a well-known phenomenon in pancreatic carcinoma of patients, especially pseudocysts are commonly found [184], however, cysts have not been described in *s.c.* xenograft models of established pancreatic cell lines. The possibility that cyst formation could be due to doxycycline administration was ruled out, since the PBS control group has also received doxycycline and was cyst-free. Only one mouse model with a polycystic kidney disease is described with cyst-acceleration upon doxycycline, due to inhibition of MMPs and changes in intracellular Ca2+ and Zn2+levels [185]. However, in BxPc-3 xenografts treated with high-dose of EpCAM mAb alone, cyst formation was observed independently of doxycycline (personal communication A. Salnikov).

Taken together, EpCAMxCD3 very efficiently retarded tumor growth in xenograft models of the tumor cell lines BxPc-3 and PC-3 in a dose-dependent manner. The use of lymphocytes as vehicles for TRAIL potently enhanced the anti-tumor effect of even very low doses of bsAb, which could provide a pharmacokinetic advantage in a clinical setting. Tumor-bearing animals did not have treatment-related side effects from either TRAIL or the bsAb. The development of cysts inside BxPc-3 xenografts could be a potential result of the EpCAMxCD3 treatment but cannot be fully explained yet.

4.5 Analysis of the anti-tumor effect of EpCAMxCD3 and transplanted TRAIL-L *in vivo* and *in vitro*

The combination of TRAIL-L with low doses of EpCAMxCD3 very efficiently retarded tumor growth in xenograft models. Although an increase in apoptosis could not be detected at the endpoint of EpCAMxCD3 treatment (active caspase 3, TUNEL) on day 23, TRAIL-L efficiently induced apoptosis in 3D *in vitro* tumor reconstructs.

Apoptosis was analysed at the endpoint of the bsAb treatment on day 23 after the co-injection of cancer cells with the respective lymphocytes. However, an increase in apoptosis could not be detected (active caspase 3, TUNEL). These results may be misleading, since tumor cells and lymphocytes were co-transplanted and may have interacted already at the time of injection. Therefore, the time of observation could be critical and we assume that apoptosis might have been visible at earlier time points. In line with this assumption, TRAIL-induced

apoptosis has been shown by Kim *et al.* used TRAIL-transduced MSCs in glioma xenografts. The strongest apoptosis was seen 7 days after injection and the effect of TRAIL declined within 2 weeks [71]. Our tumors analysed on day 23, could be persistent or apoptosis-resistent sub-populations of the initially injected tumor mass. Furthermore, treatment with EpCAMxCD3 on the days 4, 7, 10, 13 and 16 is a considerable period of time earlier than the time of analysis at day 23. Furthermore, it is possible that the anti-tumor effect of the bsAb could involve other mechanism than apoptosis.

For the study of short term effects of EpCAMxCD3 and TRAIL-L on tumor cells, apoptosis induction was analysed *in vitro*. TRAIL-L induced multiple apoptosis-related proteins in 3D tumor reconstructs after 24 and 72 hours. The detection of *in vitro* anti-tumor effect after 24 hours, is in agreement with the time of apoptosis induction mediated by other recombinant bsAb EpCAMxCD3 [118, 181, 182, 186]. In addition, the trifunctional bispecific antibody EpCAMxCD3 eliminated prostate tumor cells in co-culture experiments with PBMCs after 24 hours [182] and also in primary ovarian cancer cells *in vitro* [118]. However, EpCAMxCD3 did not enhance the effects of TRAIL in 3D reconstructs, suggesting a high impact of the lymphocytes over-expressing TRAIL. For recombinant TRAIL, a similar time frame was observed for the induction of apoptosis in glioma cell lines by others *in vitro* by terminal transferase-catalysed in situ end-labeling technique [64]. Also TRAIL-transduced MSCs induced apoptosis *in vitro* in co-culture models of lung cancer metastasis and glioma [70, 71]. However, another potential explanation for the observed cell death could be differences in death mechanisms used by lymphocytes such as cell-lytic proteins like perforin or granzyme B, which were fond to be secreted in 3D tumor reconstructs.

Furthermore, in an *in vitro* cytotoxicity assay bsAb EpCAMxCD3 significantly increased tumor cell death after incubation of tumor cells together with MOCK-L or TRAIL-L in different ratios. The cell death reached a maximum at the effector - to - target cell ratio of 10:1. However, annexinV-staining was negative and the addition of a blocking-antibody for TRAIL did not have an effect on the outcome. The cell death observed after 4 hour incubation with TRAIL-L was not mediated by TRAIL but potentially by another effector mechanism by lymphocytes. This observation is in agreement with Haas *et al.*, who showed that the single-chain bsAb EpCAMxCD3 (MT110) did not induce detectable levels of apoptosis *in vitro* before 15 hours of incubation [181]. In agreement with our data, the incubation of 24 hours and 72 hours was most effective on tumor cell eradication *in vitro* as shown by Riesenberg *et al.* and Flieger *et al.* [182, 186] who used the trifunctional bsAb EpCAMxCD3.

EpCAMxCD3 and TRAIL-L reduced the blood vessel density *in vivo*. The anti-angiogenic effect can partly be attributed to TRAIL-L. My colleague, Dr. Kallifatidis *et al.* showed that recombinant TRAIL significantly decreased CD31^{+} blood vessel density in pancreatic MIA-PaCa2 xenografts tumors *in vivo* [138]. Similar effects were shown on HUVEC cells *in vitro* (unpublished data). The anti-angiogenic effect of TRAIL has also been described by Li *et al.* and Aladina *et al.* [187, 188] by inducing apoptosis in endothelial cells. This result is supported by our data, since the treatment with EpCAMxCD3 in high doses and pre-activated lymphocytes also did not result in a major difference in the CD31^{+} blood vessel density (data not shown). Another reason for the reduced blood vessel density could be the release of IFN-γ and TNF-α by the lymphocytes. IFN-γ is known to have inhibitory effect on angiogenesis by inducing the chemokines CXCL9 (MIG), CXCL10 (IP-10) and CXCL1 (I-TAC), which inhibit the chemotaxis of endothelial cells [189-192]. In addition IFN-γ as well as TNF-α downregulate the pro-angiogenic chemokine CXCL12 (SDF-1) [193]. A local TNF-α production has also been connected to proliferation arrest and apoptosis in endothelial cells [194, 195].

EpCAMxCD3 and pre-activated lymphocytes or TRAIL-L decreased proliferation of BxPc-3 and PC-3 tumor cells *in vivo.* Compared to xenografts with pre-activated lymphocytes, TRAIL-L dramatically increased the anti-proliferative effect of bsAb. The most dramatic effect was detected in the PC-3 xenograft model. In the BxPc-3 xenograft model the decrease in proliferation was significant but not as dramatic as in PC-3. Interestingly, the localization of the highest amount of bsAb was reciprocal to the region of the highest proliferation. Ki-67^{+} cells were remarkably localized at the outer part of the tumor islets close to the tumor stroma with the blood vessels (data not shown). A possible explanation for the changes in proliferation observed in mixed xenografts of carcinoma cells with pre-activated lymphocytes/ TRAIL-L could be the interaction of the bsAb with EpCAM on tumor cells. The works of Munz *et al.* and Osta *et al.* [196, 197] underlined its role in promotion of gene transcription and cell proliferation. Cells expressing EpCAM have been demonstrated to proliferate more rapidly, grow in an anchorage-independent manner and have a reduced requirement of growth factors. Consistently, it could been shown that knock-down of endogenous EpCAM in tumor cells decreases cell proliferation and migration [196, 197]. Recently, the impact of cell-to-cell contact for EpCAM signaling and the intracellular signaling pathway has been demonstrated by Denzel *et al.* [198]. This finding high-lights the role of EpCAM as an anti-tumor target. In addition, in tumors treated with EpCAMxCD3 and

co-transplanted with TRAIL-L the reduction in proliferation was the highest, indicating the contribution from TRAIL-L.

Another reason for the decreased proliferation is the induction of cytokines by pre-activated lymphocytes or/and by the bsAbs as shown for EpCAMxCD3 in patients [117]. Alternatively EpCAMxCD3-induced IFN-γ and TNF-α production by lymphocytes may be responsible. IFN-γ and TNF-α inhibit cell proliferation. IFN-γ has been reported to inhibit cell cycle progression [199, 200]. TNF-α has been reported for a dual role in the induction of cancer cell death and angiogenesis [201]. However, TNF-α has also been descrived to contribute the local inflammation of tumors and to induce tumor cell death at high doses [195].

To mimic a clinical situation more closely, a developed tumor model was used in addition. The model of tumor cells co-injected with lymphocytes as also applied by Schlereth *et al.* [115] and Brischwein *et al.* [122] is suited for treatment studies of a tumor cell mass, like an *in vivo* cytotoxicity assay. In the literature numerous cancer treatment models are accomplished in preformed solid tumors, which are then analysed for tumor growth retardation, tumor shrinkage or even tumor eradication. Therefore, the anti-tumor effects of transplanted TRAIL-L and EpCAMxCD3 were analysed in a developed tumor model of BxPc-3 cells *s.c.* transplanted into NOD/SCID mice. The treatment in our study was started upon reaching an average tumor size of 80 mm^3. TRAIL-L were transplanted *s.c.* around the tumor and not directly into the tumor since the direct injection into the tumor may induce tumor cell death and the lymphocytes could be lost by systemic distribution. EpCAMxCD3 and TRAIL-L efficiently retarded tumor growth of developed BxPc-3 tumors, verifying the results from the previous tumor model, in which tumor wells were co-transplanted together with lymphocytes. Therefore, EpCAMxCD3 treatment in combination with TRAIL-L is also effective on the developed xenograft model of pancreatic BxPc-3, which is closer to the clinical situation.

In 3D tumor reconstructs, EpCAMxCD3 potently stimulated IFN-γ secretion by pre-activated lymphocytes, whereas the production of TNF-α was less pronounced. In contrast, TNF-α was the predominant cytokine produced in 3D reconstructs with non-stimulated PBMCs in the presence of EpCAMxCD3. The latter findings are in agreement with the clinical data showing that TNF-α level was markedly increased in ascites from ovarian cancer patients treated with EpCAMxCD3 [117]. The finding, that PC-3 and BxPc-3 tumor growth inhibition by the combined treatment with lymphocytes and EpCAMxCD3 was not associated with

therapy-related toxic side effects in tumor-bearing mice, indicates a local production of effector cytokines and an absence of TNF-α and IFN-γ in the systemic circulation. The expression of cytokines has also been shown for Catumaxomab. This hybrid mouse/rat antibody that is specific for EpCAM, CD3 and - via its Fc portion – for antigen-presenting cells, as well as for a variety of other cytotoxic immune cells, has been shown to efficiently reduce ovarian cancer patients suffering from ascites and in gastric cancer patients in phase II clinical studies. Similar results have been gained by Strauss *et al.* and Marme *et al.* with this present EpCAMxCD3 in ovarian cancer patients on ascites formation [117, 128]. Both works detected a massive induction of TNF-α, indicating a very strong local immune stimulation.

Noteworthy is that EpCAMxCD3 induced production of inhibitory cytokine IL-10 in reconstructs with PBMCs but not with pre-activated lymphocytes. This may indicate a nonspecific activation of regulatory T cells by EpCAMxCD3. Since regulatory T cells are the major source of inhibitory cytokines in PBMCs [202, 203] TGF-β1 production was analysed in 3D tumor reconstructs. The TGF-β1 level was only marginally increased in 3D tumor reconstructs with EpCAMxCD3 after 72 hours of incubation. The possibility that monocyte-derived IL-1β could contribute to the TGF-β1 production in 3D reconstructs with non-stimulated PBMCs via stimulation of fibroblasts was ruled out, because IL-1β levels were similar in all 3D reconstructs. Since the binding of bsAb containing IgG$_1$ and IgG$_{2A}$ constant heavy chain regions to human monocytes is usually weak, the potential activation of T cells via binding of EpCAMxCD3 to Fc receptors on monocytes is rather unlikely in 3D tumor reconstruct experiments.

Taken together, these results indicate that EpCAMxCD3 is a strong inducer of lymphocyte effector functions such as secretion of tumoricidal cytokines. The response of lymphocytes to EpCAMxCD3 is dependent on their activation state.

To investigate the microenvironment created in 3D tumor reconstructs and the release of cytokines, a panel of several cytokines and chemokines was analysed in 3D gels. The induction of many cytokines was detected including G-CSF, GROα, sICAM-1, IL-1α, IL-1β, IL-1ra, IL-6, IL-8, IL-16, IP-10, I-TAC, MIF, MIP-1α, MIP1β, serpin E1, RANTES, TNF-α, IFN-γ. In tumor extracts the presence of sICAM, IL-1α, IL-1ra, MIF and Serpin E1 could be detected. The presence of these cytokines in the tumors indicates that the activated lymphocytes are potentially reactive against the tumor cells. The difference in cytokine expression between *in vivo* and *in vitro* could be explained by an accumulation of the

cytokines in the 3D tumor reconstructs. *In vivo* cytokines can be distributed by the bloodflow and a tissue gradient can be created. Since the kit specifically detects human cytokines, we can conclude that the source are the lymphocytes. The majority of the detected cytokines are chemokines, which are able to induce chemotaxis of nearby responsive cells. The pro-inflammatory IL-1α, IL-1β, IL-6, sICAM-1 can promote the infiltration of immune cells to the site of production, others like MIF have an anti-migratory or chemotactic function like IL-8, MIP-1α, MIP-1β, G-CSF, IL-16, IP-10, I-TAC, RANTES, GROα and Serpin E1. TNF-α and IFN-γ released by the activated T cells also act synergistically to change endothelial cells, allowing increased blood flow, increased vascular permeability, and increased emigration of leukocytes, fluid, and protein into a site of inflammation. However, other bsAb like the irrelevant CD19xCD3 bsAb also induced the production of TNF-α and IFN-γ. On the contrary, the omission of antibodies in 3D tumor reconstructs did not induce the production of TNF-α and IFN-γ by lymphocytes.

These results indicate that EpCAMxCD3 is a strong inducer of lymphocyte effector functions such as secretion of tumoricidal cytokines and that the response of lymphocytes to EpCAMxCD3 is dependent on their activation state.

The presence of chemokines in the 3D gels and in the tumor lysates could potentially attract immune cells of the thus, could be the reason for the infiltration of tumors with immune cells. TNF-α can induce an endothelial cell activation. Endothelial cell activation can potentially facilitate activated effector T lymphocytes to enter infected tissue as well as recruiting neutrophils and macrophages. The NOD/SCID mouse model has a severe combined immunodeficiency which affects T- and B- lymphocyte development, has a NK cell functional deficit, an absence of circulating complement. These mice only possess innate immune cells such as monocytes, macrophages and granulocytes/ neutrophils. Immunohistochemistry revealed the infiltration of tumor tissues with mouse monocytes/ macrophages (CD68), mature macrophages (F4/80) and single granulocytes (Gr-1). In BxPc-3 tumors many CD68 and F4/80 positive cells were located at the rim of the tumor and in the stroma. In addition, in tumors which had been treated with EpCAMxCD3 alone, with *s.c.* injected TRAIL-L or in combination, CD68 and F4/80 positive macrophages were also found to leave the blood vessels and infiltrate the tumor islets.

The role of tumor associated macrophages (TAM) in tumor development is currently under investigation. TAMs are found in many solid tumors [204]. TAMs derive from circulating monocytes and are directed into the tumor by chemokines. Many tumor cells also produce

cytokines such as colony-stimulating factors that prolong the survival of TAMs in the tissue. Activated, TAMs can kill tumor cells or destroy the vascular endothelium of the tumor. However, TAM also produce growth factors involved in angiogenesis. Hence, TAM can stimulate tumor-cell proliferation, promote angiogenesis, and favor invasion and metastasis, which gives them a dual role in cancer biology [201, 205]. However, our results demonstrate a decreased angiogenesis and proliferation of tumor cells, which rules out a contribution of TAMs to tumor growth. The presence of these phagocytic effector cells inside the tumors could potentially contribute to the anti-tumor effect of TRAIL-L in combination with EpCAMxCD3 in both xenograft models.

4.6 Summary

In conclusion, this is the first study, which shows the effective lentiviral transduction of human lymphocytes with the death ligand TRAIL. The vector pV3TP2A effectively transduced human lymphocytes to over-express TRAIL. The majority of these TRAIL-over-expressing lymphocytes were CD8+ T cells and retained their cytotoxic functions, their migratory and proliferative properties after the transduction. Furthermore, this study showed that EpCAMxCD3 possesses a potent anti-tumor activity *in vivo*. In NOD/SCID mice, EpCAMxCD3 had a long serum half-life (t1/2 ~ 7 days). In two mouse models the combination of EpCAMxCD3 with lymphocytes significantly retarded the growth of BxPc-3 pancreatic and PC-3 prostate cancer xenografts. For mimicking a pancreatic cancer microenvironment *in vitro* a 3D tumor reconstruct system was used, in which lymphocytes were co-cultured with EpCAM-expressing tumor cells and fibroblasts in a collagen matrix. In this *in vivo*-like system EpCAMxCD3 potently stimulated the production of the effector cytokines IFN-γ and TNF-α by extracorporally pre-activated lymphocytes. Moreover, compared with a bivalent anti-CD3 antibody, EpCAMxCD3 more efficiently activated production of TNF-α and IFN-γ by non-stimulated PBMCs. We demonstrate for the first time that EpCAMxCD3 induces prolonged contacts between lymphocytes and tumor cells, which may be one of the main reason for the observed anti-tumor effects. The combination with lymphocytes over-expressing the death ligand TRAIL could effectively enhance the anti-tumor effects of bsAb EpCAMxCD3. The combination with TRAIL-L enabled us to strongly reduce the dose of EpCAMxCD3 necessary for an anti-tumor effect. This is a great advantage, which could minimize potential side effects of bsAb treatment. EpCAMxCD3 did not alter lymphocyte migration as measured by time-lapse video microscopy, which is an important prerequisite for future use in patients. Apoptosis induction in tumor cells by TRAIL-L was

confirmed *in vitro* in 3D tumor reconstructs. In cytotoxic killing assays, the anti-tumor effect of TRAIL-L was significantly enhanced by EpCAMxCD3. In 3D gels, lymphocytes were effective producers of IFN-γ, TNF-α and chemokines, which could also be detected *in vivo* from tumor lysates. An increased infiltration of the tumor islets with macrophages and granulocytes was observed upon treatment with TRAIL-L and EpCAMxCD3. A potential explanation for the demonstrated anti-tumor effect of EpCAMxCD3 and TRAIL-L combination therapy, is an enhancement of the observed effects of single treatment, namely the reduced proliferation in tumor cells, decreased blood vessels formation, local production of cytokines and chemokines, apoptosis and an increased infiltration of tumor tissue with macrophages. Conclusively, the combination of TRAIL-transduced lymphocytes and the bispecific antibody EpCAMxCD3 was very efficient in pancreatic and prostate xenograft models *in vivo*. This combination of gene therapy with immunotherapy could potentially be a possible therapeutic option for the clinical application in the future.

5   References

1.   Selley, S., et al., *Diagnosis, management and screening of early localised prostate cancer.* Health Technol Assess, 1997. **1**(2): p. i, 1-96.

2.   Society, A.C., *Cancer Facts & Figures 2009.* Atlanta: American Cancer Society; 2009, 2009.

3.   Jemal, A., et al., *Cancer statistics, 2004.* CA Cancer J Clin, 2004. **54**(1): p. 8-29.

4.   Steinberg, G.D., et al., *Family history and the risk of prostate cancer.* Prostate, 1990. **17**(4): p. 337-47.

5.   Kolonel, L.N., A.M. Nomura, and R.V. Cooney, *Dietary fat and prostate cancer: current status.* J Natl Cancer Inst, 1999. **91**(5): p. 414-28.

6.   Brawley, O.W. and H. Parnes, *Prostate cancer prevention trials in the USA.* Eur J Cancer, 2000. **36**(10): p. 1312-5.

7.   Burton, J.L., N. Oakley, and J.B. Anderson, *Recent advances in the histopathology and molecular biology of prostate cancer.* BJU Int, 2000. **85**(1): p. 87-94.

8.   Teng, D.H., et al., *MMAC1/PTEN mutations in primary tumor specimens and tumor cell lines.* Cancer Res, 1997. **57**(23): p. 5221-5.

9.   Apakama, I., et al., *bcl-2 overexpression combined with p53 protein accumulation correlates with hormone-refractory prostate cancer.* Br J Cancer, 1996. **74**(8): p. 1258-62.

10.   Mazhar, D. and J. Waxman, *Prostate cancer.* Postgrad Med J, 2002. **78**(924): p. 590-5.

11.   Coughlin, S.S., et al., *Predictors of pancreatic cancer mortality among a large cohort of United States adults.* Cancer Causes Control, 2000. **11**(10): p. 915-23.

12.   Chari, S.T., et al., *Probability of pancreatic cancer following diabetes: a population-based study.* Gastroenterology, 2005. **129**(2): p. 504-11.

13.   Malka, D., et al., *Risk of pancreatic adenocarcinoma in chronic pancreatitis.* Gut, 2002. **51**(6): p. 849-52.

14.   Howes, N. and J.P. Neoptolemos, *Risk of pancreatic ductal adenocarcinoma in chronic pancreatitis.* Gut, 2002. **51**(6): p. 765-6.

15.   Howes, N., et al., *Clinical and genetic characteristics of hereditary pancreatitis in Europe.* Clin Gastroenterol Hepatol, 2004. **2**(3): p. 252-61.

16.   Vitone, L.J., et al., *The inherited genetics of pancreatic cancer and prospects for secondary screening.* Best Pract Res Clin Gastroenterol, 2006. **20**(2): p. 253-83.

17.   Nothlings, U., et al., *Meat and fat intake as risk factors for pancreatic cancer: the multiethnic cohort study.* J Natl Cancer Inst, 2005. **97**(19): p. 1458-65.

18.   Larsson, S.C., E. Giovannucci, and A. Wolk, *Methionine and vitamin B6 intake and risk of pancreatic cancer: a prospective study of Swedish women and men.* Gastroenterology, 2007. **132**(1): p. 113-8.

19.   Ghaneh, P., E. Costello, and J.P. Neoptolemos, *Biology and management of pancreatic cancer.* Postgrad Med J, 2008. **84**(995): p. 478-97.

20.   Hanahan, D. and R.A. Weinberg, *The hallmarks of cancer.* Cell, 2000. **100**(1): p. 57-70.

21.   Dunn, G.P., L.J. Old, and R.D. Schreiber, *The three Es of cancer immunoediting.* Annu Rev Immunol, 2004. **22**: p. 329-60.

22.   Wadhwa, P.D., et al., *Cancer gene therapy: scientific basis.* Annu Rev Med, 2002. **53**: p. 437-52.

23.   Mintzer, M.A. and E.E. Simanek, *Nonviral vectors for gene delivery.* Chem Rev, 2009. **109**(2): p. 259-302.

24.   Collins, S.A., et al., *Viral vectors in cancer immunotherapy: which vector for which strategy?* Current gene therapy, 2008. **8**(2): p. 66-78.

25.   Kaplan, J.M., *Adenovirus-based cancer gene therapy.* Curr Gene Ther, 2005. **5**(6): p. 595-605.

26.   Ribacka, C., S. Pesonen, and A. Hemminki, *Cancer, stem cells, and oncolytic viruses.* Ann. of Med., 2008. **40**(7): p. 496-505.

27.   Wu, Z., A. Asokan, and R.J. Samulski, *Adeno-associated virus serotypes: vector toolkit for human gene therapy.* Mol Ther, 2006. **14**(3): p. 316-27.

28.   Lewis, P.F. and M. Emerman, *Passage through mitosis is required for oncoretroviruses but not for the human immunodeficiency virus.* J Virol, 1994. **68**(1): p. 510-6.

29.   Naldini, L., et al., *In vivo gene delivery and stable transduction of nondividing cells by a lentiviral vector.* Science, 1996. **272**(5259): p. 263-7.

30.   Korin, Y.D. and J.A. Zack, *Progression to the G1b phase of the cell cycle is required for completion of human immunodeficiency virus type 1 reverse transcription in T cells.* J Virol, 1998. **72**(4): p. 3161-8.

31.   Zufferey, R., et al., *Self-inactivating lentivirus vector for safe and efficient in vivo gene delivery.* J Virol, 1998. **72**(12): p. 9873-80.

32.   Dull, T., et al., *A third-generation lentivirus vector with a conditional packaging system.* J Virol, 1998. **72**(11): p. 8463-71.

33.   Miyoshi, H., et al., *Development of a self-inactivating lentivirus vector.* J Virol, 1998. **72**(10): p. 8150-7.

34.   Follenzi, A., et al., *Gene transfer by lentiviral vectors is limited by nuclear translocation and rescued by HIV-1 pol sequences.* Nat Genet, 2000. **25**(2): p. 217-22.

35.   Sirven, A., et al., *The human immunodeficiency virus type-1 central DNA flap is a crucial determinant for lentiviral vector nuclear import and gene transduction of human hematopoietic stem cells.* Blood, 2000. **96**(13): p. 4103-10.

36.   Zufferey, R., et al., *Woodchuck hepatitis virus posttranscriptional regulatory element enhances expression of transgenes delivered by retroviral vectors.* J Virol, 1999. **73**(4): p. 2886-92.

37.   Levine, A.J., *11th Ernst Klenk Lecture. The p53 tumor suppressor gene and product.* Biol Chem Hoppe Seyler, 1993. **374**(4): p. 227-35.

38.   Vousden, K.H. and X. Lu, *Live or let die: the cell's response to p53.* Nat Rev Cancer, 2002. **2**(8): p. 594-604.

39.   Datta, S.R., et al., *Akt phosphorylation of BAD couples survival signals to the cell-intrinsic death machinery.* Cell, 1997. **91**(2): p. 231-41.

40.   Boatright, K.M., et al., *A unified model for apical caspase activation.* Mol Cell, 2003. **11**(2): p. 529-41.

41.   Nagata, S., *Apoptotic DNA fragmentation.* Exp Cell Res, 2000. **256**(1): p. 12-8.

42.   El-Deiry, W.S., *Insights into cancer therapeutic design based on p53 and TRAIL receptor signaling.* Cell Death Differ, 2001. **8**(11): p. 1066-75.

43.   Eskes, R., et al., *Bid induces the oligomerization and insertion of Bax into the outer mitochondrial membrane.* Mol Cell Biol, 2000. **20**(3): p. 929-35.

44.   Wei, M.C., et al., *tBID, a membrane-targeted death ligand, oligomerizes BAK to release cytochrome c.* Genes Dev, 2000. **14**(16): p. 2060-71.

45.   Ashkenazi, A., *Directing cancer cells to self-destruct with pro-apoptotic receptor agonists.* Nat Rev Drug Discov, 2008. **7**(12): p. 1001-12.

46.   Wiley, S.R., et al., *Identification and characterization of a new member of the TNF family that induces apoptosis.* Immunity, 1995. **3**(6): p. 673-82.

47.   Ehrlich, S., et al., *Regulation of soluble and surface-bound TRAIL in human T cells, B cells, and monocytes.* Cytokine, 2003. **24**(6): p. 244-53.

48. Ashkenazi, A., et al., *Safety and antitumor activity of recombinant soluble Apo2 ligand.* J Clin Invest, 1999. **104**(2): p. 155-62.

49. Falschlehner, C., et al., *TRAIL signalling: decisions between life and death.* Int J Biochem Cell Biol, 2007. **39**(7-8): p. 1462-75.

50. Ashkenazi, A. and V.M. Dixit, *Apoptosis control by death and decoy receptors.* Curr Opin Cell Biol, 1999. **11**(2): p. 255-60.

51. Pitti, R.M., et al., *Induction of apoptosis by Apo-2 ligand, a new member of the tumor necrosis factor cytokine family.* J Biol Chem, 1996. **271**(22): p. 12687-90.

52. Griffith, T.S., et al., *Monocyte-mediated tumoricidal activity via the tumor necrosis factor-related cytokine, TRAIL.* J Exp Med, 1999. **189**(8): p. 1343-54.

53. Johnsen, A.C., et al., *Regulation of APO-2 ligand/trail expression in NK cells-involvement in NK cell-mediated cytotoxicity.* Cytokine, 1999. **11**(9): p. 664-72.

54. Zamai, L., et al., *Natural killer (NK) cell-mediated cytotoxicity: differential use of TRAIL and Fas ligand by immature and mature primary human NK cells.* J Exp Med, 1998. **188**(12): p. 2375-80.

55. Kayagaki, N., et al., *Expression and function of TNF-related apoptosis-inducing ligand on murine activated NK cells.* J Immunol, 1999. **163**(4): p. 1906-13.

56. Sato, K., et al., *Antiviral response by natural killer cells through TRAIL gene induction by IFN-alpha/beta.* Eur J Immunol, 2001. **31**(11): p. 3138-46.

57. Cretney, E., et al., *TNF-related apoptosis-inducing ligand as a therapeutic agent in autoimmunity and cancer*.* Immunol Cell Biol, 2006. **84**(1): p. 87-98.

58. Schaefer, U., et al., *TRAIL: a multifunctional cytokine.* Front Biosci, 2007. **12**: p. 3813-24.

59. Blankenstein, T., *The role of tumor stroma in the interaction between tumor and immune system.* Curr Opin Immunol, 2005. **17**(2): p. 180-6.

60. Mace, T.A., et al., *The potential of the tumor microenvironment to influence Apo2L/TRAIL induced apoptosis.* Immunol Invest, 2006. **35**(3-4): p. 279-96.

61. Spierings, D., *Tissue Distribution of the Death Ligand TRAIL and Its Receptors.* Journal of Histochemistry and Cytochemistry, 2004. **52**(6): p. 821-831.

62. Wiley, S.R., et al., *Identification and characterization of a new member of the TNF family that induces apoptosis.* 1995.

63. Walczak, H., et al., *Tumoricidal activity of tumor necrosis factor-related apoptosis-inducing ligand in vivo.* Nat Med, 1999. **5**(2): p. 157-63.

64. Pollack, I.F., M. Erff, and A. Ashkenazi, *Direct stimulation of apoptotic signaling by soluble Apo2l/tumor necrosis factor-related apoptosis-inducing ligand leads to selective killing of glioma cells.* Clin Cancer Res, 2001. **7**(5): p. 1362-9.

65. Gazitt, Y., *TRAIL is a potent inducer of apoptosis in myeloma cells derived from multiple myeloma patients and is not cytotoxic to hematopoietic stem cells.* Leukemia, 1999. **13**(11): p. 1817-24.

66. Mitsiades, C.S., et al., *TRAIL/Apo2L ligand selectively induces apoptosis and overcomes drug resistance in multiple myeloma: therapeutic applications.* Blood, 2001. **98**(3): p. 795-804.

67. Lawrence, D., et al., *Differential hepatocyte toxicity of recombinant Apo2L/TRAIL versions.* Nat Med, 2001. **7**(4): p. 383-5.

68. Jo, M., et al., *Apoptosis induced in normal human hepatocytes by tumor necrosis factor-related apoptosis-inducing ligand.* Nat Med, 2000. **6**(5): p. 564-7.

69. Mahalingam, D., et al., *TRAIL receptor signalling and modulation: Are we on the right TRAIL?* Cancer Treatment Reviews, 2009. **35**(3): p. 280-8.

70. Loebinger, M.R., et al., *Mesenchymal stem cell delivery of TRAIL can eliminate metastatic cancer.* Cancer Res, 2009. **69**(10): p. 4134-42.

71. Kim, S.M., et al., *Gene therapy using TRAIL-secreting human umbilical cord blood-derived mesenchymal stem cells against intracranial glioma.* Cancer Res, 2008. **68**(23): p. 9614-23.

72. Mohr, A., et al., *Mesenchymal stem cells expressing TRAIL lead to tumour growth inhibition in an experimental lung cancer model.* J Cell Mol Med, 2008. **12**(6B): p. 2628-43.

73. Luetzkendorf, J., et al., *Growth-inhibition of colorectal carcinoma by lentiviral TRAIL-transgenic human mesenchymal stem cells requires their substantial intratumoral presence.* J Cell Mol Med, 2009.

74. Armeanu, S., et al., *Adenoviral gene transfer of tumor necrosis factor-related apoptosis-inducing ligand overcomes an impaired response of hepatoma cells but causes severe apoptosis in primary human hepatocytes.* Cancer Res, 2003. **63**(10): p. 2369-72.

75. Dong, F., et al., *Eliminating established tumor in nu/nu nude mice by a tumor necrosis factor-alpha-related apoptosis-inducing ligand-armed oncolytic adenovirus.* Clin Cancer Res, 2006. **12**(17): p. 5224-30.

76. Griffith, T.S. and E.L. Broghammer, *Suppression of tumor growth following intralesional therapy with TRAIL recombinant adenovirus.* Mol Ther, 2001. **4**(3): p. 257-66.

77. Lee, J., et al., *Antitumor activity and prolonged expression from a TRAIL-expressing adenoviral vector.* Neoplasia, 2002. **4**(4): p. 312-23.

78. Lillehammer, T., et al., *Combined treatment with Ad-hTRAIL and DTIC or SAHA is associated with increased mitochondrial-mediated apoptosis in human melanoma cell lines.* J Gene Med, 2007. **9**(6): p. 440-51.

79. Seol, J.Y., et al., *Adenovirus-TRAIL can overcome TRAIL resistance and induce a bystander effect.* Cancer Gene Ther, 2003. **10**(7): p. 540-8.

80. Voelkel-Johnson, C., D.L. King, and J.S. Norris, *Resistance of prostate cancer cells to soluble TNF-related apoptosis-inducing ligand (TRAIL/Apo2L) can be overcome by doxorubicin or adenoviral delivery of full-length TRAIL.* Cancer Gene Ther, 2002. **9**(2): p. 164-72.

81. Yang, F., et al., *Recombinant adenoviruses expressing TRAIL demonstrate antitumor effects on non-small cell lung cancer (NSCLC).* Med Oncol, 2006. **23**(2): p. 191-204.

82. Bremer, E., et al., *Potent systemic anticancer activity of adenovirally expressed EGFR-selective TRAIL fusion protein.* Mol Ther, 2008. **16**(12): p. 1919-26.

83. Jeong, M., et al., *Possible novel therapy for malignant gliomas with secretable trimeric TRAIL.* PLoS ONE, 2009. **4**(2): p. e4545.

84. Strehlow, D., S. Jodo, and S.T. Ju, *Retroviral membrane display of apoptotic effector molecules.* Proc Natl Acad Sci U S A, 2000. **97**(8): p. 4209-14.

85. Wei, X.C., et al., *Killing effect of TNF-related apoptosis inducing ligand regulated by tetracycline on gastric cancer cell line NCI-N87.* World J Gastroenterol, 2001. **7**(4): p. 559-62.

86. Zhang, Y., et al., *AAV-mediated TRAIL gene expression driven by hTERT promoter suppressed human hepatocellular carcinoma growth in mice.* Life Sci, 2008. **82**(23-24): p. 1154-61.

87. Ganai, S., R.B. Arenas, and N.S. Forbes, *Tumour-targeted delivery of TRAIL using Salmonella typhimurium enhances breast cancer survival in mice.* Br J Cancer, 2009. **101**(10): p. 1683-91.

88. Wenger, T., et al., *Apoptosis mediated by lentiviral TRAIL transfer involves transduction-dependent and -independent effects.* Cancer Gene Ther, 2007. **14**(3): p. 316-26.

89. Wenger, T., et al., *Specific resistance upon lentiviral TRAIL transfer by intracellular retention of TRAIL receptors.* Cell Death Differ, 2006. **13**(10): p. 1740-51.

90. Kock, N., et al., *Tumor therapy mediated by lentiviral expression of shBcl-2 and S-TRAIL.* Neoplasia, 2007. **9**(5): p. 435-42.

91. Rosenberg, S.A., et al., *Observations on the systemic administration of autologous lymphokine-activated killer cells and recombinant interleukin-2 to patients with metastatic cancer.* N Engl J Med, 1985. **313**(23): p. 1485-92.

92. Blattman, J.N. and P.D. Greenberg, *Cancer immunotherapy: a treatment for the masses.* Science, 2004. **305**(5681): p. 200-5.

93. Fischer, N. and O. LÉGer, *Bispecific Antibodies: Molecules That Enable Novel Therapeutic Strategies.* Pathobiology, 2007. **74**(1): p. 3-14.

94. Muller, D. and R.E. Kontermann, *Recombinant bispecific antibodies for cellular cancer immunotherapy.* Curr Opin Mol Ther, 2007. **9**(4): p. 319-26.

95. Köhler, G. and C. Milstein, *Continuous cultures of fused cells secreting antibody of predefined specificity.* Nature, 1975. **256**(5517): p. 495-7.

96. Cotton, R.G. and C. Milstein, *Letter: Fusion of two immunoglobulin-producing myeloma cells.* Nature, 1973. **244**(5410): p. 42-3.

97. Suresh, M.R., A.C. Cuello, and C. Milstein, *Bispecific monoclonal antibodies from hybrid hybridomas.* Methods Enzymol, 1986. **121**: p. 210-28.

98. Glennie, M.J., et al., *Preparation and performance of bispecific F(ab' gamma)2 antibody containing thioether-linked Fab' gamma fragments.* J Immunol, 1987. **139**(7): p. 2367-75.

99. Staerz UD, K.O., Bevan MJ., *Hybrid antibodies can target sites for attack by T cells.* Nature, 1985. **314 (6012)**(Apr 18-24): p. 4.

100. Kontermann, R.E., T. Volkel, and T. Korn, *Production of recombinant bispecific antibodies.* Methods Mol Biol, 2004. **248**: p. 227-42.

101. Holliger, P., T. Prospero, and G. Winter, *"Diabodies": small bivalent and bispecific antibody fragments.* Proc Natl Acad Sci U S A, 1993. **90**(14): p. 6444-8.

102. Zeidler, R., et al., *The Fc-region of a new class of intact bispecific antibody mediates activation of accessory cells and NK cells and induces direct phagocytosis of tumour cells.* Br J Cancer, 2000. **83**(2): p. 261-6.

103. Zeidler, R., et al., *Simultaneous activation of T cells and accessory cells by a new class of intact bispecific antibody results in efficient tumor cell killing.* J Immunol, 1999. **163**(3): p. 1246-52.

104. Ruf, P. and H. Lindhofer, *Induction of a long-lasting antitumor immunity by a trifunctional bispecific antibody.* Blood, 2001. **98**(8): p. 2526-34.

105. Koprowski, H., et al., *Colorectal Carcinoma Antigens Detected by Hybridoma Antibodies* Somatic Cell Genetics, 1979. **Vol. 5**(No. 6,): p. 957-972

106. Momburg, F., et al., *Immunohistochemical study of the expression of a Mr 34,000 human epithelium-specific surface glycoprotein in normal and malignant tissues.* Cancer Res, 1987. **47**(11): p. 2883-91.

107. Went, P.T., et al., *Frequent EpCam protein expression in human carcinomas.* Hum Pathol, 2004. **35**(1): p. 122-8.

108. Winter, M.J., et al., *The epithelial cell adhesion molecule (Ep-CAM) as a morphoregulatory molecule is a tool in surgical pathology.* Am J Pathol, 2003. **163**(6): p. 2139-48.

109. Trzpis, M., et al., *Epithelial cell adhesion molecule: more than a carcinoma marker and adhesion molecule.* Am J Pathol, 2007. **171**(2): p. 386-95.

110. Amann, M., et al., *Therapeutic window of MuS110, a single-chain antibody construct bispecific for murine EpCAM and murine CD3.* Cancer Res, 2008. **68**(1): p. 143-51.

111. Ren-Heidenreich, L., et al., *Redirected T-cell cytotoxicity to epithelial cell adhesion molecule-overexpressing adenocarcinomas by a novel recombinant antibody, E3Bi, in vitro and in an animal model.* Cancer, 2004. **100**(5): p. 1095-103.

112. Morecki, S., et al., *Induction of long-lasting antitumor immunity by concomitant cell therapy with allogeneic lymphocytes and trifunctional bispecific antibody.* Exp Hematol, 2008. **36**(8): p. 997-1003.

113. Wolf, E., et al., *BiTEs: bispecific antibody constructs with unique anti-tumor activity.* Drug Discov Today, 2005. **10**(18): p. 1237-44.

114. Burges, A., et al., *Effective relief of malignant ascites in patients with advanced ovarian cancer by a trifunctional anti-EpCAM x anti-CD3 antibody: a phase I/II study.* Clin Cancer Res, 2007. **13**(13): p. 3899-905.

115. Schlereth, B., et al., *Eradication of tumors from a human colon cancer cell line and from ovarian cancer metastases in immunodeficient mice by a single-chain Ep-CAM-/CD3-bispecific antibody construct.* Cancer Res, 2005. **65**(7): p. 2882-9.

116. Salnikov, A., et al., *TARGETING OF CANCER STEM CELL MARKER EpCAM BY BISPECIFIC ANTIBODY EpCAMxCD3 INHIBITS PANCREATIC CARCINOMA.* Journal of Cellular and Molecular Medicine, 2009: p. 1-12.

117. Marme, A., et al., *Intraperitoneal bispecific antibody (HEA125xOKT3) therapy inhibits malignant ascites production in advanced ovarian carcinoma.* Int J Cancer, 2002. **101**(2): p. 183-9.

118. Wimberger, P., et al., *Efficient tumor cell lysis by autologous, tumor-resident T lymphocytes in primary ovarian cancer samples by an EP-CAM-/CD3-bispecific antibody.* Int J Cancer, 2003. **105**(2): p. 241-8.

119. Sebastian, M., et al., *Treatment of malignant pleural effusion with the trifunctional antibody catumaxomab (Removab) (anti-EpCAM x Anti-CD3): results of a phase 1/2 study.* J Immunother, 2009. **32**(2): p. 195-202.

120. Naundorf, S., et al., *In vitro and in vivo activity of MT201, a fully human monoclonal antibody for pancarcinoma treatment.* Int J Cancer, 2002. **100**(1): p. 101-10.

121. Prang, N., et al., *Cellular and complement-dependent cytotoxicity of Ep-CAM-specific monoclonal antibody MT201 against breast cancer cell lines.* Br J Cancer, 2005. **92**(2): p. 342-9.

122. Brischwein, K., et al., *MT110: a novel bispecific single-chain antibody construct with high efficacy in eradicating established tumors.* Mol Immunol, 2006. **43**(8): p. 1129-43.

123. Galon, J., et al., *Type, density, and location of immune cells within human colorectal tumors predict clinical outcome.* Science, 2006. **313**(5795): p. 1960-4.

124. Wahlin, B.E., et al., *CD8+ T-cell content in diagnostic lymph nodes measured by flow cytometry is a predictor of survival in follicular lymphoma.* Clin Cancer Res, 2007. **13**(2 Pt 1): p. 388-97.

125. Baeuerle, P.A., P. Kufer, and R. Bargou, *BiTE: Teaching antibodies to engage T-cells for cancer therapy.* Curr Opin Mol Ther, 2009. **11**(1): p. 22-30.

126. Sebastian, M., et al., *Treatment of non-small cell lung cancer patients with the trifunctional monoclonal antibody catumaxomab (anti-EpCAM × anti-CD3): a phase I study.* Cancer Immunol Immunother, 2007. **56**(10): p. 1637-1644.

127. Brischwein, K., et al., *Strictly target cell-dependent activation of T cells by bispecific single-chain antibody constructs of the BiTE class.* J Immunother, 2007. **30**(8): p. 798-807.

128. Strauss, G., et al., *Without prior stimulation, tumor-associated lymphocytes from malignant effusions lyse autologous tumor cells in the presence of bispecific antibody HEA125xOKT3.* Clin Cancer Res, 1999. **5**(1): p. 171-80.

129. Vogel, R., et al., *A single lentivirus vector mediates doxycycline-regulated expression of transgenes in the brain.* Hum Gene Ther, 2004. **15**(2): p. 157-65.

130. Leisegang, M., et al., *Enhanced functionality of T cell receptor-redirected T cells is defined by the transgene cassette.* J Mol Med, 2008. **86**(5): p. 573-583.

131. Moldenhauer, G., et al., *Epithelium-specific surface glycoprotein of Mr 34,000 is a widely distributed human carcinoma marker.* Br J Cancer, 1987. **56**(6): p. 714-21.

132. Cavalieri, S., et al., *Human T lymphocytes transduced by lentiviral vectors in the absence of TCR activation maintain an intact immune competence.* Blood, 2003. **102**(2): p. 497-505.

133. Poczatek, R.B., et al., *Ep-Cam levels in prostatic adenocarcinoma and prostatic intraepithelial neoplasia.* J Urol, 1999. **162**(4): p. 1462-6.

134. Zhang, S., et al., *Expression of potential target antigens for immunotherapy on primary and metastatic prostate cancers.* Clin Cancer Res, 1998. **4**(2): p. 295-302.

135. Li, C., et al., *Identification of pancreatic cancer stem cells.* Cancer Res, 2007. **67**(3): p. 1030-7.

136. Patrawala, L., et al., *Highly purified CD44+ prostate cancer cells from xenograft human tumors are enriched in tumorigenic and metastatic progenitor cells.* Oncogene, 2006. **25**(12): p. 1696-708.

137. Marhaba, R., et al., *CD44 and EpCAM: cancer-initiating cell markers.* Curr Mol Med, 2008. **8**(8): p. 784-804.

138. Kallifatidis, G., et al., *Sulforaphane targets pancreatic tumour-initiating cells by NF-kappaB-induced antiapoptotic signalling.* Gut, 2009. **58**(7): p. 949-63.

139. Wang, P., et al., *Inhibition of RIP and c-FLIP enhances TRAIL-induced apoptosis in pancreatic cancer cells.* Cell Signal, 2007. **19**(11): p. 2237-46.

140. Huang, S., K. Okumura, and F.A. Sinicrope, *BH3 mimetic obatoclax enhances TRAIL-mediated apoptosis in human pancreatic cancer cells.* Clin Cancer Res, 2009. **15**(1): p. 150-9.

141. Guillermet, J., et al., *Somatostatin receptor subtype 2 sensitizes human pancreatic cancer cells to death ligand-induced apoptosis.* Proc Natl Acad Sci U S A, 2003. **100**(1): p. 155-60.

142. Gill, C., et al., *Effects of cIAP-1, cIAP-2 and XIAP triple knockdown on prostate cancer cell susceptibility to apoptosis, cell survival and proliferation.* Mol Cancer, 2009. **8**: p. 39.

143. Dieterle, A., et al., *The Akt inhibitor triciribine sensitizes prostate carcinoma cells to TRAIL-induced apoptosis.* Int J Cancer, 2009. **125**(4): p. 932-41.

144. Christian, P.A., J.A. Thorpe, and S.R. Schwarze, *Velcade sensitizes prostate cancer cells to TRAIL induced apoptosis and suppresses tumor growth in vivo.* Cancer Biol Ther, 2009. **8**(1): p. 73-80.

145. Sadelain, M., I. Riviere, and R. Brentjens, *Targeting tumours with genetically enhanced T lymphocytes.* Nat Rev Cancer, 2003. **3**(1): p. 35-45.

146. Murphy, A., et al., *Gene modification strategies to induce tumor immunity.* Immunity, 2005. **22**(4): p. 403-14.

147. Coffin JM, H.S., Varmus HE, *Retroviruses.* Cold Spring Harbor Laboratory Press, 1997.

148. Voigt, K., Z. Izsvak, and Z. Ivics, *Targeted gene insertion for molecular medicine.* J Mol Med, 2008. **86**(11): p. 1205-19.

149. Ciuffi, A., *Mechanisms governing lentivirus integration site selection.* Curr Gene Ther, 2008. **8**(6): p. 419-29.

150. Cavazzana-Calvo, M., et al., *Gene therapy of human severe combined immunodeficiency (SCID)-X1 disease.* Science, 2000. **288**(5466): p. 669-72.

151. Cavazzana-Calvo, M., et al., *[Gene therapy of severe combined immunodeficiencies]*. Transfus Clin Biol, 2000. **7**(3): p. 259-60.

152. Hacein-Bey-Abina, S., et al., *LMO2-associated clonal T cell proliferation in two patients after gene therapy for SCID-X1*. Science, 2003. **302**(5644): p. 415-9.

153. Hacein-Bey-Abina, S., et al., *A serious adverse event after successful gene therapy for X-linked severe combined immunodeficiency*. N Engl J Med, 2003. **348**(3): p. 255-6.

154. Hacein-Bey-Abina, S., G. de Saint Basile, and M. Cavazzana-Calvo, *Gene therapy of X-linked severe combined immunodeficiency*. Methods Mol Biol, 2003. **215**: p. 247-59.

155. Bushman, F.D., *Retroviral integration and human gene therapy*. J Clin Invest, 2007. **117**(8): p. 2083-6.

156. Li, Z., et al., *Murine leukemia induced by retroviral gene marking*. Science, 2002. **296**(5567): p. 497.

157. Schwarzwaelder, K., et al., *Gammaretrovirus-mediated correction of SCID-X1 is associated with skewed vector integration site distribution in vivo*. J Clin Invest, 2007. **117**(8): p. 2241-9.

158. Deichmann, A., et al., *Vector integration is nonrandom and clustered and influences the fate of lymphopoiesis in SCID-X1 gene therapy*. J Clin Invest, 2007. **117**(8): p. 2225-32.

159. Kustikova, O., et al., *Clonal dominance of hematopoietic stem cells triggered by retroviral gene marking*. Science, 2005. **308**(5725): p. 1171-4.

160. Modlich, U., et al., *Leukemias following retroviral transfer of multidrug resistance 1 (MDR1) are driven by combinatorial insertional mutagenesis*. Blood, 2005. **105**(11): p. 4235-46.

161. Daniel, R. and J.A. Smith, *Integration site selection by retroviral vectors: molecular mechanism and clinical consequences*. Hum Gene Ther, 2008. **19**(6): p. 557-68.

162. Stevens, S.W. and J.D. Griffith, *Human immunodeficiency virus type 1 may preferentially integrate into chromatin occupied by L1Hs repetitive elements*. Proc Natl Acad Sci U S A, 1994. **91**(12): p. 5557-61.

163. Carteau, S., C. Hoffmann, and F. Bushman, *Chromosome structure and human immunodeficiency virus type 1 cDNA integration: centromeric alphoid repeats are a disfavored target*. J Virol, 1998. **72**(5): p. 4005-14.

164. Mitchell, R.S., et al., *Retroviral DNA integration: ASLV, HIV, and MLV show distinct target site preferences*. PLoS Biol, 2004. **2**(8): p. E234.

165. Schroder, A.R., et al., *HIV-1 integration in the human genome favors active genes and local hotspots*. Cell, 2002. **110**(4): p. 521-9.

166. Sun, Y., X. Chen, and D. Xiao, *Tetracycline-inducible expression systems: new strategies and practices in the transgenic mouse modeling*. Acta Biochim Biophys Sin (Shanghai), 2007. **39**(4): p. 235-46.

167. Zhu, Z., et al., *Tetracycline-controlled transcriptional regulation systems: advances and application in transgenic animal modeling*. Semin Cell Dev Biol, 2002. **13**(2): p. 121-8.

168. Trauzold, A., et al., *TRAIL promotes metastasis of human pancreatic ductal adenocarcinoma*. Oncogene, 2006. **25**(56): p. 7434-9.

169. Cretney, E., et al., *Increased susceptibility to tumor initiation and metastasis in TNF-related apoptosis-inducing ligand-deficient mice*. J Immunol, 2002. **168**(3): p. 1356-61.

170. Finnberg, N., A.J. Klein-Szanto, and W.S. El-Deiry, *TRAIL-R deficiency in mice promotes susceptibility to chronic inflammation and tumorigenesis*. J Clin Invest, 2008. **118**(1): p. 111-23.

171.   Grosse-Wilde, A., et al., *TRAIL-R deficiency in mice enhances lymph node metastasis without affecting primary tumor development.* J Clin Invest, 2008. **118**(1): p. 100-10.

172.   Takeda, K., et al., *Involvement of tumor necrosis factor-related apoptosis-inducing ligand in NK cell-mediated and IFN-gamma-dependent suppression of subcutaneous tumor growth.* Cell Immunol, 2001. **214**(2): p. 194-200.

173.   Smyth, M.J., et al., *Tumor necrosis factor-related apoptosis-inducing ligand (TRAIL) contributes to interferon gamma-dependent natural killer cell protection from tumor metastasis.* J Exp Med, 2001. **193**(6): p. 661-70.

174.   Seki, N., et al., *Tumor necrosis factor-related apoptosis-inducing ligand-mediated apoptosis is an important endogenous mechanism for resistance to liver metastases in murine renal cancer.* Cancer Res, 2003. **63**(1): p. 207-13.

175.   Beg, A.A. and D. Baltimore, *An essential role for NF-kappaB in preventing TNF-alpha-induced cell death.* Science, 1996. **274**(5288): p. 782-4.

176.   Van Antwerp, D.J., et al., *Suppression of TNF-alpha-induced apoptosis by NF-kappaB.* Science, 1996. **274**(5288): p. 787-9.

177.   Trauzold, A., et al., *CD95 and TRAIL receptor-mediated activation of protein kinase C and NF-kappaB contributes to apoptosis resistance in ductal pancreatic adenocarcinoma cells.* Oncogene, 2001. **20**(31): p. 4258-69.

178.   Herr, I., P. Schemmer, and M.W. Buchler, *On the TRAIL to therapeutic intervention in liver disease.* Hepatology, 2007. **46**(1): p. 266-74.

179.   Niggemann, B., et al., *Locomotory phenotypes of human tumor cell lines and T lymphocytes in a three-dimensional collagen lattice.* Cancer Lett, 1997. **118**(2): p. 173-80.

180.   Burges, A., et al., *Effective Relief of Malignant Ascites in Patients with Advanced Ovarian Cancer by a Trifunctional Anti-EpCAM x Anti-CD3 Antibody: A Phase I/II Study.* Clinical Cancer Research, 2007. **13**(13): p. 3899-3905.

181.   Haas, C., et al., *Mode of cytotoxic action of T cell-engaging BiTE antibody MT110.* Immunobiology, 2009. **214**(6): p. 441-53.

182.   Riesenberg, R., et al., *Lysis of prostate carcinoma cells by trifunctional bispecific antibodies (alpha EpCAM x alpha CD3).* J Histochem Cytochem, 2001. **49**(7): p. 911-7.

183.   Kelley, S.K., et al., *Preclinical studies to predict the disposition of Apo2L/tumor necrosis factor-related apoptosis-inducing ligand in humans: characterization of in vivo efficacy, pharmacokinetics, and safety.* J Pharmacol Exp Ther, 2001. **299**(1): p. 31-8.

184.   Garcea, G., et al., *Cystic lesions of the pancreas. A diagnostic and management dilemma.* Pancreatology, 2008. **8**(3): p. 236-51.

185.   Osten, L., et al., *Doxycycline accelerates renal cyst growth and fibrosis in the pcy/pcy mouse model of type 3 nephronophthisis, a form of recessive polycystic kidney disease.* Histochem Cell Biol, 2009: p. 1-12.

186.   Flieger, D., et al., *A bispecific single-chain antibody directed against EpCAM/CD3 in combination with the cytokines interferon alpha and interleukin-2 efficiently retargets T and CD3+CD56+ natural-killer-like T lymphocytes to EpCAM-expressing tumor cells.* Cancer Immunol Immunother, 2000. **49**(8): p. 441-8.

187.   Alladina, S.J., et al., *TRAIL-induced apoptosis in human vascular endothelium is regulated by phosphatidylinositol 3-kinase/Akt through the short form of cellular FLIP and Bcl-2.* J Vasc Res, 2005. **42**(4): p. 337-47.

188.   Li, J.H., et al., *TRAIL induces apoptosis and inflammatory gene expression in human endothelial cells.* J Immunol, 2003. **171**(3): p. 1526-33.

189.   Kanegane, C., et al., *Contribution of the CXC chemokines IP-10 and Mig to the antitumor effects of IL-12.* J Leukoc Biol, 1998. **64**(3): p. 384-92.

190. Sgadari, C., A.L. Angiolillo, and G. Tosato, *Inhibition of angiogenesis by interleukin-12 is mediated by the interferon-inducible protein 10.* Blood, 1996. **87**(9): p. 3877-82.

191. Belperio, J.A., et al., *CXC chemokines in angiogenesis.* J Leukoc Biol, 2000. **68**(1): p. 1-8.

192. Benelli, R., et al., *Cytokines and chemokines as regulators of angiogenesis in health and disease.* Curr Pharm Des, 2006. **12**(24): p. 3101-15.

193. Salvucci, O., et al., *Evidence for the involvement of SDF-1 and CXCR4 in the disruption of endothelial cell-branching morphogenesis and angiogenesis by TNF-alpha and IFN-gamma.* J Leukoc Biol, 2004. **76**(1): p. 217-26.

194. Kishore, R., et al., *Functionally novel tumor necrosis factor-alpha-modulated CHR-binding protein mediates cyclin A transcriptional repression in vascular endothelial cells.* Circ Res, 2002. **91**(4): p. 307-14.

195. Lejeune, F.J., C. Ruegg, and D. Lienard, *Clinical applications of TNF-alpha in cancer.* Curr Opin Immunol, 1998. **10**(5): p. 573-80.

196. Munz, M., et al., *The carcinoma-associated antigen EpCAM upregulates c-myc and induces cell proliferation.* Oncogene, 2004. **23**(34): p. 5748-58.

197. Osta, W.A., et al., *EpCAM is overexpressed in breast cancer and is a potential target for breast cancer gene therapy.* Cancer Res, 2004. **64**(16): p. 5818-24.

198. Denzel, S., et al., *Initial activation of EpCAM cleavage via cell-to-cell contact.* BMC Cancer, 2009. **9**: p. 402.

199. Maher, S.G., et al., *Interferon: cellular executioner or white knight?* Curr Med Chem, 2007. **14**(12): p. 1279-89.

200. Saidi, R.F., et al., *Interferon receptors and the caspase cascade regulate the antitumor effects of interferons on human pancreatic cancer cell lines.* Am J Surg, 2006. **191**(3): p. 358-63.

201. Balkwill, F. and A. Mantovani, *Inflammation and cancer: back to Virchow?* Lancet, 2001. **357**(9255): p. 539-45.

202. Roncarolo, M.G., et al., *Type 1 T regulatory cells.* Immunol Rev, 2001. **182**: p. 68-79.

203. Roncarolo, M.G., et al., *Interleukin-10-secreting type 1 regulatory T cells in rodents and humans.* Immunol Rev, 2006. **212**: p. 28-50.

204. Mantovani, A., et al., *The origin and function of tumor-associated macrophages.* Immunol Today, 1992. **13**(7): p. 265-70.

205. Allavena, P., et al., *The inflammatory micro-environment in tumor progression: the role of tumor-associated macrophages.* Crit Rev Oncol Hematol, 2008. **66**(1): p. 1-9.